Imaging in early stage cervical cancer

Jacob Pieter Hoogendam

ISBN: 9789462334496

Cover design, illustration & lay-out: Esther Beekman (www.estherontwerpt.nl)
Printed by: Gildeprint drukkerijen, Enschede

Financial support for the publication of this thesis was kindly provided by:
UMC Utrecht (division Women and Baby), AbbVie BV, ACE Pharmaceuticals BV, BMA BV (Mosos), Erbe Nederland BV, Guerbet Nederland BV, Memidis pharma BV, Sectra Benelux, Stichting Olijf.

Imaging in early stage cervical cancer

Beeldvorming van vroeg stadium baarmoederhalskanker

(met een samenvatting in het Nederlands)

Proefschrift

ter verkrijging van de graad van doctor aan de Universiteit Utrecht
op gezag van de rector magnificus, prof. dr. G.J. van der Zwaan, ingevolge het besluit van het college voor promoties in het openbaar te verdedigen op
donderdag 5 januari 2017 des middags te 4.15 uur

door

Jacob Pieter Hoogendam
geboren op 8 juni 1986 te Leidschendam

Promotores	Prof. dr. R.H.M. Verheijen
	Prof. dr. M.A.A.J. van den Bosch
Copromotores	Dr. R.P. Zweemer
	Dr. W.B. Veldhuis

CONTENTS

Discussion, Summary and Appendices

Chapter 1

General introduction

Epidemiology of cervical cancer

Worldwide, cervical cancer is the fourth most common malignancy in women with an absolute annual incidence of 454.000 – 528.000 cases, an annual absolute mortality of 200.000 – 266.000 deaths and a 5 year disease prevalence of 1.547.000 women [1,2]. In 76 – 85% of the new cases and 87% of the mortality, it occurs in developing countries (by WHO-IARC definitions) [1,2]. This is reflected by the low, age standardized incidence rates of the Netherlands (6.8/100.000 women), Western Europe (7.3/100.000) and United States (6.6/100.000) when compared to Eastern Africa (42.7/100.000), Sub-Saharan Africa (34.8/100.000) and South-Central Asia (19.3/100.000) [2]. Factors contributing to these high incidence rates include an absence of screening programs, high human papillomavirus (HPV) prevalence, limited medical resources and poor healthcare access [3]. Moreover, the anticipated long term incidence reduction due to HPV vaccination in the developed world – though prohibitively expensive for developing countries – will likely further widen this global incidence disparity in the future [4].

In the Netherlands, the absolute annual incidence – which was 715 cases in 2015 – has been stable over the past two decades (Figure 1A) [5]. This translates into a lifetime (0-85 years) cervical cancer risk of 0.63% for a Dutch woman. In context, the lifetime risks for vulvar, uterine corpus, ovarian and breast cancer are 0.30%, 1.87%, 1.14% and 12.08%, respectively [5]. Cervical cancer is often diagnosed at a relatively young age, with a peak risk interval between 30 and 50 years, and a secondary incidence rise in women over 75 years of age (Figure 1B) [5]. Like incidence, the national 5 year disease specific survival rate (adjusted for the expected other cause mortality based on annual life tables) has also remained stable around 66% over the past two decades [5].

In equally stark contrast to developing countries, in the Netherlands cervical cancer is predominately discovered at an early stage. Stage I-II disease accounts for 78.4% of all cases, of which stage IB1-2 represents the largest subgroup at 37.3%, followed by stages IA1-2 and IIB with 20.8% and 15.2% of all cases, respectively [5]. Conversely, advanced stage disease (stage III-IV) is relatively more common in developing regions [3].

Clinical staging

Staging was originally developed to allow sound group level comparisons – by setting globally uniform categories of disease status – which is important for comparing medical research and quality of care surveillance [6,7]. Nowadays, following a cervical cancer diagnosis, staging is mainly performed for optimal treatment planning and estimating prognosis.

The first staging system for cervical cancer was published in 1929 by the cancer commission of the Health Organization of the League of Nations. This made cervical

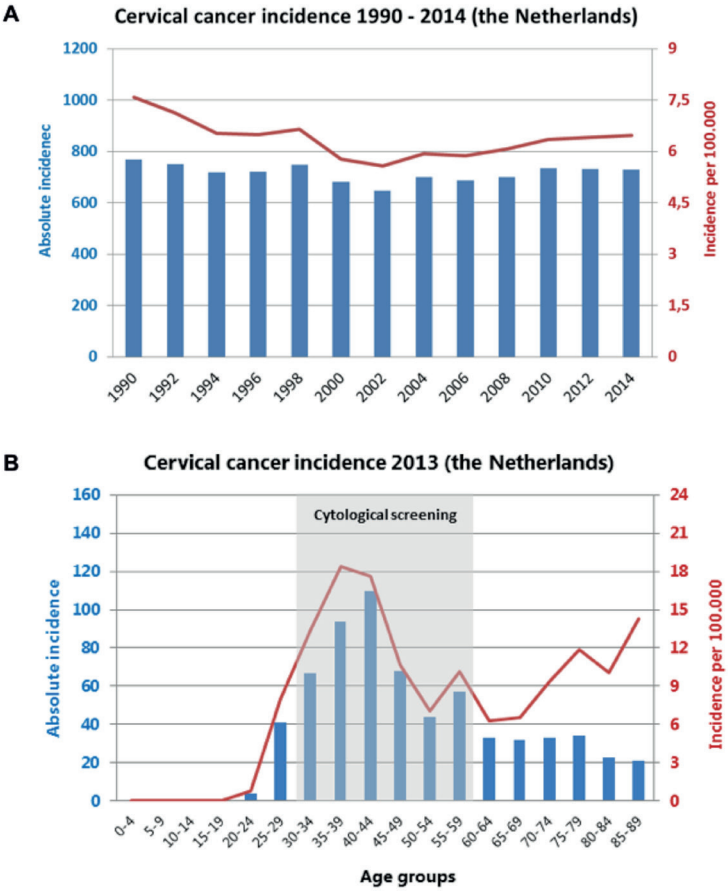

Figure 1. Absolute (blue bars, left axis) and relative (red line, right axis) cervical cancer incidence in the Netherlands plotted against year (Figure 1A) and age (Figure 1B) at diagnosis. Data collected by the Netherlands comprehensive cancer organization (IKNL) [5]. For figure 1A, the relative incidence is demography adjusted according to the world standardized model. For figure 1B, 2013 was the most recent year available with complete and verified incidence data for age groups at the time of publication.

cancer one of the first malignancies to have a formal staging system. After the Second World War, the International Federation of Gynecology and Obstetrics (FIGO) took on the role of leading organization for timely revision of the staging system [6]. From its first edition in 1958, and throughout the subsequent nine revisions, FIGO has recommended clinical (i.e. non-surgical) staging in cervical cancer [8,9].

The clinical approach centers on a thorough pelvic examination with a speculum aided inspection of the cervix and vagina, followed by (recto)vaginal palpation, which can be performed under anesthesia if assessment is impossible without relaxation. In addition, a predefined set of diagnostics may be optionally used, including colposcopy, endocervical curettage, cone biopsy, hysteroscopy, cystoscopy, proctoscopy, intravenous urography, and chest and skeletal radiography. When uncertainty between two stages persists, the less advanced of the two should be selected [10]. When a FIGO stage has been determined, based on this specific clinical approach, no future stage alterations are allowed, not even when postoperative surgico-pathological findings would suggest so [10]. Table 1 provides an overview of the current FIGO stage definitions. Consistent with its clinical approach, stages are primarily categorized based on size and the loco-regional tumor extension. In contrast to TNM staging, lymph nodal status is deliberately omitted in the FIGO system because the retroperitoneal pelvic lymphatic drainage route cannot be clinically assessed. An exception exists for those rare instances when lymph nodal metastases can be clinically found by palpation; for example in the supraclavicular chain – which results in stage IVB.

Several arguments support this clinical approach to staging. Most importantly, it is advantageous for high incidence yet underdeveloped countries because it efficiently uses the limited resources available. Clinical staging does not require advanced technology, nor comprehensive surgical staging (as used in ovarian cancer), which makes it cheap and generally accessible. Secondly, it allows for swift staging – frequently in a single visit – as it can be performed directly following the detection of a macroscopic tumor. Thirdly, when staging is performed uniformly worldwide, it enables developing countries to translate research findings and practice guidelines from more developed areas to their situation (i.e. solidarity of care principle).

However, this clinical approach also has two important limitations. First, 'erroneous' under- and overstaging may occur when clinical stages are compared to surgical findings. Studies have reported agreement between clinical stages IB1, IB2, IIA1-2 and IIB1-2 and the surgico-pathological result in only 82 – 85%, 61 – 77%, 35 – 60% and 20 – 59% of cases, respectively [11,12,13,14]. These disparities with surgical findings can lead to adjuvant treatment, for instance when parametrial invasion is found at the histology of a radical hysterectomy in a clinical stage IB1 patient. Such double modality treatment may carry an increased morbidity risk [15].

Secondly, as mentioned earlier, lymph nodal status is not incorporated into the FIGO stages, even though it is the single most important prognostic factor, and can influence the treatment plan (e.g. trachelectomy indication). In stage IB1 cervical cancer patients, the overall survival at 5 years for those with tumor-positive versus tumor-negative lymph

nodes is reported at 75.9% and 94.5% (adjusted hazard ratio: 4.7, 95%CI: 3.5 – 6.4) [11]. Ideally, a comprehensive work-up should nowadays include factors beyond those required in traditional clinical staging (e.g. lymph node status), as to allow better estimation of prognosis and minimize avoidable double modality treatment.

Cross-sectional imaging to assist clinical staging

Over the past two decades, a steady decline in diagnostics allowed by FIGO for clinical staging was reported in developed countries, while cross-sectional imaging came into routine use [16,17,18,19]. Thus, with the 2009 update of the FIGO cervical cancer stage classification system, an assisting role of cross-sectional imaging was allowed in regions where it is available. More specifically, FIGO states that the use of these imaging techniques are encouraged but not mandatory [9]. This recommendation has been supported by the WHO, the European Society for Medical Oncology, the US National Comprehensive Cancer Network, European Society for Gynaecological Oncology and various other leading health organizations [20,21,22,23].

While this recommendation formally extends to both computed tomography (CT) and magnetic resonance imaging (MRI), an extensive body of research has demonstrated the diagnostic inferiority of abdominal CT [24,25,26]. Its inability to differentiate neoplastic from healthy (para)cervical tissue makes assessing tumor size and invasion into the parametria, vagina and uterine corpus nearly impossible [27]. Hence, the current Dutch guideline advises against the use of abdominal CT, unless MRI is deemed unfeasible (e.g. in patients with a cardiac pacemaker) [28].

Value of MRI and PET-CT

Pelvic MRI is widely considered the imaging modality of choice to assess extent of disease in cervical cancer and is recommended by the Dutch guideline for those patients in who it is relevant for making or changing a treatment plan [10,27,28,29,30]. In daily clinical practice, this entails its routine use when stage ≥IB1 is suspected.

On MRI, early stage cervical cancer typically presents as a T_2 hyperintense mass relative to the T_2 hypointense cervical stroma. Contrary to physical examination, MRI allows for a tumor length assessment in the craniocaudal direction. The largest tumor diameter measurement on MRI falls within a 5mm margin of the histological measurement in 93% of cases [29,31,32]. Additionally, a meta-analysis (n=3254, 40 studies) by Thomeer et al. reported a substantially higher pooled accuracy for the detection of parametrial invasion by MRI (sensitivity: 84%, specificity: 92%) when compared to physical examination (sensitivity: 40%, specificity 93%) [33]. The commonly used criterion for parametrial invasion is an interruption of the T_2 hypointense fibrous stromal ring around the tumor

Table 1. FIGO staging for carcinoma of the cervix uteri

I		The carcinoma is strictly confined to the cervix (extension to the uterine corpus should be disregarded).
	IA	Invasive cancer identified only microscopically (all gross lesions even with superficial invasion are Stage IB cancers). Invasion is limited to measured stromal invasion with a maximum depth of 5 mm[a] and no wider than 7 mm.
		IA1 Measured invasion of stroma ≤3 mm in depth and ≤7 mm width.
		IA2 Measured invasion of stroma >3 mm and <5 mm in depth and ≤7 mm width.
	IB	Clinical lesions confined to the cervix, or preclinical lesions greater than IA.
		IB1 Clinically visible lesion ≤4 cm in size.
		IB2 Clinically visible lesion >4 cm in size.
II		The carcinoma extends beyond the uterus, but has not extended onto the pelvic wall or to the lower third of the vagina.
	IIA	Involvement of up to the upper 2/3 of the vagina. No obvious parametrial involvement.
		IIA1 Clinically visible lesion ≤4 cm in size.
		IIA2 Clinically visible lesion >4 cm in size.
	IIB[b]	Obvious parametrial involvement but not onto the pelvic sidewall.
III		The carcinoma has extended onto the pelvic sidewall. On rectal examination, there is no cancer free space between the tumor and pelvic sidewall. The tumor involves the lower third of the vagina. All cases of hydronephrosis or non-functioning kidney should be included unless they are known to be due to other causes.
	IIIA	Involvement of the lower vagina but no extension onto pelvic sidewall.
	IIIB	Extension onto the pelvic sidewall, or hydronephrosis/non-functioning kidney.
IV		The carcinoma has extended beyond the true pelvis or has clinically involved the mucosa of the bladder and/or rectum.
	IVA	Spread to adjacent pelvic organs.
	IVB	Spread to distant organs.

[a] The depth of invasion should not be more than 5 mm taken from the base of the epithelium, either surface of glandular, from which it originates. Vascular space invasion should not alter the staging.
[b] While formally not part of the FIGO system, it is clinically not uncommon to subcategorize stage IIB into IIB1 if the visible lesion is ≤4 cm and IIB2 when the lesion is >4 cm (in analogy to stages IB1-2 and IIA1-2).
Table derived from the FIGO committee on gynecologic oncology report [86].

(Figure 2) [34]. While stage III – IV disease is beyond the scope of this thesis, MRI can also be valuable for evaluating pelvic wall extension, presence of hydronephrosis and tumor invasion into the bladder or rectum.

The assessment of pelvic lymph nodes on metastases can also reliably be done on MRI. The most widely used cutoff of 10mm short axis length focuses on achieving a high specificity (range: 69 – 96%), thus conversely limiting sensitivity (range: 27% – 71%) [35,36,37,38,39]. Clinically, this means that 'non-enlarged' metastatic lymph nodes (i.e. false negatives) are not uncommon [29,40]. The second part of this thesis, particularly chapter 8, will provide a more detailed outline on the advantages and limitations of MRI based (sentinel) lymph node assessment.

In addition to MRI, ^{18}F-2-fluoro-2-deoxy-D-glucose (FDG) Positron Emission Tomography (PET) – CT may also be used to assist clinical FIGO staging. In stage I – II patients, this primarily entails noninvasive assessment of the lymph nodal status for which a variable sensitivity between 10 – 91% and an excellent specificity of 94 – 100% has been reported [41,42,43]. However, high costs and the low a priori probability of metastases, particularly in those where pelvic MRI did not show enlarged lymph nodes, discourage routine PET–CT use in early stage patients [41]. The current Dutch guideline limits its use to those patients with suspicious lymph nodes on imaging (i.e. MRI) or proven tumor-positive nodes after surgery [28]. This in contrast to the United States where – possibly in part due to medicolegal or economic factors – PET-CT is recommended for the work-up of all ≥IB1 patients [22,27].

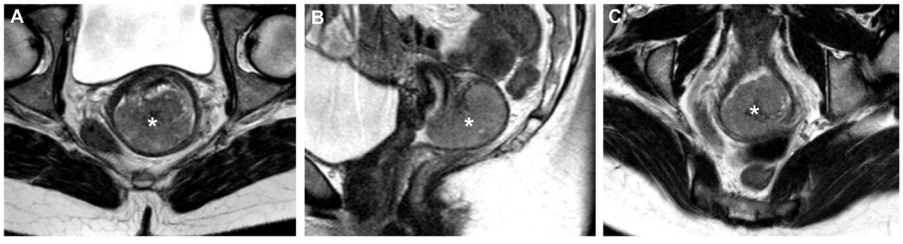

Figure 2. Pelvic T_2-weighted 1.5T MRI in the transversal (A), sagittal (B) and oblique – perpendicular to the cervical canal – plane (C) of a 44 year old women diagnosed with a clinical stage IB2 poorly differentiated adenocarcinoma of the cervix. The tumor originated from the dorsal part of the cervix (asterisk) and measured 50mm in its largest diameter. Note the low T_2 signal intensity stromal ring around the tumor, suggesting absence of parametrial invasion.

Sentinel lymph node procedure

Following a landmark study in 1977 by Ramon Cabanas on identifying the first lymphatic node of penile cancer [44], and subsequent high quality research in breast [45,46,47] and vulvar cancer [48,49,50], the sentinel lymph node (SLN) concept is now also increasingly used in cervical cancer. By definition, the SLN is the nodal station to receive the first efferent lymphatic drainage of the tumor [51,52]. This should make the SLN the site where lymph nodal metastases would first appear. Depending on the complexity, or bilateralism of the lymphatics in midline organs such as the cervix uteri, more than one SLN can be present, which should preferably all be detected [51,52].

The ultimate aim of the SLN procedure is to be able to abstain from pelvic lymph node dissection (Figure 3) when SLN's are bilaterally detected and found to be tumor-negative [53,54]. This would safeguard a majority of early stage patients from the 2 – 3% intraoperative (e.g. vascular, nerve, ureteric and bowel injury) and 2.9 – 3.5% direct postoperative complications (e.g. infections, hematoma) associated with lymph node dissections [55,56]. In addition, its long term morbidity includes chronic lower extremity lymphedema in 19 – 41%, with or without recurrent lymphangitis, which negatively influences the quality of life in these women [57]. Furthermore, pelvic lymphocele formation has been reported to occur in 20% of lymphadenectomy cases, of which 29% are symptomatic (i.e. 6% of all lymph node dissection cases) with abdominal pain, hydronephrosis, venous thrombosis or urinary urgency [58]. The much anticipated outcomes of the randomized controlled SENTICOL-2 trial will present a direct comparison on complications and morbidity between lymph node dissection and the SLN procedure [59].

In practice, the SLN procedure requires a combined effort from the gynecological oncologist, nuclear medicine physician and pathologist. First, either one day preoperatively or directly prior to surgery, the nanocolloid-bound radionuclide Technetium-99m (140 keV, $t_{1/2}$: 6.0 hours) is injected into the stroma in two or four quadrants of the cervix directly peripheral of the tumor. With an identical injection technique, a visible but biologically inert dye (e.g. Blue Patenté, Guerbet, Villepinte, France) is administered at the beginning of surgery (Figure 4A) [60]. The use of visible dye or a radionuclide alone, yields lower detection when compared to their combined use, with minimally one SLN detected in 84.0–87.5%, 88.0–90.3% and 94.3–97.0% of cases, respectively [61,62]. The same holds true for bilateral detection with a ratio of 56%, 54% and 72%, respectively [63]. Currently, this combined tracer method is considered the reference standard, though new approaches with near-infrared immunofluorescent tracers (e.g. indocyanine green) appear promising [64,65,66].

Ideally, (robot assisted) laparoscopy is used to maintain the minimally invasive aim of

the SLN concept. After pneumoperitoneal insufflation the retroperitoneum is opened bilaterally. Radioactive nodes are detected via a gamma ray detectionprobe, and blue stained SLN's are visually localized and resected (Figures 4B and 4C). Alternatively, an extraperitoneal approach can be used and may reduce intraperitoneal adhesions and the morbidity of adjuvant radiotherapy [67,68]. When the (sentinel) nodal status is needed for intraoperative decisions, optional frozen section analysis can be performed prior to confirmation by definitive paraffin embedded histology. Contrary to non-sentinel lymph nodes, serial step sectioning at relatively short intervals, between 40 – 500 µm, is performed [69,70]. Slides are stained with heamatoxylin and eosin, followed by immunohistochemical staining with pan-cytokeratin AE1/AE3 antibodies and reviewed by a pathologist specialized in gynecological oncology. This histological approach is often referred to as 'SLN ultrastaging'.

In terms of clinical relevance, the preferred accuracy parameter of the SLN procedure depends on the aim of the procedure. When used to avoid radical hysterectomy in patients with nodal involvement, given that chemoradiation is indicated anyway, a high true positive ratio is desired. However, increasingly the focus lies with avoiding full lymph node dissection in patients without nodal involvement. A low false negative ratio (i.e. a high sensitivity) is preferred. False negatives are defined as patients with tumor-negative SLN's, but tumor-positive (non-sentinel) lymph nodes.

Compared to imaging, the SLN procedure is invasive, laborious and caries an increased risk of adverse events, but is also substantially more accurate in detecting nodal metastases in early stage cervical cancer. This was confirmed by Selman et al. who performed a meta-analysis in 2008 on 72 observational studies (Table 2) [71]. However, their analysis did not include the prospective cohort study (2008) by Altgassen et al. (n=590), which showed a remarkably low sensitivity of 77.4% for surgical SLN assessment [72]. Omitting this particular study is justified by its serious methodological issues. Concerns have been raised on its poor quality assurance (e.g. absent central and uniform histology), non-standardized SLN methodology (e.g. open tracer selection for physicians), questionable inclusion criteria (e.g. all stages, including IVB) and midstudy changes to exclusion criteria [73,74]. Also, no prior experience with the SLN procedure was required for physicians and on-study training was likely insufficient with on average <5 inclusions per year for all physicians of a participating center [73].

In 2012, a multicenter study by Cibula et al. (n=645, including 115 from the VUmc / UMC Utrecht) reported that when additional quality safeguards are adopted – including bilateral SLN detection (achieved in 72%) and histopathological ultrastaging – the false negative ratio of the SLN procedure can be reduced to 1.3% [53,75]. This is in support of the earlier SENTICOL-1 trial (n=139) which did not encounter a single false-negative SLN

in the subgroup of women with bilaterally detected SLN's (achieved in 76.5%) and also concluded that bilateral detection is an important quality requirement [54].
Ultimately, the question is how low the false negative ratio for the SLN procedure needs to be before it can be considered 'safe enough' to allow omission of a full lymph node dissection. Some authors justifiably argue that the unknown false-negative ratio of full lymphadenectomy could very well be substantially larger, whereas up to 50 lymph nodes are typically reviewed without histological ultrastaging and aberrant locations (e.g. presacral) for first metastases are disregarded [76,77,78]. The SENTICOL-1 trial identified 18.1% (82/454) of its SLN's, including 4 tumor-positive SLN's, in anatomical regions outside of the standard pelvic lymphadenectomy field, highlighting the complex lymph drainage pathways from the cervix [77].

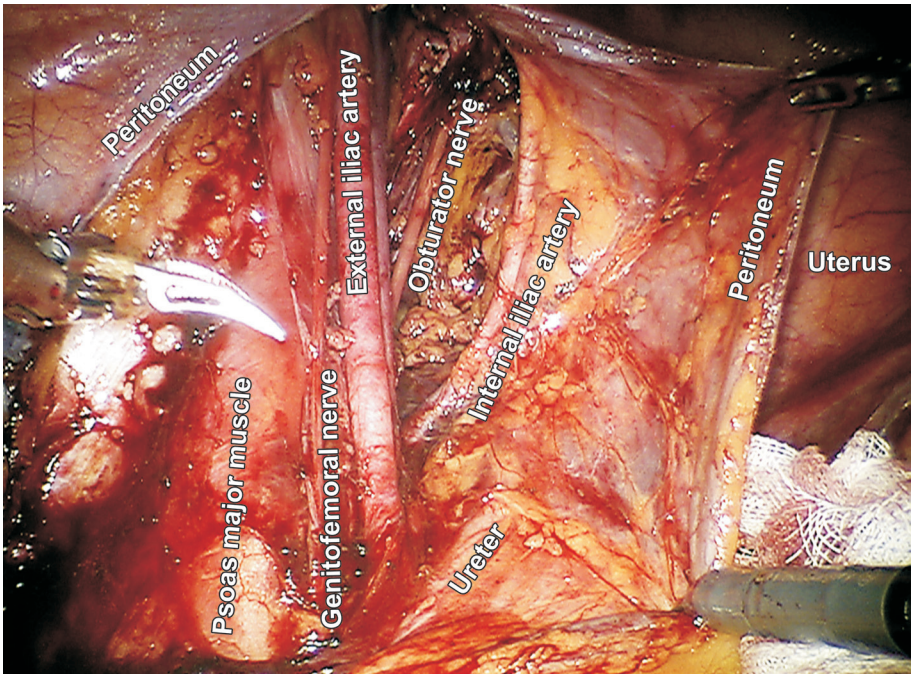

Figure 3. Intraoperative overview of the left retroperitoneal hemipelvis after a robot assisted laparoscopic pelvic lymph node dissection in a 32 year old woman with a stage IB1 poorly differentiated adenocarcinoma of the cervix. The instruments depicted are a Maryland bipolar forceps (left), monopolar curved scissors (bottom right) and a fenestrated bipolar forceps (top right).

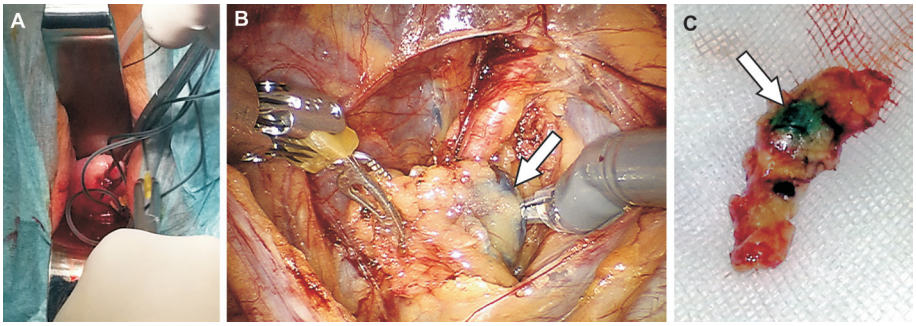

Figure 4. Exemplary sentinel lymph node procedure performed in a 32 year old women with a clinical stage IB1 poorly differentiated adenocarcinoma of the cervix. At the start of surgery – with a technique comparable to the approx. 240 MBq ^{99m}Tc-nanocolloid injection one day preoperatively – 0.5 ml patent blue dye is submucosally injected at four quadrants of the cervix around the tumor (A). Aided by a radiosensitive probe and preoperative imaging, the right sentinel lymph node (arrow) is also visually identified in the obturator fossa as a blue node (B). Following its resection and externalization the specimen (C) was found tumor-negative at histological ultrastaging. The addition of intraoperative freeze sectioning is possible depending on its clinical relevance.

Table 2. Test accuracy for diagnosing lymph node metastases in cervical cancer
Meta-analysis results from Selman et al. [71]

Modality	n	Pooled sensitivity (95%CI)	Pooled specificity (95%CI)
CT	2640	57.5% (53.5 – 61.4%)	92.3% (91.1 – 93.5%)
MRI	1206	55.5% (49.2 – 61.7%)	93.2% (91.4 – 94.0%)
PET–CT	445	74.7% (63.3 – 84.0%)	97.6% (95.4 – 98.9%)
SLN procedure	1140	91.4% (87.1 – 94.6%)	100.0% (99.6 – 100.0%)

CI: confidence interval, CT: computed tomography, MRI: magnetic resonance imaging, PET: positron emission tomography, SLN: sentinel lymph node.

Preoperative sentinel lymph node imaging

The preoperative injection with a radionuclide like Technetium-99m, as an intraoperative SLN tracer, also makes preoperative SLN imaging possible. The two imaging modalities used for this purpose are planar lymphoscintigraphy (LSG) and single photon emission computed tomography (SPECT)-CT (Figure 5). For both, an identical injection technique, radionuclide dosing and preoperative timing can be adopted.

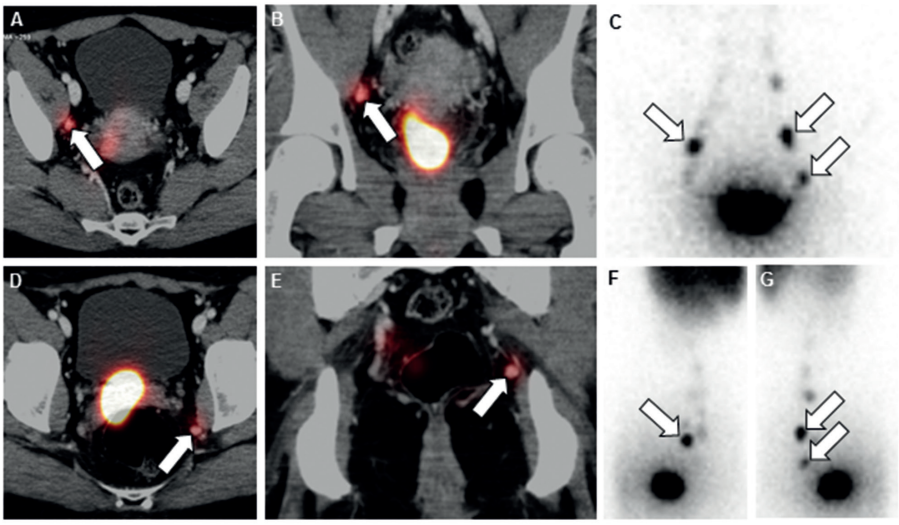

Figure 5. Axial and coronal SPECT-CT images (A,B,D,E) of a 32 year old woman with a stage IB1 poorly differentiated adenocarcinoma of the cervix. On SPECT-CT, the right sentinel node was situated in the obturator fossa (A,B) and the left in a relatively atypical location in the mesorectal fat (a region not covered by standard pelvic lymphadenectomy) (D,E). Note the activity originating from the ^{99m}Tc-nanocolloid depot in the cervix. Lymphoscintigraphy (C,F,G) of a 28 year old woman with a stage IB1 adenocarcinoma of the cervix. From anterior (C) one sentinel lymph node on the right and two on the left can be distinguished. Anatomical localization is challenging even with the aided visualization from the right (F) and left (G) lateral plane. Note the cervical ^{99m}Tc-nanocolloid depot and the higher echelon lymph nodes.

The aim of SLN imaging is to provide the surgeon with preoperative information on the location, radioactive detectability and number of SLN's per hemipelvis, which should facilitate easier intraoperative SLN localization. Unfortunately, LSG does not allow precise anatomical SLN localization which is considered an important disadvantage [79,80]. While more expensive and at an increased radiation dose, the concurrent anatomical CT reference in SPECT-CT, does allow exact SLN localization [81,82,83]. This is particularly valuable for SLN's situated in atypical locations, not covered by standard lymphadenectomy (Figure 5) [84,85]. Furthermore, it also offers all the review advantages of a cross-sectional modality. The experience with SLN imaging in a cervical cancer setting is limited, particularly for SPECT-CT, though reports are promising and further research is warranted. Several clinical questions remain, including whether it actually reduces the time in which the intraoperative SLN procedure is completed and whether a significant difference in detection ratio between LSG and SPECT-CT exists.

Aims of this thesis

This thesis focuses on the imaging modalities used after the diagnosis of cervical cancer has been made, to assist in the individualization of oncological care. This includes both traditional and experimental diagnostic strategies, which can be applied both within and outside of the framework of FIGO staging. In view of the incidence of stage I – II cervical cancer in countries with widespread access to these cross-sectional imaging modalities, we will focus the study domain on women with early stage disease.

This thesis consists of 2 parts. The first part is focused on the use of imaging – specifically chest radiography and pelvic MRI – in the initial work-up.

Chapter 2 aims to study the clinical value and efficiency of the current practice wherein chest radiography is, in adherence to guidelines, routinely used in the staging work-up of women with cervical cancer. In line with this thesis, the focus is on those women who have pre-radiograph early stage disease.

Chapters 3 and 4 will investigate - and in vivo optimize - the feasibility of ultra-high field 7.0T MRI with an endorectal monopole antenna to qualitatively improve T_2-weighted imaging of primary cervical cancer.

Chapter 5 aims to study the influence of the *b*-value combination in diffusion weighted 3.0T MRI on apparent diffusion coefficient (ADC) based detection of primary cervical cancer in early stage patients.

The second part of this thesis aims to evaluate the clinical value of preoperative SLN imaging.

Chapters 6 and 7 aim to compare ^{99m}Tc SPECT-CT to ^{99m}Tc lymphoscintigraphy SLN imaging on how they assist the intraoperative SLN procedure. Outcomes of interest will include their influence on the intra-operative SLN retrieval time, anatomical localization abilities and uni- and bilateral detection ratios.

Chapter 8 will explore the selective assessment of non-enlarged sentinel lymph nodes on MRI, through fusion with the ^{99m}Tc SPECT dataset, for diagnosing small SLN metastases in patients with early stage cervical cancer.

REFERENCES

1. Forouzanfar MH, Foreman KJ, Delossantos AM, Lozano R, Lopez AD, Murray CJ, Naghavi M. Breast and cervical cancer in 187 countries between 1980 and 2010: a systematic analysis. Lancet. 2011 Oct 22;378(9801):1461-84.
2. Ferlay J, Soerjomataram I, Ervik M, Dikshit R, Eser S, Mathers C, Rebelo M, Parkin DM, Forman D, Bray F. GLOBOCAN 2012 v1.0, Cancer Incidence and Mortality Worldwide: IARC CancerBase No. 11 [Internet]. Lyon, France: International Agency for Research on Cancer; 2013. Available from: http://globocan.iarc.fr, accessed on 2-10-15.
3. Waggoner SE, Cervical cancer. Lancet 2003; 361: 2217–25
4. Sankaranarayanan R. Overview of cervical cancer in the developing world. FIGO 26th Annual Report on the Results of Treatment in Gynecological Cancer. Int J Gynaecol Obstet. 2006 Nov;95 Suppl 1:S205-10.
5. Nederlandse Kankerregistratie, maintained by the Integraal Kankercentrum Nederland (IKNL) [Internet]. Available from: http://www.cijfersoverkanker.nl/home-27.html, accessed on 2-10-15.
6. Odicino F, Pecorelli S, Zigliani L, Creasman WT. History of the FIGO cancer staging system. Int J Gynaecol Obstet. 2008 May;101(2):205-10.
7. Hellman K, Hellström AC, Pettersson BF. Uterine cervix cancer treatment at Radiumhemmet: 90 years' experience. Time trends of age, stage, and histopathology distribution. Cancer Med. 2014 Apr; 3(2): 284–292.
8. Pecorelli S. Revised FIGO staging for carcinoma of the vulva, cervix, and endometrium. International Journal of Gynecology and Obstetrics 105 (2009) 103–104
9. Odicino F, Tisi G, Rampinelli F, Miscioscia R, Sartori E, Pecorelli S.New development of the FIGO staging system. Gynecol Oncol. 2007 Oct;107(1 Suppl 1):S8-9.
10. Wiebe E, Denny L, Thomas G. Cancer of the cervix uteri (FIGO cancer report 2012). Int J Gynaecol Obstet. 2012 Oct;119 Suppl 2:S100-9.
11. Quinn M, Benedet J, Odicino F et al. 26th annual report of the international federation of gynaecology and obstetrics on the results of treatment in gynaecological cancer. Report of 2006 (26): S43-S104.
12. Qin Y, Peng Z, Lou J, et al. Discrepancies between clinical staging and pathological findings of operable cervical carcinoma with stage IB-IIB: a retrospective analysis of 818 patients. Aust NZJ Obstet Gynaecol. 2009 49(5): 542-544.
13. LaPolla JP, Schlaerth JB, Gaddis O, Morrow CP. The influence of surgical staging on the evaluation and treatment of patients with cervical carcinoma. Gynecol Oncol. 1986 Jun;24(2):194-206.
14. Lagasse LD, Creasman WT, Shingleton HM, Ford JH, Blessing JA. Results and

complications of operative staging in cervical cancer: experience of the Gynecologic Oncology Group. Gynecol Oncol 1980 9:90–98

15. Landoni F, Maneo A, Colombo A, Placa F, Milani R, Perego P, Favini G, Ferri L, Mangioni C. Randomised study of radical surgery versus radiotherapy for stage Ib-IIa cervical cancer. Lancet. 1997 Aug 23;350(9077):535-40.
16. Amendola MA, Hricak H, Mitchell DG, Snyder B, Chi DS, Long HJ 3rd, Fiorica JV, Gatsonis C. Utilization of diagnostic studies in the pretreatment evaluation of invasive cervical cancer in the United States: results of intergroup protocol ACRIN 6651/GOG 183. J Clin Oncol. 2005 Oct 20;23(30):7454-9.
17. Tomita N, Toita T, Kodaira T, Shinoda A, Uno T, Numasaki H, Teshima T, Mitsumori M. Changing trend in the patterns of pretreatment diagnostic assessment for patients with cervical cancer in Japan. Gynecol Oncol. 2011 Dec;123(3):577-80.
18. Toita T, Kodaira T, Uno T, Shinoda A, Akino Y, Mitsumori M, Teshima T. Patterns of pretreatment diagnostic assessment and staging for patients with cervical cancer (1999-2001): patterns of care study in Japan. Jpn J Clin Oncol. 2008 Jan;38(1):26-30.
19. Russell AH, Shingleton HM, Jones WB, Fremgen A, Winchester DP, Clive R, Chmiel JS. Diagnostic assessments in patients with invasive cancer of the cervix: a national patterns of care study of the American College of Surgeons. Gynecol Oncol. 1996 Nov;63(2):159-65.
20. World Health Organization. Comprehensive cervical cancer control : a guide to essential practice. Switzerland (2006). ISBN978 9241547000.
21. Colombo N, Carinelli S, Colombo A, Marini C, Rollo D, Sessa C; ESMO Guidelines Working Group. Cervical cancer: ESMO Clinical Practice Guidelines for diagnosis, treatment and follow-up. Ann Oncol. 2012 Oct;23 Suppl 7:vii27-32.
22. NCCN Clinical practice guidelline in Oncology. Cervical cancer. Version 3.2013. Retrieved from www.nccn.org on 20th jan 2014.
23. Kesic V, Cibula D, Kimmig R, Lopes A, Marth C, Reed N, Rodolakis A, Vaitkiene D, Verheijen R, Zola P (ESGO). Algorithms for management of cervical cancer. Retrieved from www.esgo.org/explore/guidelines on 21st feb 2016.
24. Mitchell DG, Snyder B, Coakley F, Reinhold C, Thomas G, Amendola M, Schwartz LH, Woodward P, Pannu H, Hricak H.Early invasive cervical cancer: tumor delineation by magnetic resonance imaging, computed tomography, and clinical examination, verified by pathologic results, in the ACRIN 6651/GOG 183 Intergroup Study. J Clin Oncol. 2006 Dec 20;24(36):5687-94.
25. Hricak H, Gatsonis C, Coakley FV, Snyder B, Reinhold C, Schwartz LH, Woodward PJ, Pannu HK, Amendola M, Mitchell DG. Early invasive cervical cancer: CT and MR imaging in preoperative evaluation - ACRIN/GOG comparative study of diagnostic performance

and interobserver variability. Radiology. 2007 Nov;245(2):491-8.
26. Bipat S, Glas AS, van der Velden J, Zwinderman AH, Bossuyt PM, Stoker J. Computed tomography and magnetic resonance imaging in staging of uterine cervical carcinoma: a systematic review. Gynecol Oncol 2003; 91(1): 59-66.
27. Siegel CL, Andreotti RF, Cardenes HR, Brown DL, Gaffney DK, Horowitz NS, Javitt MC, Lee SI, Mitchell DG, Moore DH, Rao GG, Royal HD, Small W Jr, Varia MA, Yashar CM; American College of Radiology. ACR Appropriateness Criteria® pretreatment planning of invasive cancer of the cervix. J Am Coll Radiol. 2012 Jun;9(6):395-402.
28. Werkgroep Oncologische Gynaecologie (WOG), Integraal Kankercentrum Nederland (IKNL). Dutch national guideline cervical cancer, version: 3.0, approved 22-03-2012. Available from: http://oncoline.nl/cervixcarcinoom. Retrieved 2-10-2015.
29. Sala E, Rockall AG, Freeman SJ, Mitchell DG, Reinhold C. The added role of MR imaging in treatment stratification of patients with gynecologic malignancies: what the radiologist needs to know. Radiology. 2013 Mar;266(3):717-40.
30. Balleyguier C, Sala E, Da Cunha T, Bergman A, Brkljacic B, Danza F, Forstner R, Hamm B, Kubik-Huch R, Lopez C, Manfredi R, McHugo J, Oleaga L, Togashi K, Kinkel K.Staging of uterine cervical cancer with MRI: guidelines of the European Society of Urogenital Radiology. Eur Radiol. 2011 May;21(5):1102-10.
31. Sahdev A, Sohaib SA, Wenaden AE, Shepherd JH, Reznek RH. The performance of magnetic resonance imaging in early cervical carcinoma: a long-term experience. Int J Gynecol Cancer 2007;17(3):629–636.
32. Subak LL, Hricak H, Powell CB, Azizi L, Stern JL. Cervical carcinoma: computed tomography and magnetic resonance imaging for preoperative staging. Obstet Gynecol 1995;86(1):43–50.
33. Thomeer MG, Gerestein C, Spronk S, van Doorn HC, van der Ham E, Hunink MG. Clinical examination versus magnetic resonance imaging in the pretreatment staging of cervical carcinoma: systematic review and meta-analysis. Eur Radiol. 2013 Jul;23(7):2005-18.
34. Kinkel K. Pitfalls in staging uterine neoplasm with imaging: a review. Abdom Imaging. 2006 Mar-Apr;31(2):164-73.
35. Chung HH, Kang KW, Cho JY, et al. Role of magnetic resonance imaging and positron emission tomography/computed tomography in preoperative lymph node detection of uterine cervical cancer. Am J Obstet Gynecol. 2010;203:156.e1-5.
36. Hori M, Kim T, Murakami T, et al. Uterine cervical carcinoma: preoperative staging with 3.0-T MR imaging--comparison with 1.5-T MR imaging. Radiology. 2009;251:96-104.
37. Testa AC, Ludovisi M, Manfredi R, et al. Transvaginal ultrasonography and magnetic resonance imaging for assessment of presence, size and extent of invasive cervical

cancer. Ultrasound Obstet Gynecol. 2009;34:335-344.
38. Sheu M, Chang C, Wang J, Yen M. MR staging of clinical stage I and IIa cervical carcinoma: a reappraisal of efficacy and pitfalls. Eur J Radiol. 2001;38:225-231.
39. Choi HJ, Roh JW, Seo SS, et al. Comparison of the accuracy of magnetic resonance imaging and positron emission tomography/computed tomography in the presurgical detection of lymph node metastases in patients with uterine cervical carcinoma: a prospective study. Cancer. 2006;106:914-922.
40. Lai G, Rockall AG. Lymph node imaging in gynecologic malignancy. Semin Ultrasound CT MR. 2010;31:363-376.
41. Chou HH, Chang TC, Yen TC, Ng KK, Hsueh S, Ma SY, Chang CJ, Huang HJ, Chao A, Wu TI, Jung SM, Wu YC, Lin CT, Huang KG, Lai CH.Low value of [18F]-fluoro-2-deoxy-D-glucose positron emission tomography in primary staging of early-stage cervical cancer before radical hysterectomy. J Clin Oncol. 2006 Jan 1;24(1):123-8.
42. Sironi S, Buda A, Picchio M, Perego P, Moreni R, Pellegrino A, Colombo M, Mangioni C, Messa C, Fazio F.Lymph node metastasis in patients with clinical early-stage cervical cancer: detection with integrated FDG PET/CT. Radiology. 2006 Jan;238(1):272-9.
43. Reinhardt MJ, Ehritt-Braun C, Vogelgesang D, Ihling C, Högerle S, Mix M, Moser E, Krause TM.Metastatic lymph nodes in patients with cervical cancer: detection with MR imaging and FDG PET. Radiology. 2001 Mar;218(3):776-82.
44. Cabanas RM. An approach for the treatment of penile carcinoma. Cancer. 1977 Feb;39(2):456-66.
45. Veronesi U, Paganelli G, Viale G, Luini A, Zurrida S, Galimberti V, Intra M, Veronesi P, Robertson C, Maisonneuve P, Renne G, De Cicco C, De Lucia F, Gennari R. A randomized comparison of sentinel-node biopsy with routine axillary dissection in breast cancer. N Engl J Med. 2003 Aug 7;349(6):546-53.
46. Galimberti V, Cole BF, Zurrida S, Viale G, Luini A, Veronesi P, Baratella P, Chifu C, Sargenti M, Intra M, Gentilini O, Mastropasqua MG, Mazzarol G, Massarut S, Garbay JR, Zgajnar J, Galatius H, Recalcati A, Littlejohn D, Bamert M, Colleoni M, Price KN, Regan MM, Goldhirsch A, Coates AS, Gelber RD, Veronesi U. Axillary dissection versus no axillary dissection in patients with sentinel-node micrometastases (IBCSG 23-01): a phase 3 randomised controlled trial. Lancet Oncol. 2013 Apr;14(4):297-305.
47. Krag DN, Anderson SJ, Julian TB, Brown AM, Harlow SP, Costantino JP, Ashikaga T, Weaver DL, Mamounas EP, Jalovec LM, Frazier TG, Noyes RD, Robidoux A, Scarth HM, Wolmark N. Sentinel-lymph-node resection compared with conventional axillary-lymph-node dissection in clinically node-negative patients with breast cancer: overall survival findings from the NSABP B-32 randomised phase 3 trial. Lancet Oncol. 2010 Oct;11(10):927-33.

48. Oonk MH, van Hemel BM, Hollema H, de Hullu JA, Ansink AC, Vergote I, Verheijen RH, Maggioni A, Gaarenstroom KN, Baldwin PJ, van Dorst EB, van der Velden J, Hermans RH, van der Putten HW, Drouin P, Runnebaum IB, Sluiter WJ, van der Zee AG. Size of sentinel-node metastasis and chances of non-sentinel-node involvement and survival in early stage vulvar cancer: results from GROINSS-V, a multicentre observational study. Lancet Oncol. 2010 Jul;11(7):646-52.
49. Van der Zee AG, Oonk MH, De Hullu JA, Ansink AC, Vergote I, Verheijen RH, Maggioni A, Gaarenstroom KN, Baldwin PJ, Van Dorst EB, Van der Velden J, Hermans RH, van der Putten H, Drouin P, Schneider A, Sluiter WJ. Sentinel node dissection is safe in the treatment of early-stage vulvar cancer. J Clin Oncol. 2008 Feb 20;26(6):884-9.
50. Levenback CF, Ali S, Coleman RL, Gold MA, Fowler JM, Judson PL, Bell MC, De Geest K, Spirtos NM, Potkul RK, Leitao MM Jr, Bakkum-Gamez JN, Rossi EC, Lentz SS, Burke JJ 2nd, Van Le L, Trimble CL. Lymphatic mapping and sentinel lymph node biopsy in women with squamous cell carcinoma of the vulva: a gynecologic oncology group study. J Clin Oncol. 2012 Nov 1;30(31):3786-91.
51. Sentinel lymph node biopsy. National Cancer Institute website. http://www.cancer.gov/about-cancer/diagnosis-staging/staging/sentinel-node-biopsy-fact-sheet#q2. Updated: August 11, 2011. Retrieved: September 22, 2015.
52. Eiriksson LR, Covens A.Sentinel lymph node mapping in cervical cancer: the future? BJOG. 2012 Jan;119(2):129-33.
53. Cibula D, Abu-Rustum NR, Dusek L, Slama J, Zikán M, Zaal A, Sevcik L, Kenter G, Querleu D, Jach R, Bats AS, Dyduch G, Graf P, Klat J, Meijer CJ, Mery E, Verheijen R, Zweemer RP. Bilateral ultrastaging of sentinel lymph node in cervical cancer: Lowering the false-negative rate and improving the detection of micrometastasis. Gynecol Oncol. 2012 Dec;127(3):462-6.
54. Lécuru F, Mathevet P, Querleu D, Leblanc E, Morice P, Daraï E, Marret H, Magaud L, Gillaizeau F, Chatellier G, Dargent D. Bilateral negative sentinel nodes accurately predict absence of lymph node metastasis in early cervical cancer: results of the SENTICOL study. J Clin Oncol. 2011 May 1;29(13):1686-91.
55. Querleu D, Leblanc E, Cartron G, Narducci F, Ferron G, Martel P. Audit of preoperative and early complications of laparoscopic lymph node dissection in 1000 gynecologic cancer patients. Am J Obstet Gynecol. 2006 Nov;195(5):1287-92.
56. Köhler C, Klemm P, Schau A, Possover M, Krause N, Tozzi R, Schneider A. Introduction of transperitoneal lymphadenectomy in a gynecologic oncology center: analysis of 650 laparoscopic pelvic and/or paraaortic transperitoneal lymphadenectomies. Gynecol Oncol. 2004 Oct;95(1):52-61.
57. Bergmark K, Avall-Lundqvist E, Dickman PW, Henningsohn L, Steineck G. Lymphedema

and bladder-emptying difficulties after radical hysterectomy for early cervical cancer and among population controls. Int J Gynecol Cancer. 2006 May-Jun;16(3):1130-9.

58. Zikan M, Fischerova D, Pinkavova I, Slama J, Weinberger V, Dusek L, Cibula D. A prospective study examining the incidence of asymptomatic and symptomatic lymphoceles following lymphadenectomy in patients with gynecological cancer. Gynecol Oncol. 2015 May;137(2):291-8.
59. Comparison of Pelvic Lymphadenectomy Versus Isolated Sentinel Lymph Node Biopsy Procedure for Early Stages of Cervical Cancers : a Multicenter Study With Evaluation of Medico-economic Impacts (SENTICOL2). From: https://clinicaltrials.gov/. Under Identifier: NCT01639820. Last updated: August 21, 2013. Retreived 29 September 2015.
60. Smith B, Backes F. The role of sentinel lymph nodes in endometrial and cervical cancer. J Surg Oncol. Epub ahead of print; 2015 sep 9.
61. Wu Y, Li Z, Wu H, Yu J. Sentinel lymph node biopsy in cervical cancer: A meta-analysis. Mol Clin Oncol. 2013 Nov;1(6):1025-1030.
62. van de Lande J, Torrenga B, Raijmakers PG, Hoekstra OS, van Baal MW, Brölmann HA, Verheijen RH. Sentinel lymph node detection in early stage uterine cervix carcinoma: a systematic review. Gynecol Oncol. 2007 Sep;106(3):604-13.
63. Tax C, Rovers MM, de Graaf C, Zusterzeel PL, Bekkers RL. The sentinel node procedure in early stage cervical cancer, taking the next step; a diagnostic review. Gynecol Oncol. 2015 Sep 28. [Epub ahead of print]
64. Bats AS, Mathevet P, Lécuru F. Response to Rossi et al. (Gynecol oncol. 2012; 124(1):78-82). Gynecol Oncol. 2012 Jun;125(3):764; author reply 765.
65. Rossi EC, Ivanova A, Boggess JF. Robotically assisted fluorescence-guided lymph node mapping with ICG for gynecologic malignancies: a feasibility study. Gynecol Oncol. 2012 Jan;124(1):78-82.
66. Jewell EL, Huang JJ, Abu-Rustum NR, Gardner GJ, Brown CL, Sonoda Y, Barakat RR, Levine DA, Leitao MM.Detection of sentinel lymph nodes in minimally invasive surgery using indocyanine green and near-infrared fluorescence imaging for uterine and cervical malignancies. Gynecol Oncol. 2014 May;133(2):274-7.
67. Occelli B, Narducci F, Lanvin D, Querleu D, Coste E, Castelain B, Gibon D, LeBlanc E. De novo adhesions with extraperitoneal endosurgical para-aortic lymphadenectomy versus transperitoneal laparoscopic para-aortic lymphadenectomy: a randomized experimental study. Am J Obstet Gynecol. 2000 Sep;183(3):529-33.
68. Fine BA, Hempling RE, Piver MS, Baker TR, McAuley M, Driscoll D. Severe radiation morbidity in carcinoma of the cervix: impact of pretherapy surgical staging and previous surgery. Int J Radiat Oncol Biol Phys. 1995 Feb 15;31(4):717-23.
69. Euscher ED, Malpica A, Atkinson EN, Levenback CF, Frumovitz M, Deavers MT

Ultrastaging improves detection of metastases in sentinel lymph nodes of uterine cervix squamous cell carcinoma. Am J Surg Pathol. 2008 Sep;32(9):1336-43.

70. Zaal A, Zweemer RP, Zikán M, Dusek L, Querleu D, Lécuru F, Bats AS, Jach R, Sevcik L, Graf P, Klát J, Dyduch G, von Mensdorff-Pouilly S, Kenter GG, Verheijen RH, Cibula D. Pelvic lymphadenectomy improves survival in patients with cervical cancer with low-volume disease in the sentinel node: a retrospective multicenter cohort study. Int J Gynecol Cancer. 2014 Feb;24(2):303-11.
71. Selman TJ, Mann C, Zamora J, Appleyard TL, Khan K. Diagnostic accuracy of tests for lymph node status in primary cervical cancer: a systematic review and meta-analysis. CMAJ. 2008;178:855-862.
72. Altgassen C, Hertel H, Brandstädt A, Köhler C, Dürst M, Schneider A; AGO Study Group. Multicenter validation study of the sentinel lymph node concept in cervical cancer: AGO Study Group. J Clin Oncol. 2008 Jun 20;26(18):2943-51.
73. Gien LT, Covens A. Quality control in sentinel lymph node biopsy in cervical cancer. J Clin Oncol. 2008 Jun 20;26(18):2930-1.
74. Oonk MH, van de Nieuwenhof HP, de Hullu JA, van der Zee AG. The role of sentinel node biopsy in gynecological cancer: a review. Curr Opin Oncol. 2009 Sep;21(5):425-32.
75. Cibula D, Abu-Rustum NR, Dusek L, Zikán M, Zaal A, Sevcik L, Kenter GG, Querleu D, Jach R, Bats AS, Dyduch G, Graf P, Klat J, Lacheta J, Meijer CJ, Mery E, Verheijen R, Zweemer RP. Prognostic significance of low volume sentinel lymph node disease in early-stage cervical cancer. Gynecol Oncol. 2012 Mar;124(3):496-501.
76. Vicus D, Covens A. Role of Sentinel Lymph Node Biopsy in Cervical Cancer: Pro. 2010 20(11) Supplement 2: S34-S36
77. Bats AS, Mathevet P, Buenerd A, Orliaguet I, Mery E, Zerdoud S, Le Frère-Belda MA, Froissart M, Querleu D, Martinez A, Leblanc E, Morice P, Daraï E, Marret H, Gillaizeau F, Lécuru F. The sentinel node technique detects unexpected drainage pathways and allows nodal ultrastaging in early cervical cancer: insights from the multicenter prospective SENTICOL study. Ann Surg Oncol. 2013 Feb;20(2):413-22.
78. Gortzak-Uzan L, Jimenez W, Nofech-Mozes S, Ismiil N, Khalifa MA, Dubé V, Rosen B, Murphy J, Laframboise S, Covens A. Sentinel lymph node biopsy vs. pelvic lymphadenectomy in early stage cervical cancer: is it time to change the gold standard? Gynecol Oncol. 2010 Jan;116(1):28-32.
79. Frumovitz M, Coleman RL, Gayed IW, Ramirez PT, Wolf JK, Gershenson DM, Levenback CF. Usefulness of preoperative lymphoscintigraphy in patients who undergo radical hysterectomy and pelvic lymphadenectomy for cervical cancer. Am J Obstet Gynecol. 2006 Apr;194(4):1186-93;
80. Vieira SC, Sousa RB, Tavares MB, Silva JB, Abreu BA, Santos LG, da Silva BB, Zeferino LC.

Preoperative pelvic lymphoscintigraphy is of limited usefulness for sentinel lymph node detection in cervical cancer. Eur J Obstet Gynecol Reprod Biol. 2009 Jul;145(1):96-9.

81. Klapdor R, Mücke J, Schneider M, Länger F, Gratz KF, Hillemanns P, Hertel H. Value and advantages of preoperative sentinel lymph node imaging with SPECT/CT in cervical cancer. Int J Gynecol Cancer. 2014 Feb;24(2):295-302.
82. Pandit-Taskar N, Gemignani ML, Lyall A, Larson SM, Barakat RR, Abu Rustum NR.Single photon emission computed tomography SPECT-CT improves sentinel node detection and localization in cervical and uterine malignancy. Gynecol Oncol. 2010 Apr;117(1):59-64.
83. Buda A, Elisei F, Arosio M, Dolci C, Signorelli M, Perego P, Giuliani D, Recalcati D, Cattoretti G, Milani R, Messa C. Integration of hybrid single-photon emission computed tomography/computed tomography in the preoperative assessment of sentinel node in patients with cervical and endometrial cancer: our experience and literature review. Int J Gynecol Cancer. 2012 Jun;22(5):830-5.
84. Bats AS, Frati A, Mathevet P, Orliaguet I, Querleu D, Zerdoud S, Leblanc E, Gauthier H, Uzan C, Deandreis D, Darai E, Kerrou K, Marret H, Lenain E, Froissart M, Lecuru F. Contribution of lymphoscintigraphy to intraoperative sentinel lymph node detection in early cervical cancer: Analysis of the prospective multicenter SENTICOL cohort. Gynecol Oncol. 2015 May;137(2):264-9
85. Bats AS, Frati A, Froissart M, Orliaguet I, Querleu D, Zerdoud S, Leblanc E, Gauthier H, Uzan C, Deandreis D, Darai E, Kerrou K, Marret H, Lenain E, Mathevet P, Lecuru F. Feasibility and performance of lymphoscintigraphy in sentinel lymph node biopsy for early cervical cancer: results of the prospective multicenter SENTICOL study. Ann Nucl Med. 2015 Jan;29(1):63-70.
86. FIGO Committee on Gynecologic Oncology. FIGO staging for carcinoma of the vulva, cervix, and corpus uteri. Int J Gynaecol Obstet. 2014 May;125(2):97-8.

PART 1:

Imaging for the primary evaluation of cervical cancer

Chapter 2

No value for routine chest radiography in the work-up of early stage cervical cancer patients

Jacob P. Hoogendam
Ronald P. Zweemer
Helena M. Verkooijen
Pim A. de Jong
Maurice A.A.J. van den Bosch
René H.M. Verheijen
Wouter B. Veldhuis

PLoS ONE. 2015. 10(7): e0131899.

ABSTRACT

Aim: Evidence supporting the recommendation to include chest radiography in the work-up of all cervical cancer patients is limited. We investigated the diagnostic value of routine chest radiography in cervical cancer staging.

Methods: All consecutive cervical cancer patients who presented at our tertiary referral center in the Netherlands (January 2006 – September 2013), and for whom ≥6 months follow-up was available, were included. As part of the staging procedure, patients underwent a routine two-directional digital chest radiograph. Findings were compared to a composite reference standard consisting of all imaging studies and histology obtained during the 6 months following radiography.

Results: Of the 402 women who presented with cervical cancer, 288 (71.6%) underwent chest radiography and had ≥6 months follow-up. Early clinical stage (I/II) cervical cancer was present in 244/288 (84.7%) women, while 44 (15.3%) presented with advanced disease (stage III/IV). The chest radiograph of 1 woman – with advanced pre-radiograph stage (IVA) disease – showed findings consistent with pulmonary metastases. Radiographs of 7 other women – 4 early, 3 advanced stage disease – were suspicious for pulmonary metastases which was confirmed by additional imaging in only 1 woman (with pre-radiograph advanced stage (IIIB) disease) and excluded in 6 cases, including all women with early stage disease. In none of the 288 women were thoracic skeletal metastases identified on imaging or during 6 months follow up. Radiography was unremarkable in 76.4% of the study population, and showed findings unrelated to the cervical carcinoma in 21.2%.

Conclusion: Routine chest radiography was of no value for any of the early stage cervical cancer patients presenting at our tertiary center over a period of 7.7 years.

Keywords: cervical cancer, staging, routine chest radiography, pulmonary metastases.

INTRODUCTION

Cervical cancer is the third most common malignancy in women worldwide, with the highest incidence in developing countries [1,2]. The staging system devised by the International Federation for Gynecology and Obstetrics (FIGO) is centered around the gynecologic examination, aided by a limited number of universally available diagnostic tests (including chest radiography) [3,4,5]. Over the past decades, this clinically oriented approach has allowed for globally uniform, inexpensive cervical cancer staging.

Numerous (inter)national cervical cancer guidelines still adhere to these staging principles, and all include routine chest radiography as the primary diagnostic instrument for detection of thoracic metastatic disease [6,7,8,9,10,11,12]. For example, the US guideline advises its use in all patients except for those with microscopic stage IA1-2, wherein it is considered an optional test [7]. However, limited original research exists to support the routine use of chest radiography in the staging work-up of cervical cancer [12]. Indeed, guidelines [6,7,8,9,10,11] are frequently unable to cite specific references, beyond the FIGO expert opinion based recommendation which was the first to endorse radiography use. However, clear disadvantages such as the radiation exposure, patient strain, healthcare costs and the consequences of false-positive findings, justify a critical assessment of this practice.

The primary aim was to investigate the diagnostic yield of routine chest radiography as part of staging of cervical cancer patients in a tertiary referral center in the Netherlands. Specifically, we evaluated the efficiency of the current practice and whether the addition of a chest radiograph results in upstaging to FIGO IVB (i.e. tumor extension beyond the true pelvis). In addition, we will report the rate of coincidental radiographic findings unrelated to cervical carcinoma.

METHODS AND MATERIALS

Design

In this cross-sectional, diagnostic study we included all consecutive patients who presented to our center between January 1st 2006 and September 1st 2013. Inclusion criteria were: 1) histopathological proof of a malignancy primary to the cervix uteri, and 2) staging was performed at our institution. Patients were excluded when they were lost to follow up within the first 6 months, and when chest radiography was absent or performed with a mobile x-ray unit (i.e. bedside examination). No exclusion based on medical history, including prior malignancies, was performed to prevent selecting an abnormally healthy study population.

All procedures in the presented study followed standard clinical care. Authors RZ, RV and WV were the physicians treating the included patients and obtained verbal informed consent for the diagnostic workup (incl. chest radiography) and subsequently documented this in the patient's medical file. Author JH anonymized the dataset prior to analysis. Patients were not informed that their results would be anonymously used in this analysis. This practice adheres to all applicable Dutch law, specifically the Medical Research Involving Human Subjects Act (WMO). Likewise, institutional review board approval is implicit under Dutch law because only anonymized and already existing (i.e. retrospective) data were used.

Staging practice

In the Netherlands, all cervical cancer cases are referred to a specialized – tertiary referral – center. At our institution, the standardized cervical cancer staging protocol adheres to national guidelines and consists of a detailed history, full physical and gynecological examination, and chest radiography [10]. In addition, abdominal ultrasound (before 2008) or contrast enhanced pelvic magnetic resonance imaging (from 2008 onwards) are routinely performed to detect ureteric obstruction. An examination under anesthesia is performed when outpatient based (recto)vaginal examination is inadequate for clinical staging.

Histopathological proof of cervical cancer is required by protocol prior to the initiation of therapy. All histological material, including the original samples provided by referring hospitals, is reviewed by an institutional pathologist specialized in gynecological oncology. The work-up findings are presented in a multidisciplinary meeting to reach consensus on the diagnosis, stage and treatment plan.

Chest radiography

X-ray radiography of the chest was performed on a digital flat panel detector radiography system (DigitalDiagnost, Philips Healthcare, Best, the Netherlands). The x-ray tube potential was maintained at 125 kV while the exposure intensity was automatically optimized per patient (typically: 1 – 3 mAs). Radiologic technologists followed an institutional protocol which prescribed the methodology for complete depiction of the thoracic cage in the posterior-anterior and lateral plane. During the examination, patients assumed an upright standing position with elevated arms and full inspiration. The upper body was unclothed, including removal of jewelry, and any draping long hair was lifted. Nipple marking was not routinely performed.

Chest radiographs were reviewed by board certified radiologists who had access to all prior radiological examinations available in the Picture Archiving and Communication

System (PACS, Sectra AB, Linköping, Sweden). Clinical information indicating the cervical cancer staging purpose was available. When present, the frequency and location of suspected pulmonary or skeletal metastases were registered for each case, as was the incidence of diagnostic findings unrelated to cervical cancer. Additional diagnostic tests performed to confirm the radiographic suspicion of cervical cancer metastases were also scored. Additional tests included computed tomography (CT) of the chest, positron emission tomography (PET)-CT, repeat chest radiography, referral to a pulmonologist and/or targeted histologic sampling. Adverse events hereof were recorded in adherence to the 'Common Terminology Criteria for Adverse Events' version 4.03 guideline created by the department of health of the United States (US) government [13].
The reference standard was defined as detection of pulmonary or thoracic skeletal metastasis within 6 months following the staging chest radiograph determined by a composite of chest CT, PET-CT, repeat chest radiography, histopathological (including autopsy) or cytological sampling when available.

Statistical analysis

Statistical calculations were performed with the 'Statistical Package for the Social Sciences' version 20.0.0 (SPSS, International Business Machines, Armonk, United States of America). Summary statistics and (non-)parametric tests were chosen based on the data type and its distribution. Statistical significance was preset at an alpha of <0.05.

RESULTS

Study population

From a total 402 eligible patients, 114 were excluded based on an absent staging chest radiograph (n=97; 24.1%) or <6 months follow-up (n=17; 4.2%) (Figure 1). None of these excluded lost-to-follow-up cases had radiographic findings suspicious for pulmonary or thoracic skeletal metastases. In the group with no radiograph, 26/97 women had already undergone chest CT (n=23) or PET-CT (n=3) in the referring hospital and chest radiography was omitted during formal staging at our institution. This group included a total 5 IVB cases, in all of whom stage IVB cervical cancer was already diagnosed prior to imaging (i.e. no upstaging occurred). A second reason for omitting a chest radiograph – in 24/97 patients – was microscopic, stage IA1-2 cervical cancer. At 63.2%, omission of radiography was much more common in stage IA1-2 patients than in other FIGO stages (p<0.001). The median percentage of cases with no chest imaging in stage IB1 – IVB was 11.7% (range: 0.0 – 16.5%), with no statistically significant differences among these stages (Figure 2).

Thus, the study population comprised 288 patients of which 171 (59.4%), 73 (25.3%), 29 (10.1%) and 15 (5.2%) women had stage I, II, III or IV respectively (Table 1). A total of 268 patients (93.1%) were treated with curative intent by either surgery (n=96; 35.8%), (chemo) radiotherapy (n=110; 41.0%) or a combination of both (n=62; 23.1%). Of those, 'no evidence of disease' was achieved in 256 (95.5%), of which 35 women (13.7%) had a recurrence after a median of 14 months follow-up (range: 7 – 50 months). Hereof, 7 women presented with a recurrence which included pulmonary metastases (median 14 months, range 10 – 24 months follow-up) while all had unremarkable chest radiographies at workup. The 5-year overall and disease specific survival rates (n=288) were 71.9% and 79.2%, respectively.

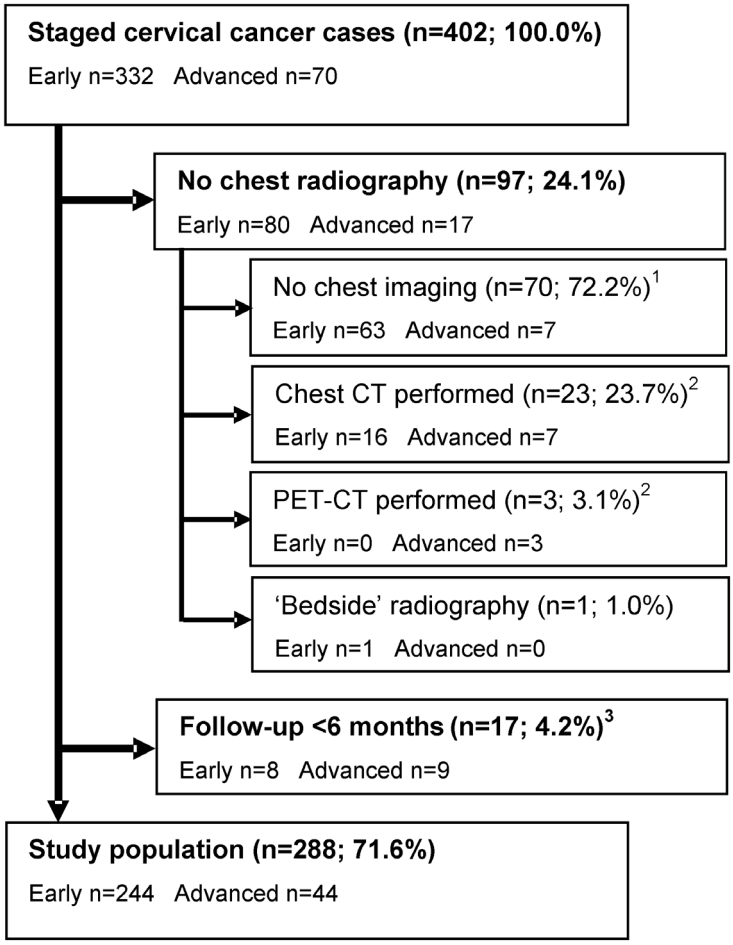

Figure 1. Flowchart displaying the formation of the study population.

[1] None of these 70 cases had findings during the available follow-up period that would have induced a stage change to IVB. Follow-up of at least 6 months was available in 58/70 (82.9%) cases, including 6 of the 7 advanced cases (85.7%).

[2] In 20/23 chest CT (87.0%) and all PET-CT cases, imaging was already performed by the referring center. Consequently, chest radiography was not repeated upon formal staging at our institution. In 1 subject (3.8%) pulmonary metastases were found, though in none of the in total 5 FIGO IVB cases (19.2%) upstaging was performed based on chest imaging.

[3] None of these cases had radiographic findings suspicious for pulmonary or thoracic skeletal metastases. Two patients did have stage IVB cervical cancer, but based on supraclavicular lymph nodal and intrahepatic metastases, not on pulmonary or skeletal metastases that could have been detected on a chest radiograph.

CT: Computed tomography; PET: Positron Emission Tomography;

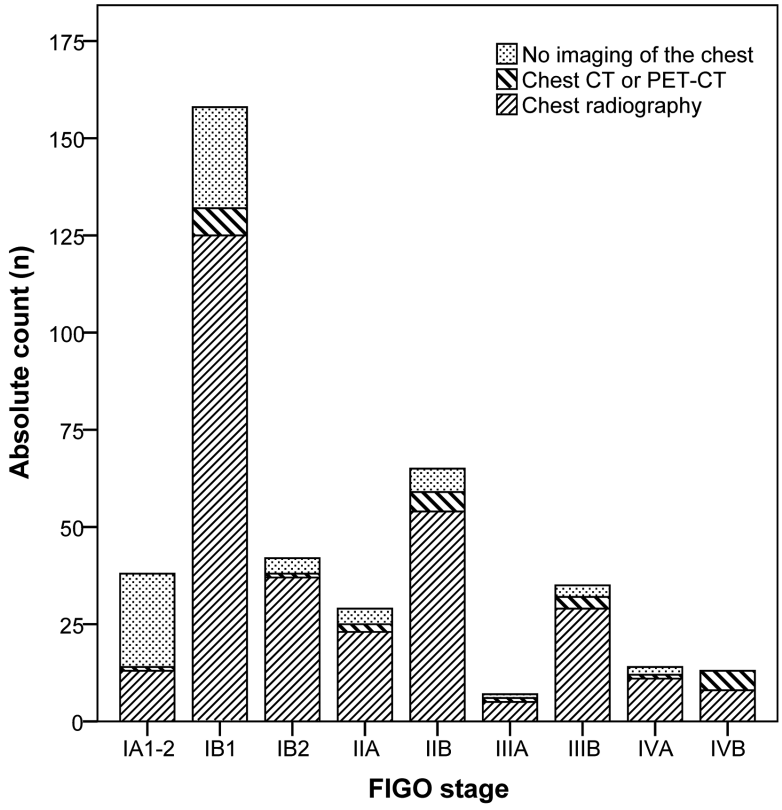

Figure 2. Stacked bar graph of the primary thoracic imaging examinations performed during the staging of all eligible patients (n=402).
CT: Computed Tomography; PET: Positron Emission Tomography; FIGO: International Federation for Gynecology and Obstetrics;

Table 1. Baseline characteristics of the study population (n=288)

Median age at presentation (range)		46.4 (24.3 – 89.8) years	
		n	**percentage**
Pulmonary history	Asthma	11	3.8%
	COPD	9	3.1%
	Tuberculosis	1	0.3%
	Other	1	0.3%
Smoking status	Current	94	32.6%
	Stopped	52	18.1%
	Never smoked	134	46.5%
	Unknown	8	2.8%
History of a prior malignancy[1]		10	3.5%
FIGO stage cervical cancer	IA1-2	12	4.2%
	IB1-2	159	55.2%
	IIA1-2	22	7.6%
	IIB1-2	51	17.7%
	IIIA	4	1.4%
	IIIB	25	8.7%
	IVA	9	3.1%
	IVB	6	2.1%
Tumor histology	Squamous cell carcinoma	219	76.0%
	Adenocarcinoma	58	20.1%
	Adenosquamous cell carcinoma	7	2.4%
	Other	4	1.4%
Tumor differentiation grade	I	27	9.4%
	II	163	56.6%
	III	76	26.4%
	Undefined	22	7.6%
Lymph-vascular space invasion		95	33.3%

[1] Excluding all types of skin cancer except melanoma.
COPD: chronic obstructive pulmonary disease, FIGO: International Federation for Gynecology and Obstetrics.

Chest radiography

Chest radiography was unremarkable in 220/288 women (76.4%). In one woman (0.3%) radiography showed findings consistent with pulmonary metastases. The radiographs of 7 (2.4%, 95% confidence interval (CI): 1.1 – 5.2%) other women – 4 early, 3 advanced stage disease – were suspicious for pulmonary metastases. In those 7 cases, 4 chest CT's, 2 PET-CT's and 2 repeat chest radiography exams were performed, confirming pulmonary metastases in only 1 case. The remaining 6 cases, including all women with early stage disease, were false-positives (2.1%, 95%CI: 0.8 – 4.7%) with imaging demonstrating only non-specific benign pulmonary nodules. Two of these women were active smokers and 4 never smoked. Not a single patient was referred for further examination by a pulmonologist. At six month's follow-up no false-negatives had occurred.

Of the 244 women with pre-radiograph stage I/II disease none showed evidence of pulmonary metastases at initial radiography or during 6 months follow up. Two women with already advanced pre-radiograph stage IIIB and IVA disease were upstaged to stage IVB due to pulmonary metastases. In both, the management plan changed to palliative care. This corresponds to a 4.5% (95%CI: 0.8 – 16.7%) prevalence of pulmonary metastases in women with pre-radiograph stage III/IV cervical cancer (Table 2).

No thoracic skeletal metastases were identified on the staging chest radiography or during the 6 months follow up.

In addition to the false-positive radiographs, in another 61/288 women (21.2%) one or more findings unrelated to cervical cancer were identified. These included thoracic spondylosis (n=25; 8.7%), cardiomegaly (defined as cardiothoracic ratio ≥0.5) (n=20; 6.9%), pulmonary emphysema (n=10; 3.5%), thoracic scoliosis (n=9; 3.1%), atelectasis (n=3; 1.0%), old clavicle/rib fractures (n=2; 0.7%) and various other abnormalities (n=6; 2.1%). In none of these cases did the radiograph mandate or result in immediate intervention.

Table 2. Outline of FIGO stage IVB cervical cancer cases in the study population

	Case description	IVB defining disease site(s)	Pre-radiograph stage	Radiography outcome	Secondary diagnostics[1]
1	49 years, gr 2 SCC, palliative chemotherapy	Supraclavicular LN	IVB	No abnormalities	None
2	65 years, gr 2 SCC, palliative radiotherapy	Lung	IIIB	Solitary lung metastasis	None
3	31 years, gr 2 SCC, palliative chemotherapy	Para-aortal LN, Mediastinal LN, Supraclavicular LN	IVB	No abnormalities	None
4	54 years, gr 2 SCC, experimental therapy (trial)	Liver	IVB	No abnormalities	None
5	48 years, gr 3 SCC, palliative chemoradiotherapy	Lung	IVA	Multiple lung metastases	Chest CT
6	60 years, gr 3 SCC, palliative chemotherapy	Inguinal LN	IVB	Emphysema	None

Cases no. 1 through 5 ultimately died due to cervical cancer while case 6 received palliative care at the conclusion of this study.

[1] Indicated solely by chest radiography.

Gr: differentiation grade, SCC: squamous cell carcinoma, LN: lymph node(s)

DISCUSSION

Limited original research exists to support the routine use of chest radiography in the staging work-up of cervical cancer. Here, we have analyzed the data from all consecutive cervical cancer patients presented to our tertiary referral center over a 7½ year period.

Routine chest radiography did not identify pulmonary or skeletal metastases in any of 244 patients with stage I/II disease. Consequently, no stage shift occurred. Nor did radiography in these patients yield any secondary health benefits by detection of unrelated pathology. We fear that routine chest radiography exposes early stage cervical cancer patients to ionizing radiation, raises cost-utility concerns and places them at risk for false-positive findings, without a clear benefit in return.

Radiography did lead to upstaging to FIGO stage IVB in 2 patients with already advanced, pre-radiograph stage IIIB and IVA, cervical cancer. This is consistent with the results of Massad et al., in which radiography only identified pulmonary metastases in pre-radiograph stage IIIB patients [14]. In developed countries, these advanced pre-radiograph stage patients are likely to undergo additional cross-sectional imaging, allowing the aforementioned radiograph to still be omitted. However, especially in low resource settings where alternatives are scarce, continued used of radiography in this subgroup of patients can be defended.

Overall, we found a prevalence of pulmonary metastases of 0.7% (2/288). This is in line with the 0.4 - 1.6% reported in older studies and supports the generalizability of the findings reported here [15,16,17,18,19,20]. Two studies specified the pre-radiograph stage and both reported pulmonary metastases in 0.6% of early stage cases (disregarding cases with a second primary tumor) and 2.0 – 2.7% in advanced patients [15,16].

The low pretest probability of finding metastases relative to the high background prevalence of non-specific pulmonary nodules on CT (comparable age group, non-cancer patients: 13 - 18% [21,22]), can raise additional uncertainty when cross-sectional imaging is unselectively used. In a minority of our initial patient population chest CT (n=23) or PET-CT (n=3) had been performed as the initial thoracic imaging method. Although 1 patient did have pulmonary metastases, in none of the in total 5 FIGO IVB cases did the chest CT or PET-CT findings alter the clinical stage. This is consistent with 4 of the ultimately 6 IVB cases of the radiography population (Table 2: cases 1, 3, 4 and 6). Overall, this reaffirms that thoracic metastatic disease is rarely an isolated reason for upstaging, and even if so, only in cases which have otherwise already been diagnosed with advanced stage disease.

From a statistical standpoint, the absence of any metastases among our 'sample' of 244 early stage patients does not necessarily equal a population probability of 0.00%. It is possible, due to random chance, that our series of 244 negative cases was encountered

by accident only. However, based on a power of 80% (5% alpha, one sided test), we can state that our sample size is sufficient to exclude that the real population probability lies above 0.63% ('pwr' package version 1.1-2 within R version 3.0.3, R foundation for statistical computing, Vienna, Austria). Furthermore, our significant underrepresentation of IA1-2 patients likely allows for an even lower boundary.

Certain limitations of this study merit further clarification. Firstly, a substantial proportion (28.4%) of eligible patients could not be included, mainly because of absent radiography in low risk patients. We found that stage IA1-2 patients were selectively underrepresented, which likely strengthens rather than refutes our conclusions on radiography's absent value. Also, as stated earlier, in the subgroup which received immediate cross-sectional imaging instead of a radiograph, no stage changing findings were detected.

Secondly, despite our 7.5 year inclusion interval the population size and especially the number of 'event' cases remains limited, which influences precision. This is unfortunately inherent to the rarity of pulmonary and thoracic skeletal metastases in cervical cancer.

Thirdly, the cut-off of 6 months follow-up incorporated into our reference standard can be considered arbitrary. Current literature does not offer any guidance on an optimal length of time for this purpose. Though to minimize the risk of bias in our study, this cut-off was determined before the data-collection was started.

Finally, the radiography data used in our study were generated during the initial clinical review and no 'expert' revision was performed. Such a revision could ensure a standardized review and scoring method to minimize – or even exclude when only one expert is used – any inter-observer variability. However, we deliberately chose to follow regular clinical reality to increase the external validity (i.e. generalizability) of our study.

In conclusion, our study showed no value for routine chest radiography in the workup of early stage (stage I/II) cervical cancer patients. In none of these women did the radiograph identify pulmonary metastases or alter the FIGO stage. In advanced cases (stage III/IV), the continued use of routine chest radiography can be considered if cross-sectional imaging is not routinely employed or available. Nevertheless, even in these patients, pulmonary and skeletal metastases remain an infrequent finding at staging and are mostly diagnosed in patients already staged as IVB, making upstaging through radiography (its primary aim) uncommon. While further studies on advanced stage patients are preferred, careful consideration should be given to abandoning the current unselective use of chest radiography in early stage patients.

REFERENCES

1. Forouzanfar MH, Foreman KJ, Delossantos AM, Lozano R, Lopez AD, Murray CJ, et al. Breast and cervical cancer in 187 countries between 1980 and 2010: a systematic analysis. Lancet. 2011 Oct 22;378(9801):1461-84.
2. Ferlay J, Soerjomataram I, Ervik M, Dikshit R, Eser S, Mathers C, et al. GLOBOCAN 2012 v1.0, Cancer Incidence and Mortality Worldwide: IARC CancerBase No. 11 [Internet]. Lyon, France: International Agency for Research on Cancer; 2013. Available from: http://globocan.iarc.fr. retrieved on 30th Dec 2013.
3. FIGO Committee on Gynecologic Oncology. FIGO staging for carcinoma of the vulva, cervix, and corpus uteri. Int J Gynaecol Obstet. 2014 May;125(2):97-8.
4. Pecorelli S, Zigliani L, Odicino F. Revised FIGO staging for carcinoma of the cervix. Int J Gynaecol Obstet. 2009 May;105(2):107-8.
5. Moore DH. Cervical cancer. Obstet Gynecol. 2006 May;107(5):1152-61.
6. Colombo N, Carinelli S, Colombo A, Marini C, Rollo D, Sessa C; ESMO Guidelines Working Group. Cervical cancer: ESMO Clinical Practice Guidelines for diagnosis, treatment and follow-up. Ann Oncol. 2012 Oct;23 (Suppl 7:vii 27-32).
7. National Comprehensive Cancer Network (NCCN). NCCN Clinical Practice Guidelines in Oncology: Cervical Cancer. Version 3.2013. Available from "http://www.nccn.org", retrieved on Jan 20th, 2014.
8. World Health Organization, department of reproductive health and research and department of chronic diseases and health promotion. Comprehensive Cervical Cancer Control: A guide to essential practice (2006). Available from: http://www.who.int/reproductivehealth/publications/cancers/en/, retrieved on Jan 20th, 2014.
9. Kesic V, Cibula D, Kimmig R, Lopes A, Marth C, Reed N, et al (ESGO Educational Committee). Algorithms for management of Cervical cancer. Available from: http://www.esgo.org/Education/Pages/Algorithms.aspx, retrieved on Jan 20th, 2014.
10. Comprehensive Cancer Centre the Netherlands (IKNL). National cervical cancer guideline. Version 3.0 (approved on march 22th, 2012). Available from: http://oncoline.nl/cervixcarcinoom, retrieved on Jan 23th, 2014.
11. Oaknin A, Díaz de Corcuera I, Rodríguez-Freixinós V, Rivera F, del Campo JM; SEOM (Spanish Society of Clinical Oncology). SEOM guidelines for cervical cancer. Clin Transl Oncol. 2012 Jul;14(7):516-9.
12. Scottish Intercollegiate Guidelines Network (SIGN) and National Health services (NHS). Management of cervical cancer: A national clinical guideline (2008). Available from http://www.sign.ac.uk/guidelines/fulltext/99/index.html, retrieved on Jan 23th, 2014.
13. United States government, department of health, National Institutes of Health and

National Cancer Institute (2008). Common Terminology Criteria for Adverse Events (CTCAE), version 4.0, published: May 28th, 2009 (version 4.03: June 14th , 2010). Available from: http://evs.nci.nih.gov/ftp1/CTCAE, retrieved on 31th May 2013.

14. Massad LS, Calvello C, Gilkey SH, Abu-Rustum NR. Assessing disease extent in women with bulky or clinically evident metastatic cervical cancer: yield of pretreatment studies. Gynecol Oncol. 2000 Mar;76(3):383-7.
15. Gordon RE, Mettler FA Jr, Wicks JD, Bartow SA. Chest X-rays and full lung tomograms in gynecologic malignancy. Cancer. 1983 Aug 1;52(3):559-62.
16. Griffin TW, Parker RG, Taylor WJ. An evaluation of procedures used in staging carcinoma of the cervix. AJR Am J Roentgenol. 1976 Nov;127(5):825-7.
17. Barter JF, Soong SJ, Hatch KD, Orr JW, Shingleton HM. Diagnosis and treatment of pulmonary metastases from cervical carcinoma. Gynecol Oncol. 1990 Sep;38(3):347-51.
18. Imachi M, Tsukamoto N, Matsuyama T, Nakano H. Pulmonary metastasis from carcinoma of the uterine cervix. Gynecol Oncol. 1989 May;33(2):189-92.
19. Gunasekera PC, Fernando RJ, Abeykoon SC. Pulmonary metastases from cervical cancer in Sri Lanka. J Obstet Gynaecol. 1999 Jan;19(1):65-8.
20. Tellis CJ, Beechler CR. Pulmonary metastasis of carcinoma of the cervix: a retrospective study. Cancer. 1982 Apr 15;49(8):1705-9.
21. Hall WB, Truitt SG, Scheunemann LP, Shah SA, Rivera MP, Parker LA, et al. The prevalence of clinically relevant incidental findings on chest computed tomographic angiograms ordered to diagnose pulmonary embolism. Arch Intern Med. 2009 Nov 23;169(21):1961-5.
22. Burt JR, Iribarren C, Fair JM, Norton LC, Mahbouba M, Rubin GD, et al; Incidental findings on cardiac multidetector row computed tomography among healthy older adults: prevalence and clinical correlates. Arch Intern Med. 2008 Apr 14;168(7):756-61.

Chapter 3

Boosting the SNR by adding a receive-only endorectal monopole to an external antenna array for high-resolution T_2-weighted imaging of early stage cervical cancer with 7T MRI

Irene M.L. van Kalleveen
Jacob P. Hoogendam
Alexander J.E. Raaijmakers
Fredy Visser
Catalina S. Arteaga de Castro
René H.M. Verheijen
Peter R. Luijten
Ronald P. Zweemer
Wouter B. Veldhuis
Dennis W.J. Klomp

Submitted.

ABSTRACT

We aimed to image early stage cervical cancer at ultra-high field MRI (e.g. 7T) using a combination of multiple external and a single endorectal antenna. Here we study the Signal-to-Noise Ratio (SNR) increase and improvement of cervix MR imaging when including an endorectal monopole antenna. This should allow high resolution T_2-weighted images which facilitates the local tumor status assessment, including whether or not invasion into the surrounding connective tissue (parametria) has occurred.

In a prospective feasibility study, five healthy female volunteers and six histologically proven stage IB1-IIB cervical cancer patients were scanned at 7T. We used seven external fractionated dipole antennas for transmit-receive (transceive) and an endorectally placed monopole antenna for reception only. A region of interest, containing both normal cervix and tumor tissue, was selected for the SNR measurement. Separated signal and noise measurements were obtained in the region of the cervix for each element and in the near field of the monopole antenna (radius <30 mm) to calculate the SNR gain of the endorectal antenna per patient.

We obtained high resolution T_2-weighted images with a voxel size of 0.7x0.8x3.0 mm^3. In four cases with optimal placement of the endorectal antenna (verified on the T_2-weighted images) a mean gain of 2.2 in SNR was obtained at the overall cervix and tumor tissue area. Within a radius of 30 mm from the monopole antenna, a mean SNR gain of 3.7 was achieved in the four optimal cases. In the optimal cases, overlap between the two different regions of the SNR calculations, was around 24%.

We have demonstrated that the use of an endorectal monopole antenna substantially increased the SNR of 7T MRI at the (para)cervical anatomy. Combined with the intrinsic high SNR of ultra-high field MRI, this gain can be used to enhance spatial resolutions to assess tumor invasion.

INTRODUCTION

Cervical cancer is the fourth most common malignancy in women worldwide and 1.5T - 3T MRI of the pelvis is the modality of choice to assist the clinical international federation of gynecology and obstetrics (FIGO) local tumor staging [1,2]. Specifically, high spatial resolution T_2-weighted images in multiple orthogonal planes are used for the detection of parametrial invasion (i.e. into the connective tissue directly surrounding the cervix) [3]. This is clinically relevant as parametrial invasion changes stage, prognosis and treatment. In analogy with the detection of capsular extension of prostate cancer [4], higher spatial resolutions are likely beneficial for the assessment of parametrial invasion. The improved detection of capsular extension in prostate cancer was demonstrated after boosting the SNR with an endorectal Radio Frequency (RF) coil at 3T.

For imaging the cervix using endovaginal RF coil, an equal setup is being used at 1.5 and 3T [5,6,7]. Applying a small coil around the cervix for receive only can boost the SNR in the cervical region [8]. However, these coils are placed around the cervix which limits application to small malignancies confined to the cervix. Since we are interested in detecting parametrial invasion, an alternative approach to image the cervix is required. Besides internal antennas, the SNR can be further increased by the use of a stronger B_0 magnetic field (e.g. 7T) [9,10,11]. Consequently, at ultra-high field the increased spatial resolution of T_2-weighted imaging of the cervix can potentially result in better detection of parametrial invasion.

However, at ultra-high field strengths, body MRI becomes challenging. The RF transmit field (B_1^+) is severely non-uniform, and the RF power deposition (i.e. the Specific Absorption Rate, SAR) limits effective use of RF pulse intensive sequences, commonly the case in T_2-weighted MRI. With a local transceive array, driven with optimized phase settings, the B_1^+ field can be focused at a region of interest [12]. Moreover, using antenna arrays rather than conventional coil arrays, SAR can be reduced which might enable a more efficient T_2-weighted MRI in the body at 7T [13].

The female cervix is located centrally in the inner pelvis and is situated directly ventral to the rectum. Hence, using an endorectal coil for signal reception may boost the SNR. While loop [14] and stripline [10] designs for endorectal coils have been reported and showed successful results when applied to prostate MRI, recently also monopole antennas were demonstrated to work as an internal transceiver for 7T MRI [15]. The advantages of the monopole over the loop or stripline designs, are its relatively thin size [15], and potential higher SNR efficiency at depth [16]. The close anatomical distance between the cervix and the rectum allows the perpendicular B_1 field of the antenna to be used to image the cervix.

However, as the transmit field is severely non-uniform when using the monopole as a transceiver, B_1^+ compensating RF pulses are required for uniform flip angles. Erturk et al. [15] have demonstrated the use of composite pulses in rabbits. For Gradient Echo imaging (GRE), using the small tip angle (STA) approximation [17], images of the rectum [18] have been shown where 2D RF pulses are used to compensate the non-uniform B_1^+ field, when using the antenna as a transceiver. A more elegant way to benefit from the high SNR is to only use the internal antenna as a receiver, while providing a relatively uniform transmit field with an external local transmit or transceive array. This way, conventional RF pulses and sequences may be used facilitating the exploration of T_2-weighted MRI at maximized SNR.

We therefore propose to use an endorectal monopole antenna for receive purposes, in addition to an external transceive coil array, to boost the SNR of T_2-weighted MRI of the human cervix, using a 7T MR system. This study aims to quantify the gain in SNR achieved with the internal antenna versus the external antennas only in the first ever obtained high resolution T_2-weighted 7T MR images of stage IB1-IIB cervical cancer patients.

EXPERIMENTAL METHODS

Study design and population

A pilot study was conducted with five healthy female volunteers to optimize logistical and technical protocols. Due to the far field of the antenna, a measurement of the SNR gain of the monopole antenna in a phantom will not result is trustworthy values [18]. Therefore we used a healthy volunteer to check whether the increase in SNR was enough to use the monopole antenna on patients. After we used one healthy volunteer for SNR calculations in the uterus and cervix to explore the SNR gain, we started a prospective feasibility study in patients. Six women diagnosed with cervical cancer were scanned between March and October 2014. Women were included if they had histologically proven stage IB1, IB2, IIA1-2 or IIB cervical cancer and were at least 18 years old. Patients were excluded when contra-indicated for MRI or if treatment with radical surgery had already been carried out or if chemo-radiation therapy had already been started. Subjects with severe uterine prolapse were also excluded. Additionally, we obtained T_2-weighted images in a patient with and without the monopole antenna to show the effects in the B_1 transmit field by the physical presence of the antenna. The institutional review board approved the study protocol (NL41056.041.13) and written informed consent was provided by patients, as well as the healthy volunteers. This study was registered prospectively at clinicaltrials.gov under identifier NCT02083848.

Setup

A 7T whole body MR system (Achieva, Philips Medical systems, Cleveland, United States of America) equipped with 8-channel multi-transmit functionality was used in combination with a local transceiver coil array of fractionated dipole antennas [13] (MR Coils B.V., Drunen, The Netherlands) and the internal monopole antenna (Machnet B.V., Maarn, The Netherlands). The seven external antennas were placed around the pelvis (Figure 1a, b). We combined these elements with a single endorectally placed monopole antenna (Figure 1c, d), used for receive purposes only.

The monopole antenna was encapsulated in a 14 Fr urinary catheter to enable easy insertion and for microbiological safety was placed in a single use sterile probe cover (Ultracover 200 mm, Microtek medical B.V., Zutphen, The Netherlands). Endorectal insertion, performed on the MR bed, was facilitated by sterile lubricating gel and performed by a qualified physician from the gynecological oncology department (JH). The receive optimum of the monopole antenna was positioned 6-10 cm beyond the anal verge to obtain the optimal signal. To ensure immobilization during imaging, the external part of the antenna was fixed with tape to the medial part of the left upper leg. No antispasmodic medication was administered.

For the volunteer low resolution sagittal SNR images (Multi-Slice (MS) GRE, TE = 1.49 ms, TR = 15 ms and resolution = 2x2x6 mm^3) were obtained. To support our findings, we also obtained three times the same sagittal T_2-weighted image where respectively the monopole antenna, the external antennas and both monopole and external antennas were used for receiving. B_1^+ shimming was performed with a phase-based shimming method [12] to focus on the (para)cervical anatomy. For this we used a single slice GRE sequence (TE = 1.97 ms, TR = 45 ms, FOV = 250x500x35 mm^3) repeated 7 times, each time driving a different transmit antenna, while receiving with all 8 elements. A low resolution T_2-weighted sagittal image (MS (Turbo Spin Echo (TSE), TE = 272 ms, scan time= 70 s, resolution = 1.4x1.6x5 mm^3) was obtained to localize the cervix and the tumor and to determine its orientation. On the sagittal images a high resolution single-shot T_2-weighted transversal and double oblique (i.e. perpendicular to the cervical canal) sequences (MS TSE, TE = 70 ms, TR = 13 s, resolution = 0.7x0.8x2.5 mm^3) were planned.

Signal to noise measurements (MS GRE, TE = 1.49 ms, TR = 15 ms, resolution = 2x2x6 mm^3) were obtained in the same double oblique scan plane as the high resolution T_2-weighted sequence. For each patient, the scan was obtained twice; first with a nominal flip angle of 15° followed by a sequence without excitation (flip angle of 0°). The measurements were recorded with only the endorectal monopole antenna as a receiver and with only each of the external elements separate as a receiver. The separate external elements were finally combined in a SNR optimal setting [19].

Data processing

We used MATLAB version 2014b (MathWorks, Natick, USA) to create a patient based mask (to select the region of interest) which included the cervix and the tumor. To determine the optimal gain in SNR of the monopole antenna, we also created a mask in the region around the antenna (with a radius of 30 mm). The difference in SNR was calculated using the mean signal over the area contained within the mask divided by the standard deviation of the noise scan from the same area [19]. The SNR in the selected volume was calculated per patient, when using only the monopole antenna, or when using only the external antennas. In the latter calculation we used complex weighted averaging of the signal from each element, where the weighting factor was determined from the highest SNR images [20]. For the noise scan reconstruction identical weighting factors were used as for the signal images. Finally, the SNR was calculated per patient over a region in the cervix and in the vicinity of the antenna containing around 2,000 and 9,000 voxels on average respectively.

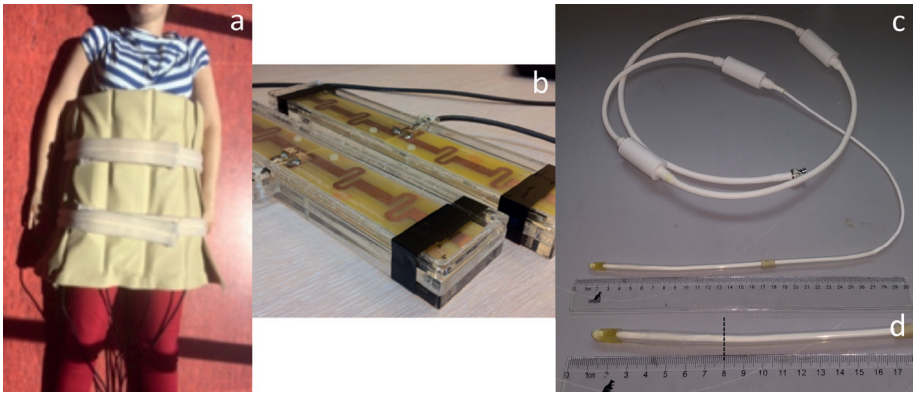

Figure 1. A) The external array of fractionated dipole antennas. Elements are contained in the leather sleeve. B) Two single fractionated dipole antenna elements. C) The endorectal monopole antenna. The part of the antenna which is placed inside the rectum is covered by a 14 Fr urinary catheter. D) A close-up of the endorectal antenna next to a ruler to indicate its size. The dotted line indicates the location of the receive optimum.

RESULTS

A healthy female volunteer (26 years) was scanned to visualize the gain in SNR when using only the external antennas, the internal antenna or both the external and internal antennas for receive (Figure 2). Due to a lower resolution scan, the region of interest for this volunteer was chosen over the complete cervix and uterus. The SNR gain from this volunteer (white region) was a factor of 3.2.

Table 1 provides the baseline characteristics of the six patients. The outlined coil setup enabled T_2-weighted visualization of the entire true pelvis (pelvis minor) (Figure 2-4). Sagittal T_2-weighted images (Figure 3a, 4a) were obtained to locate the cervix and plan the high resolution double oblique T_2-weighted scan (Figure 3b, 4b) perpendicular to the cervical canal to image the cervix and the tumor.

We compared the SNR of the internal antenna with the optimal combination of signals from the external antennas [19]. See Table 2 for an overview per patient. Using the internal antenna as an extra receiver, we gained a mean factor of 1.8 in SNR in the cervical region. In patients 5 and 6 the antenna was not fixed properly, as after the examination it had turned out to be shifted more than 5 cm out of the rectum. In these two patients, the SNR gain of the antenna is substantially reduced and therefore contributing less to the external array. However excluding these two patients, we gained a mean factor of 2.2 in SNR. We also calculated the SNR for the internal and external antennas in the surrounding tissue of the internal antenna (in a radius of 30 mm) at the height of the cervix. In this case the overall SNR gain was a factor of 2.9, or even a factor of 3.7 in SNR gain when excluding patients 5 and 6.

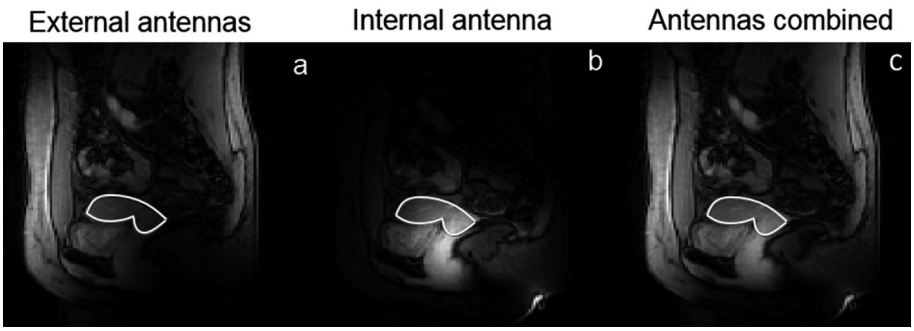

Figure 2. A sagittal slice of the SNR maps (MS GRE, TE = 1.49 ms, TR = 15 ms and resolution = 2x2x6 mm^3) through the uterus and cervix (white region) of a healthy volunteer where for receive A) only the external antennas, B) the monopole antenna and C) both the external and internal antennas combined were used.

Additionally, we obtained T_2-weighted images with all the antennas (external and internal antennas) and excluding the monopole antenna to show that the antennas do not couple (Figure 5).

Table 1. Baseline characteristics of six patients

	Age (years)	BMI (kg/m²)	Prior LETTZ	Prior conisation	Largest tumor diameter (mm)	FIGO Stage	Histological type and grade	LVSI	Relevant medical history
1	40	22.4	+	+	45	IIB2	SCC, III	+	None
2	32	18.4	+	-	0*	IB1	SCC, II	-	None
3	65	26.2	-	-	50	IIB2	SCC, II	-	Excisional Haemorr-hoidectomy 4 years earlier
4	30	20.2	-	+	0**	IB1	AC, I	-	None
5	33	19.2	-	-	39	IIA1	Neuro-endocrine small cell carcinoma	+	M. Marfan
6	44	22.2	-	-	58	IB2	SCC, III	-	Laparotomy for appendicitis

Clinical characteristics of the patients. BMI: body mass index, LLETZ: large loop excision of the transformation zone, FIGO: international federation for gynecology and obstetrics, LVSI: lymphovascular space invasion, SCC: squamous cell carcinoma.
⁺ Positive, ⁻ Negative.
* Following the LETTZ, no residual tumor was visible.
** Following the conisation, no residual tumor was visible.

Table 2. SNR ratios of monopole antenna when used as a receiver only vs the external antennas only for each patient

SNR ratio of monopole versus external antennas in the cervix and tumor			SNR ratio of monopole versus external antennas near the antenna (radius<30 mm)		
Cervix and tumor	SNR monopole / SNR external	Number of voxels in mask	Near monopole (r<30 mm)	SNR monopole / SNR external	Number of voxels in mask
Patient 1	1.765	2229	Patient 1	3.718	9253
Patient 2	2.495	1386	Patient 2	3.163	15101
Patient 3	1.642	2017	Patient 3	2.045	9969
Patient 4	2.978	1114	Patient 4	5.834	13932
Patient 5	0.922	1911	Patient 5	1.484	3178
Patient 6	0.858	3213	Patient 6	1.268	2099
Mean Summary Statistics	**1.777**	**1978**	**Mean Summary Statistics**	**2.919**	**8922**

The SNR gain was calculated in the cervix and tumor tissue and in the near field of the antenna (radius < 30 mm).

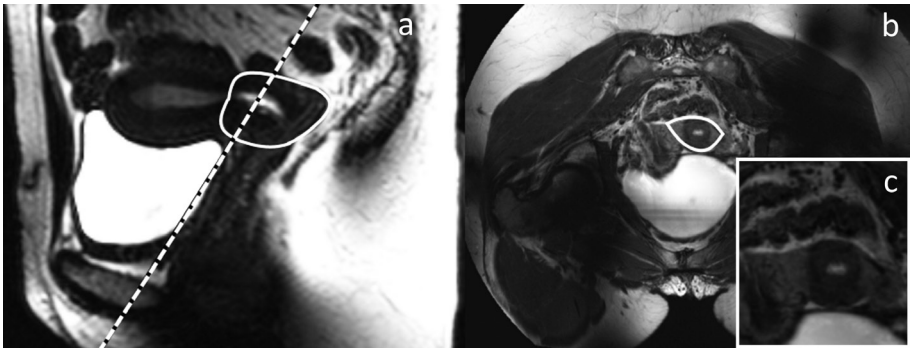

Figure 3. A) Sagittal T_2-weighted image of patient 1 (MS TSE, TE = 272 ms, TR = 70 s, resolution = 1.4x1.6x5.0 mm^3, FOV = 246x375x105 mm^3). The dashed white line indicates the planning of the double oblique high resolution T_2-weighted scan which is placed perpendicular to the cervix. The white delineation represents the region of the cervix and the tumor in the sagittal plane on which the SNR calculations were based. B) The high resolution single-shot double oblique T_2-weighted image of patient 1 (MS TSE, TE = 70 ms, TR = 13 s, resolution = 0.7x0.8x2.5 mm^3, FOV = 350x400x47 mm^3), where the cervix and the tumor tissue are clearly visible. C) A zoomed version of the cervix taken from b).

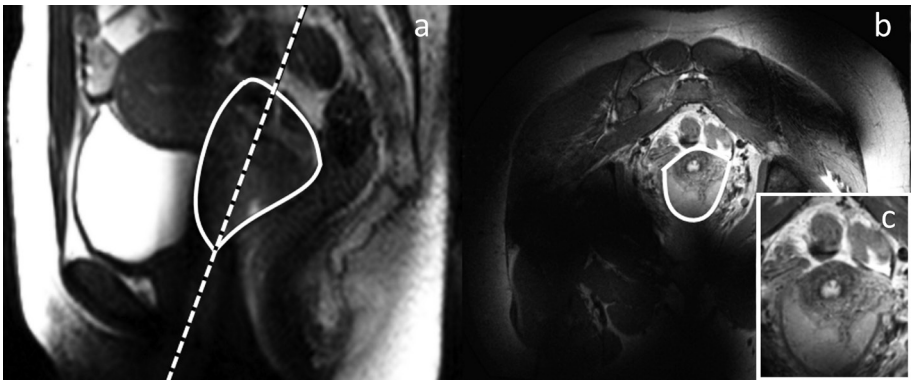

Figure 4. A) Sagittal T_2-weighted image of patient 6 (MS TSE, TE = 170 ms, TR = 50 s, resolution = 0.9x1.6x5.0 mm^3, FOV = 375x375x85 mm^3). The dashed white line indicates the planning of the double oblique high resolution T_2-weighted scan which is placed perpendicular to the cervix. The white delineation represents the region of the cervix and the tumor in the sagittal plane on which the SNR calculations are based. B) The high resolution single-shot double oblique T_2-weighted image of patient 6 (MS TSE, TE = 70 ms, TR = 7 s, resolution = 0.7x0.8x3.0 mm^3, FOV = 350x400x39 mm^3), where the cervix and the tumor tissue are clearly visible. In b) the white delineation represents the region of interest which is used for the SNR comparison within the cervix and the cervical tumor. C) A zoomed version of the cervix taken from b).

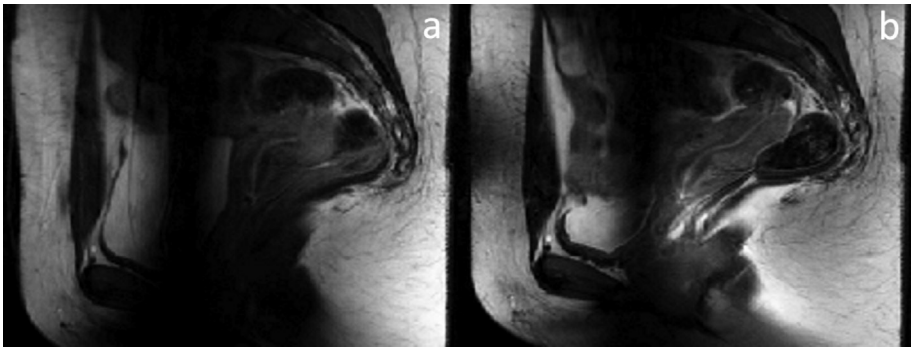

Figure 5. Sagittal T_2-weighted images of a patient (MS TSE, TE = 70 ms, TR = 7 s, resolution = 0.5x0.8x4.9 mm^3, FOV = 400x250x73 mm^3). In A) the external antennas are used for transmit and receive. No endorectal monopole antenna is present. In B) the external antennas are used for transmit and receive and the endorectal monopole antenna is used as an additional receiver. Due to the time between both scans, the bladder was filled further, causing a change in planning of the multi-slice T_2-weighted scan. Note that the absence of signal voids and symmetric contrast surrounding the antenna reflects a uniform flip angle hence negligible RF interaction of the transmit antennas to the internal antenna.

DISCUSSION

We have demonstrated a strong increase in SNR using an endorectal monopole antenna in 7T MR imaging of early stage cervical cancer compared to using external antennas only. Furthermore, while internal antenna use has been reported in rabbits [15], this study is the first to report the use of internal monopole antennas in humans at ultra-high field strengths. To show the benefits of the internal monopole antenna, an SNR comparison has been made between a state of the art external fractionated dipole antenna array and the internal monopole antenna. First in a healthy volunteer, to check the benefits of an additional monopole antenna. And finally in cervical tumor patients, to investigate the SNR boost in cervical tumors. For small tumors, this method might work even better, due to the smaller tumor size and a closer location to the antenna (due to the reduced size).

The intrinsic SNR scales by approximation linear to the main magnetic field. Therefore MRI at 7T is expected to have about 2.3 fold more SNR than a similar scan at 3T. An additional similar gain is observed by inserting a monopole antenna resulting in an overall gain is SNR of approximately 5.5-fold. The SNR is linearly related to the volume pixel size, hence potentially could be traded to a 5.5-fold reduced pixel volume or a 1.8-fold reduction in pixel size in all three dimensions.

We also added results of removing the endorectal antenna physically, and compared it to the case where the endorectal antenna is still present. In these images (Figure 5) it is clear that the influence of the antenna is very local, as expected. Removing the antenna results in a loss of signal near the cervix, as already pointed out by the SNR measurement, however the signal beyond the field of view of the antenna is not harmed by the removal of the endorectal antenna. Giving us no proof of any coupling between the external antennas and the internal antenna. Furthermore, would a coupling occur between the endorectal antenna and the external antennas, the strong inhomogeneous B_1^+ field of the monopole antenna would create a strong deviation of the flip angle near the antenna, which is also present in the cervix for this patient. This would cause image distortions, especially in T_2-weighted images.

Parametrial invasion is difficult to assess using an endovaginal coil, because such an RF coil cannot be placed alongside the full length of the cervix, the parametria are at least partially excluded from the field of view. Because we wanted to focus on the parametrial invasion of the cervix cancer patients the method of using an endovaginal coil is not suitable for our study. Especially for patients with larger tumors, a small angular displacement or an anatomical difference in structure or a full bladder might change the orientation of the coil with respect to the cervix and the tumor. This might reduce the SNR in the cervix drastically.

The gain in SNR depends strongly on the positioning of the monopole antenna and on the anatomical location of the uterus in relation to the antenna. After the antenna has been endorectally inserted and is taped to the upper inner leg, the peristaltic motion and other patient motion might still reposition the antenna. Therefore the gain in SNR may not be optimal. To overcome this problem an external socket might keep the antenna at the right location. Examples of cases where the antenna was dislocated are shown in table 2 (patient 5 and 6). Nevertheless, in these cases a more modest SNR gain is still present.

Comparing Figures 3 and 4 (patient 1 and 6 resp.) shows how many factors play a role in obtaining an optimal SNR setting for the best case scenario. The SNR boost of the antenna is in the case of patient six is a factor 2 lower than in the case of patient 1. However comparing the T_2-weighted images of both patients, this is not obvious at first sight. There are other factors which play a role, like the anatomy and the tumor itself. Another reason for still obtaining a high resolution T_2-weighted image is the increased SNR in the cervix of the external antennas (which are calculated in the best case scenario [19]), and in combination with a less efficient placement of the endorectal antenna the SNR ratio between the internal and external antennas will drop. Another option for using the monopole antenna could be to use it for transmit and receive without the external antenna array. Hereby the FOV can be reduced and as an effect we might boost the spatiotemporal resolution. However, the reduced field of view, caused by the limited transmit and receive field of the monopole antenna, can make diagnostics more difficult. This challenge might be reduced by designing RF pulses, which might restore a part of the limited field of the monopole antenna [15,18]. The use of the monopole antenna solely as a transceiver depends strongly on its placement making the fixation of the antenna even more important. In addition, if using the internal antenna for transmit, the inhomogeneous B_1^+ field of it has to be considered. The inhomogeneous B_1^+ field results in an inhomogeneous flip angle distribution, which compromises tissue contrast. A method to overcome the inhomogeneous flip angle distribution is to use adiabatic RF pulses [21,22]. However these pulses are SAR intensive and may not be feasible to use within safety guidelines. Another method might be to use a selective excitation in the cervix that incorporates the non-uniformity in B_1^+. Other groups have already shown successfully the use of selective excitation in the brain [23,24].

The challenge with these so-called multi-dimensional RF pulses is that turbo spin echo images (T_2-weighted) require a high flip angle excitation and refocusing pulses and these 2D RF pulses are normally designed using low flip angle assumptions (Small Tip angle Approximation method [17]) and used in GRE sequences. High flip angle optimizations are more challenging [24], particularly when considering the severe non-uniformities in

B_1^+ when using the endorectal antenna as a transceiver.
We used a single-shot T_2-weighted scan to overcome the peristaltic movement. By using medication (e.g. butylscopolamine or glucagon [25,26,27]) in combination with a multi-shot TSE or an increased number of averages, it might be possible to even gain more SNR. At 1.0T and 1.5T this approach has already been shown to be successful [28].
Boosting the SNR by combining an ultra-high field MRI and an endorectal monopole antenna in combination with external antennas, we are able to obtain high resolution T_2-weighted images. Using these images earlier detection of parametrial invasion might be possible, resulting in additional information for radiologist. Based on this additional information patient treatment planning might change; whether or not surgery and/or radiation fits the best in the treatment plan of the patient.
To conclude, we demonstrated that adding an endorectal monopole antenna to an external antenna array can substantially boost the SNR at the cervix. This enables higher resolution T_2-weighted image acquisitions, relevant for assessing the local tumor status in early stage cervical cancer.

Conflict of interest disclosure
Fredy Visser is an employee at Philips Healthcare in Best and Dennis Klomp has a minority interest of 4.9% in MR Coils B.V. The other authors declare that they have no conflict of interest relevant for the presented research.

Funding
The development of the endorectal antenna was made possible by the Dutch Technical Science Foundation (STW 10882).

Abbreviations

2D RACE	2-Dimensional Radially Compensating Excitation
SNR	Signal-to-Noise Ratio
FIGO	International Federation for Gynecology and Obstetrics
SAR	Specific Absorption Rate
MS	Multi-Slice
GRE	Gradient Echo
TSE	Turbo Spin Echo
BMI	Body Mass Index
LLETZ	Large Loop Excision of the Transformation Zone
LVSI	Lymphovascular Space Invasion
SCC	Squamous Cell Carcinoma

REFERENCES

1. Balleyguier C, Sala E, Da Cunha T., Bergman A, Brkljacic B., Danza F, Forstner R, Hamm B, Kubik-Huch R, Lopez C, Manfredi R, McHugo J, Oleaga L, Togashi K, Kinkel K. Staging of uterine cervical cancer with MRI: guidelines of the European Society of Urogenital Radiology. Eur Radiol 2011;21:1102-1110.
2. Pecorelli S. Revised FIGO staging for carcinoma of the vulva, cervix and endometrium. Int J Gynaecol Obstet 2009;105:103-104.
3. Sala E, Wakely S, Senior E, Lomas D. MRI of malignant neoplasms of the uterine corpus and cervix. A J R 2007;188:1577-1587.
4. Futterer JJ, Heijmink SWTPJ, Scheenen TWJ, Jager GJ, Hulsbergen-Van de Kaa CA, Witjes JA, Barentsz JO. Prostate Cancer: Local Staging at 3-T Endorectal MR Imaging - Early Experience. Invest Radiol 2006;238:184-191.
5. Charles-Edwards E, Morgan V, Attygalle AD, Giles SL, Ind TE, Davis M, Shepherd J, McWhinney N, deSouza NM Endovaginal magnetic resonance imaging of stage 1A/1B cervical cancer with a T2- and diffusion-weighted magnetic resonance technique: Effect of lesion size and previous cone biopsy on tumor detectability. Gynecol Oncol 2011;120:368-373.
6. Downey K, Shepherd JH, Attygalle AD, Hazell S, Morgan VA, Giles SL, Ind TEJ, deSouza NM Preoperative imaging in patients undergoing trachelectomy for cervical cancer: Validation of a combined T2- and diffusion-weighted endovaginal MRI technique at 3.0 T. Gynecol Oncol 2014;133:326-332.
7. Charles-Edwards EM, Messiou C, Morgan VA, De Silva SS, McWhinney NA, Katesmark, M, Attygalle AD, DeSouza NM. Diffusion-weighted imaging in cervical cancer with an endovaginal technique: potential value for improving tumor detection in stage Ia and Ib1 disease. Radiology 2008;249:541-550.
8. deSouza NM, Dina R, McIndoe GA, Soutter WP. Cervical cancer: Value of an endovaginal coil magnetic resonance imaging technique in detecting small volume disease and assessing parametrial extension. Gynecol Oncol 2006;102:80-85.
9. Metzger GJ, Van de Moortele PF, Akgun C, Snyder CJ, Moeller S, Strupp J, Andersen P, Shrivastava D, Vaughan T, Ugurbil K, Adriany G. Performance of external and internal coil configurations for prostate investigations at 7 T. Magn Reson Med 2010;64:1625-1639.
10. Arteaga de Castro CS, van den Bergen B, Luijten PR, Van der Heide UA, van Vulpen, M, Klomp DWJ. Improving SNR and B1 transmit field for an endorectal coil in 7 T MRI and MRS of prostate cancer. Magn Reson Med 2012;68:311-318.
11. Erturk MA, Tian J, Van de Moortele PF, Adriany G, Metzger GJ Development and

evaluation of a multichannel endorectal RF coil for prostate MRI at 7T in combination with an external surface array. J Magn Reson Imaging 2016;43:1279-1287.
12. Metzger GJ, Snyder C, Akgun C, Vaughan T, Ugurbil K, van de Moortele PF. Local B1+ shimming for prostate imaging with transceiver arrays at 7T based on subject-dependent transmit phase measurements. Magn Reson Med 2008;59:396-409.
13. Raaijmakers AJ, Italiaander M, Voogt IJ, Luijten PR, Hoogduin JM, Klomp DW, van den Berg CA. The fractionated dipole antenna: A new antenna for body imaging at 7 Tesla. Magn Reson Med 2016;75:1366-1374.
14. Klomp DWJ, Bitz AK, Heerschap A, Scheenen TW. Proton spectroscopic imaging of the human prostate at 7 T. NMR biomed 2009;22:495-501.
15. Erturk MA, El-Sharkawy AM, Moore J, Bottomley PA. 7 tesla MRI with a transmit/receive loopless antenna and B1-insensitive selective excitation. Magn Reson Med 2014;72:220-226.
16. Raaijmakers AJE, Ipek O, Klomp DWJ, Possanzini C, Harvey PR, Lagendijk JJW, van den Berg CAT. Design of a radiative surface coil array element at 7 T: the single-side adapted dipole antenna. Magn Reson Med 2011;66:1488-1497.
17. Pauly J, Nishimura D, Macovski A. A k-space analysis of small-tip-angle excitation. J Magn Reson 1989;81:43-56.
18. van Kalleveen IML, Kroeze H, Sbrizzi A, Boer VO, Reerink O, Phillipens MEP, van den Berg CAT, Luijten PR, Klomp DWJ. 2D radially compensating excitation pulse in combination with an internal transceiver antenna for 3D MRI of the rectum at 7 T. Med Phys 2016;43:http://dx.doi.org/10.1118/1111.4954204.
19. Hayes CE, Roemer PB. Noise correlations in data simultaneously acquired form mulitple surface coil arrays. Magn Reson Med 1990;16:181-191.
20. Hargreaves BA, Cunningham CH, Nishimura DG, Conolly SM. Variable-rate selective excitation for rapid MRI sequences. Magn Reson Med 2004;52:590-597.
21. Garwood M, DeLaBarre L. The return of the frequency sweep: Designing adiabatic pulses for contemporary NMR. J Magn Reson 2001;153:155-177.
22. Van Kalleveen IML, Koning W, Boer VO, Luijten PR, Zwanenburg JJM, Klomp DWJ. Adiabatic Turbo Spin Echo in Human Applications at 7 T. Magn Reson Med 2012;68:580-587.
23. Moore J, Jankiewicz M, Zeng H, Anderson AW, Gore JC. Composite RF pulses for B1+-insensitive volume excitation at 7 Tesla. JMR 2010;205:50-62.
24. Grissom WA, Xu D, Kerr AB, Fessler JA, Noll DC. Fast large-tip-angle multidimensional and parallel RF pulse design in MRI. IEEE Trans Med Imaging 2009;10:1548-1559.
25. Froehlich JM, Patak MA, Von Weymarn C, Juli CF, Zollikofer CL, Wentz KU. Small bowel motility assessment with magnetic resonance imaging. J Magn Reson 2005;21:370-375.

26. Horsthuis K, Bipat S, Bennink RJ, Stoker J. Inflammatory bowel disease diagnosed with US, MR, Scintigraphy, and CT: Meta-analysis of prospective studies. Radiology 2008;247:64-79.
27. Florie J, Wasser, MNJM, Arts-Cieslik K, Akkerman EM, Siersema PD, Stoker, J. Dynamic contrast-enhanced MRI of the bowel wall for assessment of disease activity in Crohn's disease. Am J Roentgenol 2006;186:1384-1392.
28. Wagner M, Rief M, Busch J, Scheurig C, Taupitz M, Hamm B, Franiel T. Effect of butylscopolamine on image quality in MRI of the prostate. Clin Radiol 2010;65:460-464.

Chapter 4

High resolution T_2-weighted cervical cancer imaging: a feasibility study on ultra-high field 7.0T MRI with an endorectal monopole antenna

Jacob P. Hoogendam
Irene M.L. Kalleveen
Catalina S. Arteaga de Castro
Alexander J.E. Raaijmakers
René H.M. Verheijen
Maurice A.A.J. van den Bosch
Dennis W.J. Klomp
Ronald P. Zweemer
Wouter B. Veldhuis

Eur Radiol, in press.

ABSTRACT

Objectives: We studied the feasibility of high resolution T_2-weighted cervical cancer imaging on an ultra-high field 7.0T magnetic resonance imaging (MRI) system using an endorectal antenna of 4.7mm thickness.

Methods: A feasibility study on 20 stage IB1 – IIB cervical cancer patients was conducted. All underwent pre-treatment 1.5T MRI. At 7.0T MRI, an external transmit/receive array with seven dipole antennas and a single endorectal monopole receive antenna were used. Discomfort levels were assessed. Following individualized phase-based B_1^+ shimming, T_2-weighted turbo spin echo sequences were completed.

Results: Patients had stage IB1 (n=9), IB2 (n=4), IIA1 (n=1) or IIB (n=6) cervical cancer. Discomfort (10 point scale) was minimal at placement and removal of the endorectal antenna with a median score of 1 (range: 0-5) and 0 (range: 0-2) respectively. Its use did not result in adverse events or preterm session discontinuation. To demonstrate feasibility, T_2-weighted acquisitions from 7.0T MRI are presented in comparison to 1.5T MRI. Artefacts on 7.0T MRI were due to motion, locally destructive B_1 interference, excessive B_1 under the external antennas and SENSE reconstruction.

Conclusions: High resolution T_2-weighted 7.0T MRI of stage IB1 – IIB cervical cancer is feasible. The addition of an endorectal antenna is well tolerated by patients.

Keywords: uterine cervical neoplasms, magnetic resonance imaging, feasibility studies, antenna, neoplasm staging.

INTRODUCTION

Accurate staging of cervical cancer is crucial for treatment planning and determines prognosis. Historically, to allow efficient and comparable staging in high incidence underdeveloped areas, the International Federation of Gynaecology and Obstetrics (FIGO) requires clinical (i.e. non-surgical) staging by physical examination [1]. This inherently introduces under- and overstaging, particularly for intermediate stages wherein estimation of (subtle) parametrial invasion by rectovaginal examination remains difficult, yet determines operability [2]. Studies comparing clinical and post-surgical histological stages in IB1, IB2, IIA1-2 and IIB have reported concordance in 82-85%, 61-77%, 35-60% and 20-59% of cases, respectively [2,3,4].

Following the 2009 FIGO update, and supported by (inter)national guidelines, MRI may be added to the work-up to assist clinical staging [5,6,7]. A meta-analysis (n=3254, 40 studies) showed a pooled sensitivity of 84% for detection of parametrial invasion by MRI, substantially superior to the 40% achieved by clinical examination [8]. This study also identified higher B_0 field strengths and the use of fast spin echo sequences as statistically significant factors to improve the accuracy in detecting parametrial invasion [8].

Increasing the B_0 field strength to 7.0T, increases the signal-to-noise ratio (SNR) and consequently allows for higher spatial or temporal resolution acquisitions [9]. While more expensive, this is potentially advantageous for the assessment of loco-regional invasion which is a predominantly anatomic, spatial resolution-dependent assessment made on T_2-weighted MR images. Moreover, at 7.0T, the MRI signals are obtained at much shorter wavelengths than at lower fields, facilitating the use of ultra-thin antennas [10]. While using such an antenna in close proximity to the cervix is more laborious, SNR and thereby resolution is expected to increase even further.

We built an endorectal monopole antenna and aimed to develop dedicated T_2-weighted TSE sequences for 7.0T imaging with that antenna combined with an external coil array, to image the (para)cervical anatomy in early stage cervical cancer patients. To date, no published research exists which has attempted this. We assessed patient tolerance of using an endorectal antenna. In addition, we will present the T_2-weighted images acquired at 7.0T, and clinical 1.5T MRI as a visual reference.

MATERIALS AND METHODS

Design

We conducted a monocenter, prospective cohort study to develop, optimize and assess the feasibility of high resolution pelvic T_2-weighted in-vivo imaging on a 7.0T MRI system using a purpose designed endorectal antenna. Inclusion criteria were: 1) a histologically proven primary malignancy of the cervix uteri, 2) FIGO stage IB1, IB2, IIA1-2 or IIB disease, and 3) a minimum age of 18 years. Patients were excluded when 1) general contra-indications for MRI existed, 2) radical surgery had already been performed or chemo- and/or radiotherapy had been initiated, or 3) uterine prolapse existed (C ≥ -6cm, POP-Q classification [11]). When eligible, subjects were consecutively counselled between March 2014 and November 2015.

The institutional review board approved this study (clinicaltrials.gov: NCT02083848). Participants provided written informed consent. Data quality, protocol adherence and safety were independently monitored by qualified staff. At our tertiary oncologic referral centre, clinical staging adheres to FIGO and national cervical cancer guidelines [1,6]. Supplemental file 1 provides details on the clinical 1.5T MRI and treatment [12].

7.0T MRI

Participants completed a safety checklist and underwent metal detector testing prior to imaging on a whole body 7.0T MRI system (Achieva, Philips medical systems, Cleveland, USA) equipped with 8-channel multi-transmit functionality. Intravenous contrast agents were not administered, nor was spasmolytic medication. Adverse events were monitored in adherence to the common terminology criteria for adverse events criteria [13].

The shortened B_1 wavelength at ultra-high field MRI, which limits signal penetration and increases the risk of destructive interference, challenges cervical cancer imaging given its anatomical position deep in the female inner pelvis. To alleviate these issues, a local transmit/receive array consisting of seven 30cm fractionated dipole antennas (MR Coils, Drunen, Netherlands) was used. This setup allows for per patient optimization of the B_1 field distribution. The technical specifications of this array, including the corresponding Specific-Absorption-Rate (SAR) implications, were recently published [14].

The internal monopole B_1 receive antenna was created in-house and specifically designed for endorectal use in 7.0T MRI, and subsequently commercialized by Machnet, Maarn, Netherlands. It was positioned in a 14Fr Foley urinary catheter with a desufflated balloon for an optimal balance between rigidity and flexibility, yielding a 4.7mm outer diameter (Figure 1). In addition to its sterilization in-between sessions, a single use, sterile cover (Ultracover 200mm, Microtek medical, Zutphen, Netherlands) was used. Water based

lubricating gel (K-Y, Johnson & Johnson, Sézanne, France) facilitated easy endorectal positioning. The region with optimal signal strength was located 6-10cm beyond the anal verge. Patient reported levels of discomfort related to the antenna – on a Likert scale from 0 (i.e. none whatsoever) to 10 (i.e. worst imaginable) – was assessed directly after introduction and removal.

Sequence parameters were optimized for each patient in the first half of the study. From inclusion 10 and on, a standardized protocol with only minor individual adaptations was used. After a multidirectional survey was obtained for anatomical localization, phase-based B_1^+ shimming was performed per patient to maximize and homogenize the B_1^+ on the (para)cervical anatomy [15]. Herein, a single slice gradient echo sequence was repeated 7 times, each time transmitting with a different transmit antenna, while receiving with all 8 antennas. Next, following a shimmed survey, T_2-weighted TSE sequences in the transverse (repetition time (TR) / echo time (TE)=7000/100ms, radiofrequency (RF) echo train length=16, flip angle=90 degrees, matrix=640x640, field of view (FoV)=250x400x59mm, slice thickness/gap=3/1mm, duration=294s) and sagittal plane (TR/TE=7000/100ms, RF echo train length=16, flip angle=90 degrees, matrix=640x640, FoV=250x400x73mm, slice thickness/gap=3/1mm, duration=294s) were created. Also, a T_2-weighted TSE axial oblique sequence (TR/TE=7000/100ms, RF echo train length=16, flip angle=90 degrees, matrix=512x512, FoV=350x250x39mm, slice thickness/gap=3/1mm, duration=322s) angled perpendicular to the cervical canal was performed. All T_2-weighted acquisitions had a voxel size of 0.7x0.8x3.0mm and used a SENSE parallel acquisition technique (parallel reduction factor: 3). All sequences remained within the maximum local SAR limit of 10W/kg [16].

RESULTS

Endorectal antenna tolerance

Of the 25 women who waived participation, only 1 chose not to partake because of objections against the use of the endorectal antenna. In addition to the predetermined sample of 20 patients, 3 women provided informed consent but could not be imaged due to system unavailability. See supplemental file 2 for the corresponding flowchart. The baseline characteristics of the scanned population are outlined in table 1.

Tolerance of the endorectal antenna was excellent, discomfort on the 10 point scale was 'minimal' at placement with a median score of 1 (range 0-5) and reported as 'none whatsoever' for removal with a median score of 0 (range 0-2). The single outlier of 5 at placement occurred in a patient who had undergone ligation of multiple haemorrhoids

1 month earlier. In contrast, a subject with a history of excisional haemorrhoidectomy 4 years earlier had uneventful placement (score: 0) and removal (score: 1). Comparable results were found in cases with irritable bowel syndrome, chronic obstipation and deep infiltrating endometriosis.

None of the participants reported pain or a heating sensation at any time, nor did any subject request preterm termination of the MRI session. The duration in the MRI with the antenna in situ was 48.0±7.3 minutes. One adverse event – unrelated to the antenna – was reported, namely <30 seconds of mild vertigo upon entering the 7.0T MRI bore.

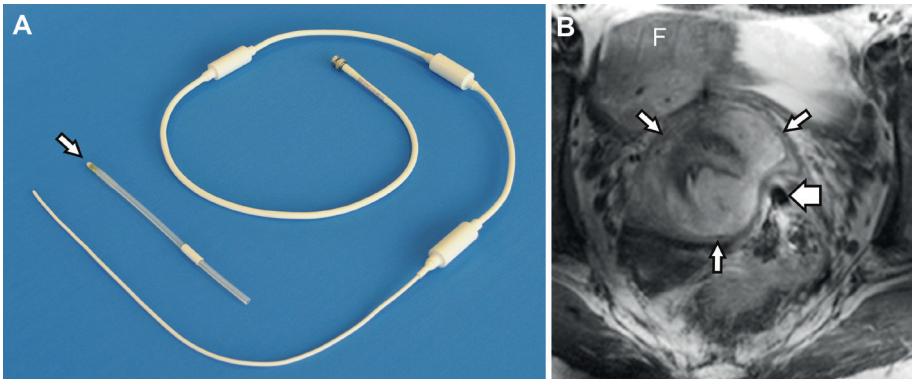

Figure 1. A) Overview of the monopole antenna shown with the 14 Fr Foley urinary catheter (arrow) removed. B) Transverse T_2-weighted 7.0T MRI of the inner female pelvis which demonstrates the close proximity of the endorectal monopole antenna (broad arrow) to this stage IB2 poorly differentiated papillary squamotransitional cell carcinoma of the cervix. Note the uterine fundus (F) and the T_2 hypointense fibrostromal ring surrounding the tumour (narrow arrows) indicative of absent parametrial invasion.

Cervical cancer imaging

Key to our focus on T_2-weighted imaging was the visualization of parametrial invasion, which is particularly challenging when subtle and in large tumours. Here, we present three exemplary cases which represent the range of physical examination and imaging results encountered. First, figure 2 presents a woman in whom the physical examination led to a stage IB2, in agreement with 1.5T and 7.0T MRI which indicated bilaterally absent parametrial invasion. The second example was clinically staged as IB2, though right sided parametrial invasion was suspected on both MRI's (Figure 3). This was motivated by unclear tumour demarcation against the parametrial fat on the right – more distinct on

7.0T MRI – and a locally interrupted T_2-hypointense fibrostromal ring. The third example was a bulky IIB based on left sided parametrial invasion at rectovaginal examination. However, the 7.0T MRI was considered suggestive of bilateral parametrial invasion (Figure 4). All three cases received chemoradiation, hence no definitive histological proof of invasion was provided. The mean interval between the clinical 1.5T and experimental 7.0T MRI was 13.7±11.8 days. None of the 9 included women with a clinical stage IB1 tumour had an unexpected histological finding of parametrial invasion following their radical surgery.

A prior loop excision, sharp conisation or both were performed in 3, 1 and 2 women, respectively. The interval of this surgery to the clinical 1.5T and 7.0T MRI was a median 42 days (range 32-44 days) and 47 days (range 41-57 days) respectively. After radical surgery, final histology did not show residual invasive tumour in any of these cases.

Artefacts

On sagittal acquisitions motion artefacts in the phase encoding direction, caused by breathing, occurred relatively frequent (Figure 5a). Secondly, non-essential anatomical regions were variably obscured by signal voids caused by destructive interference of B_1 – due to the short RF wavelength at 7.0T – from the multiple independent external transmit antennas (Figure 5b). Thirdly, superficial black semicircular inversion bands were present due to the inherently much higher B_1 levels directly under the elements of the external transmit/receive antenna array (Figure 5c). While encountered in all participants, it posed no clinical problem as only the subcutaneous fat was obscured. Fourthly, small SENSE reconstruction artefacts were incidentally seen, and are likely caused by destructive interference in the receive signals of the SENSE reference scan (Figure 5d).

Table 1. Baseline characteristics of the 20 women who underwent 7.0T MRI

Median age (range)	39.3 (25.3 – 66.5) years
Median BMI (range)	22.3 (18.4 – 36.7) kg/m^2
	N (percentage)
Parity	
0	9 (45%)
1	3 (15%)
2	8 (40%)
WHO performance status	
0	17 (85%)
1	3 (15%)
ASA classification	
1	13 (65%)
2	7 (35%)
Stage	
IB1	9 (45%)
IB2	4 (20%)
IIA1	1 (5%)
IIB	6 (30%)
Tumor histology	
Squamous cell carcinoma	10 (50%)
Adenocarcinoma	8 (40%)
Other	2 (10%)
Tumour differentiation	
Grade 1	3 (15%)
Grade 2	8 (40%)
Grade 3	7 (35%)
Not applicable	2 (10%)
LVSI present	5 (25%)
Lymph node metastases[1]	4 (20%)
Treatment	
Robot ass. laparoscopic SLN + PLND + RVT or RH	7 (35%)
Robot ass. laparoscopic SLN + PLND + RH + adjuvant Rth[2]	1 (5%)
Robot ass. laparoscopic SLN + PLND + Chemoradiation[3]	1 (5%)
PLND + RH via laparotomy[4]	1 (5%)
Chemoradiation	10 (50%)

[1] Determined by a composite of the SLN procedure, PLND or PET-CT as available.
[2] Adjuvant radiotherapy was indicated due to a <5mm resection margin.
[3] Chemoradiation substituted radical hysterectomy because of intraoperatively detected tumor-positive sentinel lymph nodes.
[4] After diagnosis and staging at our centre, this patient preferred treatment at a different hospital where no laparoscopic radical surgery was performed.

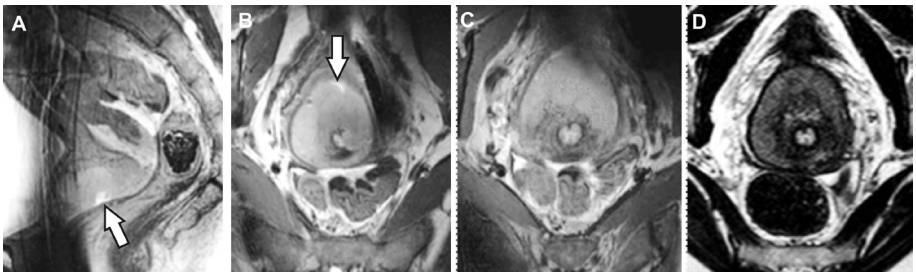

Figure 2. A) Mid-sagittal and B) axial oblique (perpendicular to the cervical canal) T_2-weighted slice at 7.0T of a 44 year old patient diagnosed with a 70 mm, stage IB2, poorly differentiated squamous cell carcinoma originating from the ventral part of the cervix. Note the visible biopsy site (arrow). C) Slice from the same sequence, though 12 mm cranially as figure 2B, depicting part of the healthy (T_2 hypointense) cervix invaded by tumour. D) axial oblique T_2-weighted slice from the clinical 1.5T MRI, created 17 days earlier, matched to figure 2C for comparison. Note the T_2 hypointense fibrostromal ring surrounding the tumour.

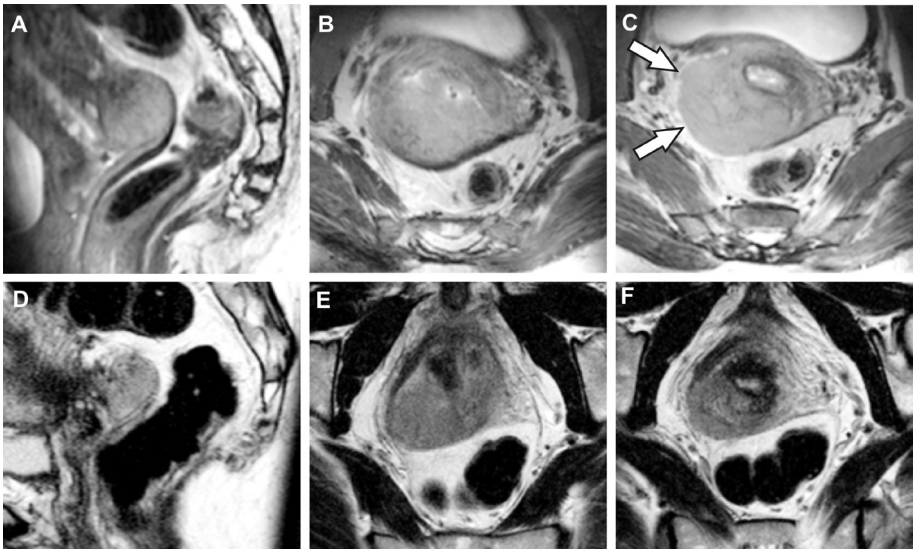

Figure 3. A) Sagittal and B) axial oblique T_2-weighted acquisitions from the 7.0T MRI of a 48 year old women diagnosed with a 80 mm poorly differentiated squamous cell carcinoma of the dorsal cervix. C) Slice from the same acquisition as (B), though positioned 12 mm cranially. Parametrial invasion was judged absent at rectovaginal palpation, leading to a clinical stage IB2. However, the unclear tumour demarcation and absent T_2 hypointense fibrostromal ring on the right (arrows) are suggestive of right sided parametrial invasion (i.e. stage IIB). D,E,F) The matched T_2-weighted axial oblique slices from the clinical 1.5T MRI, created 24 days earlier, are provided for comparison.

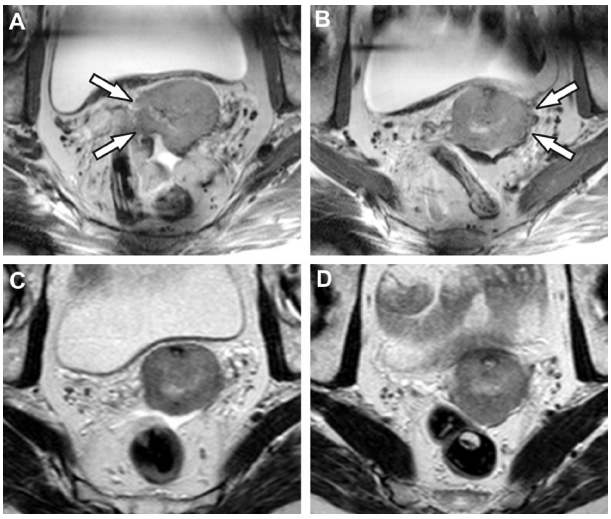

Figure 4. A) Transverse T_2-weighted acquisition from the 7.0T MRI of a 65 year old women diagnosed with a 50 mm moderately differentiated squamous cell carcinoma of the cervix. B) Slice from the same acquisition as (A), though positioned 8 mm cranially. Only left sided parametrial invasion was judged present at rectovaginal palpation, leading to a clinical stage IIB. However, the bilaterally unclear tumour demarcation and absent T_2 hypointense fibrostromal ring are suggestive of bilateral sided parametrial invasion (arrows). C,D) The matched transverse T_2-weighted slices from the clinical 1.5T MRI, created 16 days earlier, are provided for comparison. Note the free fluid in the rectouterine pouch (Douglas).

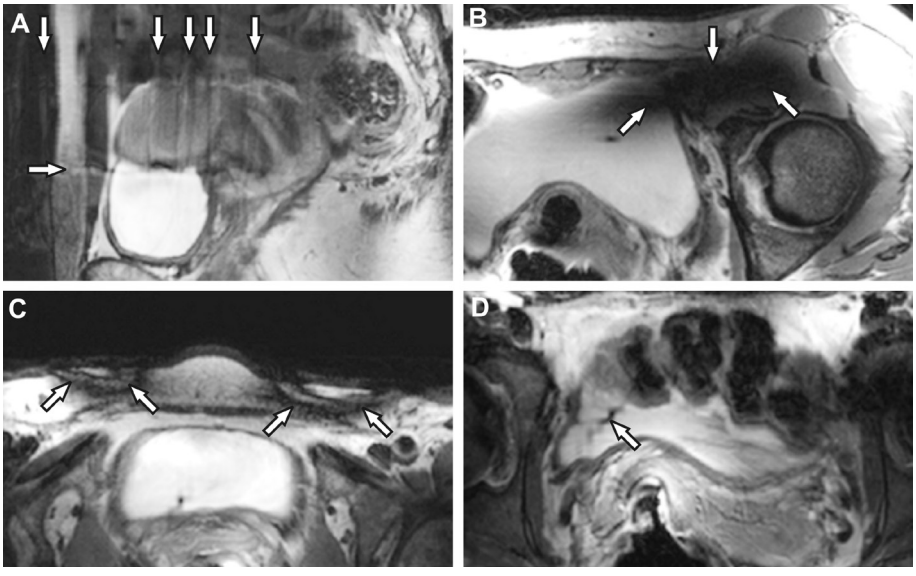

Figure 5. Image artefacts that were encountered on 7.0T MRI were A) motion artefacts, B) locally destructive B_1 interference, C) inversion bands due to too much B_1 under the external transmit/receive antennas and D) SENSE reconstruction artefacts. Note the unrelated vaginal tampon (asterisk) in (B).

DISCUSSION

This feasibility study showed that T_2-weighted cervical cancer imaging at 7.0T is achievable and that the incorporation of an endorectal antenna is well tolerated by patients. We have presented the acquired images, referenced against 1.5T MRI, relevant for local tumour assessment. To our knowledge, no literature currently exists on 7.0T MRI in cervical cancer, which in the past has been termed 'a considerable challenge' [17]. The presented study demonstrates a feasible approach to body imaging for pathology in the female pelvis.

Earlier research on 7.0T MRI in the female pelvis was obtained with an external coil array only, limited to healthy volunteers and reported moderate image quality of T_2-weighted sequences [18]. Our approach incorporated an endorectal monopole antenna for optimal signal capture, improving the SNR, deep in the inner pelvis [19]. Its use was not judged as uncomfortable, nor did it prohibit study accrual. Furthermore, in our small sample, no adverse events related to the antenna were encountered.

The research group led by Nandita deSouza has published extensively on their in-house build 37mm ring-shaped solenoid receive coil, placed endovaginally around the cervix, for 0.5-3.0T MRI in stage IA, IB1 and IIA cervical cancer [20,21]. Its application appears limited to relatively small lesions, though accurate in tumour detection and volume calculation [22,23,24]. Unfortunately, for parametrial invasion detection on T_2-weighted imaging no conclusions have thus far been reached on the added value of this solenoid receive coil [25]. In a recent study on radical surgery (n=25), only 1 patient had unexpected parametrial extension which was missed on MRI with the solenoid receive coil [25].

In line with the above, a limitation of our study is that none of the women clinically suspected of parametrial invasion had histological confirmation. The risk of partial verification bias is inherent to current practice guidelines which precludes radical surgery for women with tumour extension outside the cervix [6,7,26]. While definitive proof would have strengthened our case presentation, this was prohibited by the inherent design of our study which was not aimed at diagnostic accuracy.

Several technical challenges in our study on pelvic imaging at ultra-high field strength merit further explanation. The SNR advantage of the endorectal antenna is local, which limits the high resolution field of view in the feet-head direction and does not – for example – permit enhanced visualization of lymph nodes at the common iliac arteries [19]. While relevant for a clinical MRI protocol, this was not an objective of the current study which focused on the feasibility of primary tumour imaging. Secondly, at ultra-high field strengths the tissue RF power deposition is substantial and, in RF pulse intensive sequences like TSE used for T_2-weighted imaging, leads to SAR constraints. As a

consequence, the repetition time has to be increased, which lengthens the scan protocol. Internal antennas may, however, alleviate this by taking advantage of its highly non-uniform spatial field distribution that can be used for zoomed imaging or high imaging accelerations [14]. In addition, the short B_1 wavelength at ultra-high field strengths causes B_1 inhomogeneity and destructive interference, yielding artefacts which may obscure relevant parts of the inner pelvic anatomy. Using multi-dimensional RF pulses, these artefacts may be removed [27]. Our individualized B_1 shimming approach, made possible by using an external body array coil with multiple elements in parallel transmission, ensured that key anatomical regions of interest (i.e. the cervix) remained visible. Finally, the SENSE reconstruction algorithm that was implemented by the manufacturer, uses at the time of the study a reference scan with a constant amplitude and phase weighting during reception. This can cause destructive interferences during reception, causing artefacts (figure 5d). These artefacts can be mitigated using interferometry techniques [28].

Future studies should focus on whether our experimental imaging technique improves clinical decision making. This includes quantifying both the diagnostic test accuracy and observer variability (i.e. reproducibility). Furthermore, we focused on T_2-weighted imaging as it is relevant for local tumour assessment, though for clinical implementation additional sequences such as T_1-weighted MRI are desired [29]. The addition of functional imaging such as ^{1}H or ^{31}P MR spectroscopy – current experience in cervical cancer is limited to 1.5- 3.0T MRI – may benefit from the increased spectral and spatial resolution at ultra-high B_0 field strengths [30,31].

In conclusion, the use of an endorectal monopole antenna to improve the SNR at the level of the cervix was well tolerated by participants and not associated with any real discomfort, nor did it lead to adverse events or hinder study accrual. We established the feasibility of T_2-weighted cervical cancer imaging with 7.0T MRI. While further research is needed to reduce artefacts and substantiate its clinical impact, we demonstrated that high resolution T_2-weighted acquisitions deep in the female pelvis can be achieved with ultra-high field MRI. This combination of ultra-high field MRI and an internal antenna is promising and merits further research, including pelvic imaging for indications beyond cervical cancer.

Disclosure

The scientific guarantor of this publication is WB Veldhuis, MD PhD. The authors of this manuscript declare relationships with the following companies: DW Klomp has an interest of 4.9% in MR Coils BV. This study has received funding by the Dutch government via the STW (Stichting Technische Wetenschappen) technology foundation for the

development of the endorectal monopole antenna (grant 10822).
Institutional Review Board approval was obtained (reference: NL41056.041.13). Written informed consent was obtained from all subjects (patients) in this study. Methodology: prospective, experimental, performed at one institution.

Supplemental file 1. Standard clinical care, including 1.5T MRI sequence protocol.

At our tertiary referral centre, clinical staging adheres to FIGO and national cervical cancer guidelines. This includes a re-examination under anaesthesia when the outpatient exam is deemed or unreliable. All patients routinely undergo pelvic MRI on a 1.5T system (Achieva/Intera, Philips Medical systems, Best, the Netherlands) with an external sensitivity encoding (SENSE) torso coil only. The protocol consists of a transversal T_2-weighted TSE sequence (repetition time (TR) / echo time (TE)=6667/100ms, flip angle=90 degrees, matrix=400x280, Field of View (FoV)=320x320mm, slice thickness/gap=4/0mm), a sagittal T_2-weighted TSE sequence (TR/TE=2800/100ms, flip angle=90 degrees, matrix=424x280, FoV=300x240mm, slice thickness/gap=4/0mm) and a double-oblique T_2-weighted TSE sequence angled perpendicular to the cervical canal (TR/TE=3030/100ms, flip angle=90 degrees, matrix=400x280, FoV=320x320mm, slice thickness/gap=4/0mm). In addition, a transversal diffusion-weighted sequence (*b*-values: 0 and 800 s/mm^2), a transversal fat-saturated T_1-weighted sequence before and after intravenous gadolinium, and a transversal proton-density-weighted sequence of the entire abdomen were performed. In cases where a diathermic loop excision or a cold knife cone had been performed the clinical MRI was scheduled at least 30 days after such procedure to minimize tissue reaction, which may obscure residual tumour.
Stage IB1 and IIA1 patients were scheduled for a sentinel lymph node procedure with frozen section, pelvic lymph node dissection and radical hysterectomy or – in eligible patients desiring fertility preservation – a radical vaginal trachelectomy. In patients with tumour-positive (sentinel) lymph nodes, chemoradiation substituted radical uterine surgery. Stage IB2, IIA2 and IIB patients were treated primarily with chemoradiation. By design, treatment and stage decisions were uninfluenced by 7.0T MRI findings, which were not reported to clinicians.

Supplemental file 2. Flowchart of patient accrual into the study.

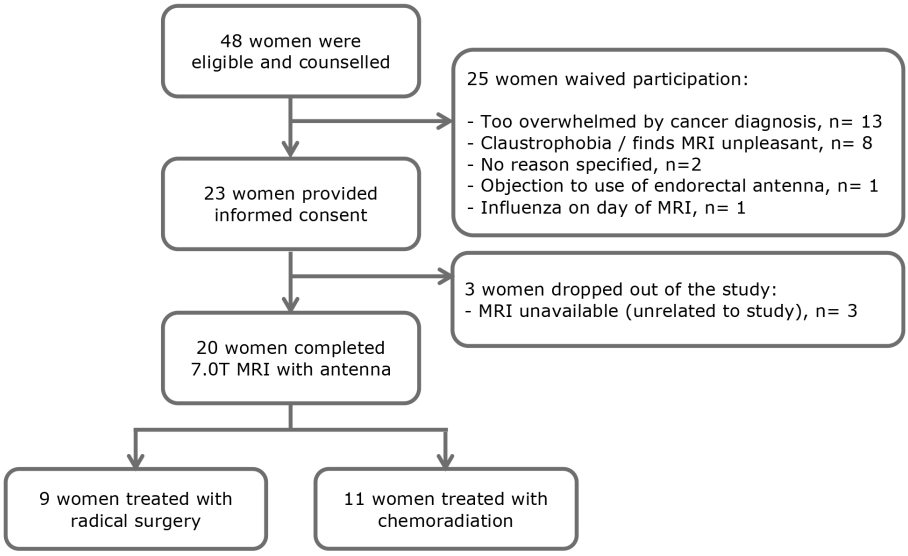

REFERENCES

1. FIGO Committee on Gynecologic Oncology. FIGO staging for carcinoma of the vulva, cervix, and corpus uteri. Int J Gynaecol Obstet. 2014 May;125(2):97-98.
2. Quinn M, Benedet J, Odicino F et al. 26th annual report of the international federation of gynaecology and obstetrics on the results of treatment in gynaecological cancer. Report of 2006 (26): S43-S104.
3. Qin Y, Peng Z, Lou J, et al. Discrepancies between clinical staging and pathological findings of operable cervical carcinoma with stage IB-IIB: a retrospective analysis of 818 patients. Aust NZJ Obstet Gynaecol. 2009 49(5): 542-544.
4. LaPolla JP, Schlaerth JB, Gaddis O, Morrow CP. The influence of surgical staging on the evaluation and treatment of patients with cervical carcinoma. Gynecol Oncol. 1986 Jun;24(2):194-206.
5. Odicino F, Tisi G, Rampinelli F, et al. New development of the FIGO staging system. Gynecol Oncol 2007;107(1 Suppl 1): S8–S9
6. Guideline cervical cancer, version 3.0, subsection; diagnostics. Available at www.oncoline.nl, a website from the Integraal kankercentrum Nederland (IKNL). Accessed January 15, 2014.
7. NCCN Clinical practice guidelline in Oncology. Cervical cancer. Version 3.2013. Available at www.nccn.org. Accessed January 20, 2014.
8. Thomeer MG, Gerestein C, Spronk S, van Doorn HC, van der Ham E, Hunink MG. Clinical examination versus magnetic resonance imaging in the pretreatment staging of cervical carcinoma: systematic review and meta-analysis. Eur Radiol. 2013 Jul;23(7):2005-2018.
9. Kuhl CK, Träber F, Schild HH. Whole-body high-field-strength (3.0-T) MR Imaging in Clinical Practice. Part I. Technical considerations and clinical applications. Radiology. 2008 Mar;246(3):675-696.
10. Ertürk MA, El-Sharkawy AM, Bottomley PA. Interventional loopless antenna at 7 T. Magn Reson Med. 2012 Sep;68(3):980-988.
11. Bump RC, Mattiasson A, Bø K, et al. The standardization of terminology of female pelvic organ prolapse and pelvic floor dysfunction. Am J Obstet Gynecol. 1996 Jul;175(1):10-17.
12. Hoogendam JP, Verheijen RH, Wegner I, Zweemer RP. Oncological outcome and long-term complications in robot-assisted radical surgery for early stage cervical cancer: an observational cohort study. BJOG. 2014 Nov;121(12):1538-1545.
13. National Cancer Institute, US department of health and human services. Common Terminology Criteria for Adverse Events (CTCAE), version 4.03. Available at http://evs.nci.nih.gov. Accessed May 31, 2013.

14. Raaijmakers AJ, Italiaander M, Voogt IJ, et al. The fractionated dipole antenna: A new antenna for body imaging at 7 Tesla. Magn Reson Med. 2015 DOI: 10.1002/mrm.25596.
15. Metzger GJ, Snyder C, Akgun C, Vaughan T, Ugurbil, K., van de Moortele PF. Local B1+ shimming for prostate imaging with transceiver arrays at 7T based on subject-dependent transmit phase measurements. Magn Reson Med 2008;59:396-409.
16. International Commission on Non-Ionizing Radiation Protection. Medical Magnetic Resonance (MR) Procedures: Protection of patients. Health Physics 2004;87(2):197-216
17. Norris DG. High field human imaging. J Magn Reson Imaging. 2003 Nov;18(5):519-29.
18. Umutlu L, Kraff O, Fischer A, et al. Seven-Tesla MRI of the female pelvis. Eur Radiol. 2013 Sep;23(9):2364-2373.
19. Kalleveen IM, Hoogendam JP, Raaijmakers AJ, et al. Boosting SNR with an internal antenna and external antennas in the human cervix uteri in TSE at 7T. Available at http://www.ismrm.org/14/program_files/EP05.htm. Accessed November 27, 2015.
20. Charles-Edwards EM, Messiou C, Morgan VA, et al. Diffusion-weighted imaging in cervical cancer with an endovaginal technique: potential value for improving tumor detection in stage Ia and Ib1 disease. Radiology. 2008 Nov;249(2):541-550.
21. deSouza NM, Scoones D, Krausz T, Gilderdale DJ, Soutter WP. High-resolution MR imaging of stage I cervical neoplasia with a dedicated transvaginal coil: MR features and correlation of imaging and pathologic findings. Am J Roentgenol. 1996 Mar;166(3):553-559.
22. Soutter WP, Hanoch J, D'Arcy T, Dina R, McIndoe GA, DeSouza NM. Pretreatment tumour volume measurement on high-resolution magnetic resonance imaging as a predictor of survival in cervical cancer. BJOG. 2004 Jul;111(7):741-747.
23. deSouza NM, Whittle M, Williams AD, et al. Magnetic resonance imaging of the primary site in stage I cervical carcinoma: A comparison of endovaginal coil with external phased array coil techniques at 0.5T. J Magn Reson Imaging. 2000 Dec;12(6):1020-1026.
24. deSouza NM, McIndoe GA, Soutter WP, et al. Value of magnetic resonance imaging with an endovaginal receiver coil in the pre-operative assessment of Stage I and IIa cervical neoplasia. BJOG 1998 May;105(5):500-507.
25. Downey K, Attygalle AD, Morgan VA, et al. Comparison of optimised endovaginal vs external array coil T2-weighted and diffusion-weighted imaging techniques for detecting suspected early stage (IA/IB1) uterine cervical cancer. Eur Radiol. 2015 Jul 11. [Epub ahead of print]
26. Colombo N, Carinelli S, Colombo A, Marini C, Rollo D, Sessa C. Cervical cancer: ESMO Clinical Practice Guidelines for diagnosis, treatment and follow-up. Ann Oncol. 2012 Oct;23 Suppl 7:vii27-32.
27. Malik SJ, Keihaninejad S, Hammers A, Hajnal JV. Tailored excitation in 3D with spiral

nonselective (SPINS) RF pulses. Magn Reson Med. 2012 May;67(5):1303-1315.
28. Brunner DO, Pruessmann KP. B1(+) interferometry for the calibration of RF transmitter arrays. Magn Reson Med. 2009 Jun;61(6):1480-1488.
29. Balleyguier C, Sala E, Da Cunha T, et al. Staging of uterine cervical cancer with MRI: guidelines of the European Society of Urogenital Radiology. Eur Radiol. 2011 May;21(5):1102-1110.
30. Payne GS, Schmidt M, Morgan VA, et al. Evaluation of magnetic resonance diffusion and spectroscopy measurements as predictive biomarkers in stage 1 cervical cancer. Gynecol Oncol. 2010 Feb;116(2):246-252.
31. Booth SJ, Pickles MD, Turnbull LW. In vivo magnetic resonance spectroscopy of gynaecological tumours at 3.0 Tesla. BJOG. 2009 Jan;116(2):300-303.

Chapter 5

The influence of the *b*-value combination on apparent diffusion coefficient based differentiation between malignant and benign tissue in cervical cancer

Jacob P. Hoogendam
Wenche M. Klerkx
Gerard A.P. de Kort
Shandra Bipat
Ronald P. Zweemer
Daisy M.D.S. Sie-Go
René H.M. Verheijen
Willem P.T.M. Mali
Wouter B. Veldhuis

J Magn Reson Imaging. 2010 Aug; 32(2):376-382.

ABSTRACT

Purpose: The purpose of this study was to analyze the influence of different *b*-value combinations on apparent diffusion coefficient (ADC)-based differentiation of known malignant and benign tissue in cervical cancer patients.

Methods: 35 patients with stage IB1, IB2, IIA cervical cancer underwent a 3.0T Magnetic Resonance Imaging scan prior to radical hysterectomy and pelvic lymph node dissection. Conventional T_1 and T_2-weighted sequences and a diffusion-weighted sequence (*b*=0,150,500,1000 s/mm²) were performed. Regions-of-interest were drawn on ADC maps derived from five different *b*-value combinations (0,500; 0,150,500; 0,1000; 0,150,500,1000; 150,500,1000 s/mm²). The influence of the *b*-value combination on ADC-based differentation of benign and malignant tissue was analyzed using receiver-operating-characteristics curves.

Results: For all *b*-value combinations, ADCs were significantly ($p<0.001$) lower in cervical malignancies ($1.15\pm0.21\cdot10^{-3}$; $1.10\pm0.21\cdot10^{-3}$; $0.97\pm0.18\cdot10^{-3}$; $0.97\pm0.23\cdot10^{-3}$ and $0.85\pm0.18\cdot10^{-3}$ mm²/s respectively to the aforementioned *b*-value combinations) than in benign cervix ($2.08\pm0.31\cdot10^{-3}$; $2.00\pm0.29\cdot10^{-3}$; $1.62\pm0.23\cdot10^{-3}$; $1.54\pm0.21\cdot10^{-3}$ and $1.42\pm0.22\cdot10^{-3}$ mm²/s respectively). The diagnostic accuracy was high for all *b*-value combinations and without statistical differences between the combinations.

Conclusion: ADC-based differentiation of benign from malignant cervical tissue is independent of the tested *b*-value combinations. The results support the inclusion and possible pooling of studies using different *b*-value combinations in meta-analyses on ADC-based tissue differentiation in cervical cancer.

Keywords: diffusion magnetic resonance imaging, apparent diffusion coefficient, uterine cervical neoplasms, sensitivity and specificity, *b*-value.

INTRODUCTION

Signal intensity in diffusion-weighted magnetic resonance (MR) imaging (DWI) is sensitive to the diffusion of intra- and extracellular watermolecules, which varies with anatomical structure and with pathology [1]. Changes in cellular architecture [2,3] and increases in cellularity [4,5], associated with cervical malignancy, result in hindered water diffusion compared to healthy cervix [6]. This difference between benign and malignant cervical tissue allows for DWI-based tumor detection [1,7,8,9,10]. The apparent diffusion coefficient (ADC) is a derived quantitative measure of water diffusion in a voxel. ADC mapping allows for a more objective comparison between tissues (e.g. malignant versus benign) than evaluation of DWI signal intensity alone. An additional advantage of parametric mapping is the removal of T_2-shine-through effects that are associated with the long echo-time needed for diffusion-weighting [11].

The ADC is calculated by fitting the signal intensities from DWI datasets acquired with a minimum of two different *b*-values (the *b*-value combination) to the Stejskal-Tanner equation [12]. A frequently used combination is 0 and 1000 s/mm^2, but even within studies regarding the same primary tumors, *b*-values vary widely between investigators [13]. Furthermore, curve-fitting with more than two *b*-values reduces the error in ADC calculation, leading to even more variation in choice of *b*-values [14]. For cervical cancer there is no clear evidence what constitutes an ideal *b*-value combination for ADC calculation leading to a lack of standardization in the use of DWI for the detection of (cervical) malignancies. This variability raises uncertainty about whether individual ADC outcomes can be generalized and compared.

The objective of this study is to investigate the influence of the *b*-value combination on the diagnostic accuracy of ADC-based differentiation of malignant and benign tissue in cervical cancer patients.

MATERIALS AND METHODS

Population

Between January 2006 and September 2008, we included all patients with biopsy proven cervical cancer who were about to undergo a presurgical MRI scan in one of two tertiary referral centers before undergoing radical hysterectomy. We subsequently excluded all patients in whom final pathological analysis showed the surgical specimen to be tumor-free (which can result from prior exconisation of the transformation zone). Since this is a descriptive study without a hypothesis to be tested, no formal sample size calculation

was performed. The inclusion criteria were: 1) histologically proven cervical cancer FIGO (International Federation of Gynecology and Obstetrics) stage IB1 to IIA, 2) A score >70 out of 100 on the Karnofsky performance status scale, which quantifies the general well-being of cancer patients, 3) age >18 years. Exclusion criteria were general contraindications to MRI, such as pacemaker, aneurysm clips or claustrophobia. This study was approved by both institutional Medical Research Ethics Committees. All patients provided informed consent prior to participation.

Magnetic Resonance Imaging

In both centers patients were scanned on a 3.0T Philips MRI scanner (Philips Medical Systems, Best, the Netherlands) with either a 6-channel sensitivity encoding (SENSE) torso coil or a 6-channel SENSE cardiac coil. The scanning parameters were identical for both centers. The conventional sequences consisted of a transversal T_2-weighted turbo spin echo (TSE) (matrix: 800x800, field of view (FOV): 360x360 mm, repetition time (TR) / echo time (TE): 3441/80 ms, slice thickness/gap: 4/0 mm, number of signal averaging (NSA): 3, sequence duration: 4:48 min); a T_2-weighted TSE sequence with SPAIR (spectral attenuation and inversion recovery) fat suppression, in a transversal and sagittal plane (matrix: 800x800, FOV: 360x360 mm, TR/TE: 2888/80 ms, slice thickness/gap: 4/0 mm, NSA: 3, sequence duration: 6:43 min); and a transversal T_1-weighted fast field echo (FFE) (matrix: 512x512, FOV: 360x360 mm, TR/TE: 393/2.3 ms, slice thickness/gap: 4/0 mm, NSA: 2, sequence duration: 5:02 min). Free breathing diffusion-weighted images were acquired using a single shot echo planar imaging sequence (matrix: 256x256, FOV: 400x400 mm, TR/TE: 5000/54 ms, b=0,150,500,1000 s/mm^2, slice thickness/gap: 4/0 mm, NSA: 3, sequence duration: 8:30 min).

Data analysis

A radiologist with 8 years of experience in pelvic MRI reviewed all conventional T_1- and T_2-weighted scans according to standard clinical practice. The radiologist was informed that all patients underwent this MRI scan in a research setting for cervical cancer patients, but he was blinded to all other data, including information concerning the aim of the study, clinical and pathological results. During review, malignant cervical tissue was marked using standard vendor supplied software (Sectra PACS, Philips Medical Systems, Best, The Netherlands) in three orthogonal directions on the transversal and sagittal fat-suppressed T_2-weighted dataset. The radiologist was allowed to consult all available conventional sequences while evaluating the cervical tumor. Remaining representative benign cervical tissue was marked on a single transversal T_2-weighted slice if possible. During review, tumor invasion into the uterus, parametria, vagina, bladder and rectum

was scored. Image quality was scored as well, moderate or poor, and the corresponding reason was noted.

Further image-analysis was done using in-house software created in MATLAB (Mathworks, USA). Regions-of-interest (ROIs) of the tumor were drawn on all slices of the fat-suppressed T_2-weighted data set, as indicated by the reviewing radiologist. ADC maps were calculated by fitting the assumed-mono-exponential signal decay to the Stejskal-Tanner equation using a least-squares approach. Five ADC maps were calculated based on different *b*-value combinations for each patient: 1) ADC map based on *b*=0,500 s/mm^2, 2) *b*=0,150,500 s/mm^2, 3) *b*=0,1000 s/mm^2, 4) *b*=0,150,500,1000 s/mm^2, and 5) *b*=150,500,1000 s/mm^2. ROIs were automatically copied from the T_2-weighted dataset to the ADC maps (Figure 1). After automatic copying, manual adaptation of the ROI was allowed to correct for any patient movement or image distortion. Tumor ADC was determined by averaging the ADC values of all voxels in the ROI from the largest transversal cross section of the tumor. Benign ADCs were calculated by drawing a ROI on the ADC map, based on the marked remaining cervical tissue by the reviewing radiologist.

Histopathologic analysis

After MR imaging, all patients underwent a radical hysterectomy combined with pelvic lymph node dissection. The specimen, consisting of the uterus including cervix, vaginal cuff, parametria and locoregional lymph nodes, was analyzed by a pathologist with over 20 years' experience in gynaecological oncology, who was blinded to MRI findings. After a macroscopic review, formaldehyde fixation, sectioning, hematoxylin and eosin staining the specimen was, amongst others, reviewed for tumorspread, its histological type and tumor differentiation scored as either well, moderate or poor. The lymph nodes were examined for locoregional metastasis.

Statistical analysis

For the five different *b*-value combinations ADCs from malignant tumor and benign cervical stroma were compared using a paired Student's t-test. Receiver operating characteristics (ROC) curves were then plotted for analysis of optimal ADC cut-off values, defined by the highest Youden index (sensitivity + specificity – 1). Corresponding sensitivity, specificity and area under the curve (AUC) with 95% confidence intervals (CI) were calculated. The AUCs of all combinations were statistically compared using the DeLong test. P-values <0.05 were considered statistically significant. Statistical Package for the Social Sciences (SPSS inc, Chicago, Illinois, USA) version 15.0 for windows was used.

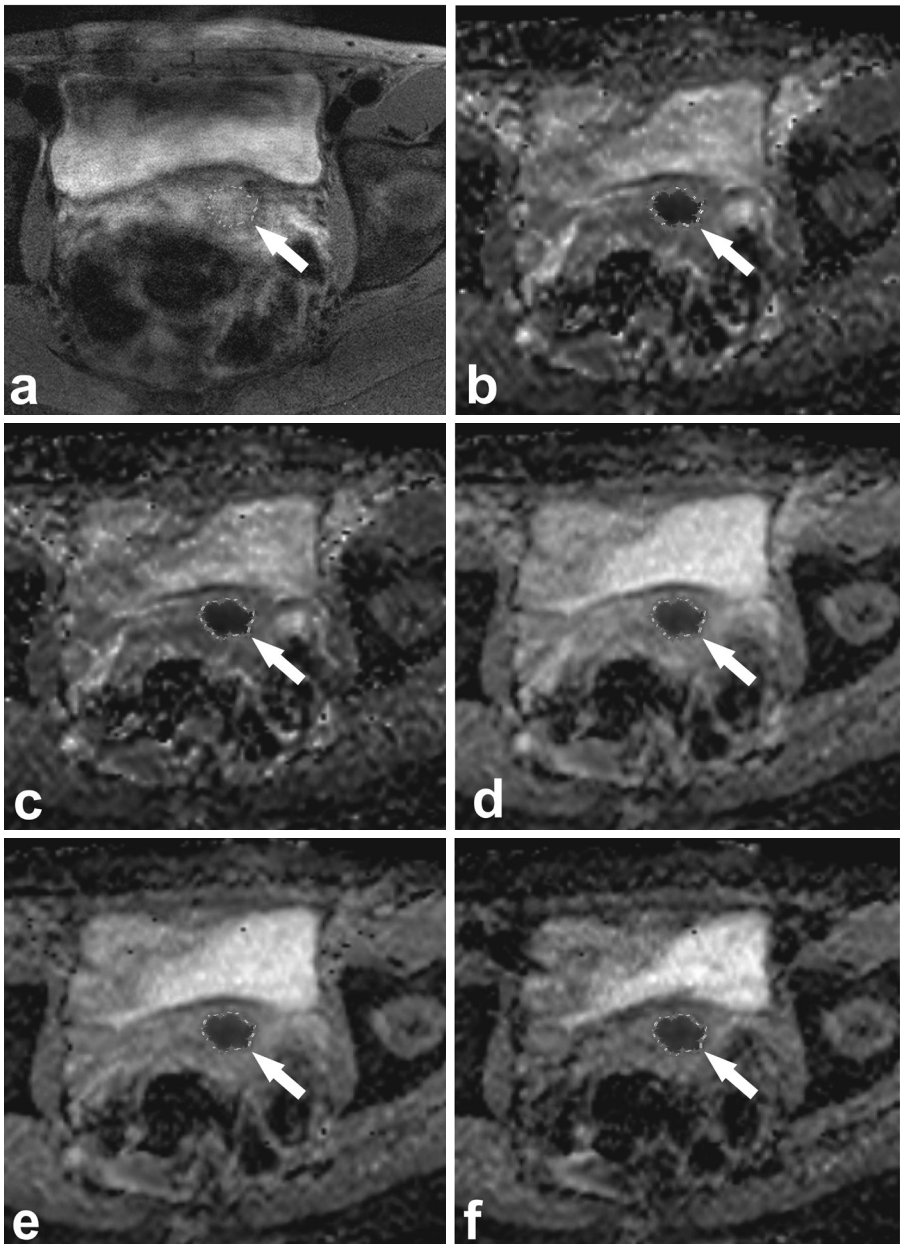

Figure 1. Patient with stage IB1 cervical cancer (white arrow), marked with a ROI. A) fatsuppressed T_2-weighted sequence, B) corresponding ADC map from b=0,500 s/mm^2, C) b=0,150,500 s/mm^2, D) b=0,1000 s/mm^2, E) b=0,150,500,1000 s/mm^2, F) b=150,500,1000 s/mm^2.

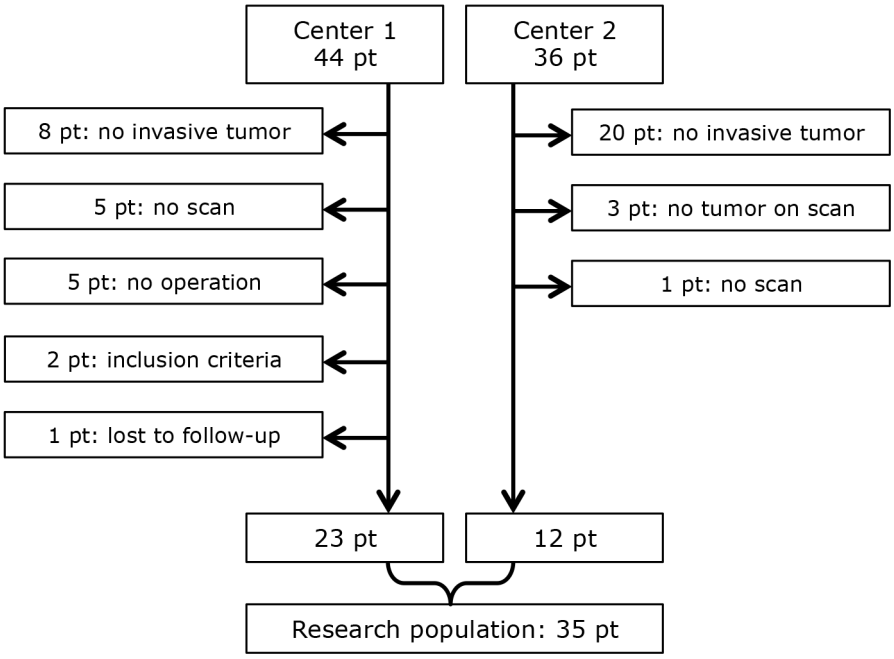

Figure 2. Flowchart of patient exclusion. Pt = patients.

RESULTS

Patient population

A flowchart of the total number of included patients is shown in Figure 2. From 80 eligible patients, 28 (35.0%) patients were excluded because no invasive tumor in the final surgical specimen was found. In most cases a prior procedure - cone biopsy or loop excision - had produced insufficient margins making a re-operation necessary. Six (7.5%) patients did not receive a preoperative scan because of too limited time between inclusion in the study and surgery. Five (6.3%) patients did not undergo a radical hysterectomy because an alternative treatment was chosen. Three (3.8%) patients did not have a tumor visible on MRI, but a small malignancy was present at histopathological examination. Retrospectively, two patients (2.5%) did not meet the inclusion criteria due to misclassification of tumor-type or -stage. One (1.3%) patient was transferred to another center and lost during follow-up.

Table 1 summarizes the baseline characteristics of the research population from both referral centers (n=35). The median age was 43.2 years (range 38.0-49.4), the predominant stage and histologic type were IB1 (n=30; 85.7%) and squamous cell carcinoma respectively (n=24; 68.6%). No statistically significant differences were found in the demographics, tumor grade and histologic type, between both centers.

Image quality

Image quality of the conventional datasets was well in 25 (71.4%), moderate in eight (22.9%) and poor in two (5.7%) cases. The main cause of reduced quality was motion artifacts (n=6/10). Other causes were: artifacts related to a prior invasive procedure to the cervix (n=3/10) and vaginal fluids around the tumor with comparable signal intensity (n=1/10). No significant difference in scan quality was found between both centers (p=0.733). Image quality of the diffusion weighted data sets was well in 27 (77.1%), moderate in six (17.1%) and poor in two (5.7%) cases. The cause of reduced quality was ghosting artifacts from patient motion (n=8/8). The image quality of the DWI datasets was comparable in both centers (p=0.111).

Influence of *b*-value combination on ADC-based tissue differentiation

For all *b*-value combinations, ADCs were significantly ($p<0.001$) lower in cervical malignancies ($1.15\pm0.21\cdot10^{-3}$ mm^2/s; $1.10\pm0.21\cdot10^{-3}$ mm^2/s; $0.97\pm0.18\cdot10^{-3}$ mm^2/s; $0.97\pm0.23\cdot10^{-3}$ mm^2/s and $0.85\pm0.18\cdot10^{-3}$ mm^2/s respectively to the combinations *b*=0,500; 0,150,500; 0,1000; 0,150,500,1000; 150,500,1000 s/mm^2) than in benign cervix ($2.08\pm0.31\cdot10^{-3}$ mm^2/s; $2.00\pm0.29\cdot10^{-3}$ mm^2/s; $1.62\pm0.23\cdot10^{-3}$ mm^2/s; $1.54\pm0.21\cdot10^{-3}$ mm^2/s and $1.42\pm0.22\cdot10^{-3}$ mm^2/s respectively) (Table 2). For these very low p-values, correcting for multiple comparisons still resulted in statistically significant results. Figure 3 shows the mean ADCs of malignant and benign cervical tissue for all combinations of *b*-values used.

Figure 4 shows the ROC curves created for all the *b*-value combinations. Table 3 presents the derived optimal ADC cut-off values based on the highest Youden index, and the corresponding diagnostic accuracy. The *b*-value combinations are equally accurate in differentiating between benign and malignant tisue, for there are no statistically significant differences between all combinations tested. (Table 4)

There were two false negative cases (i.e. malignant ADC higher than the benign ADC): both found with *b*=0,150,500,1000 s/mm^2 and both showing a relatively high malignant ADC of 1.50 and $1.35\cdot10^{-3}$ mm^2/s, and a benign ADC in the normal range for the *b*-value combination, 1.42 and $1.28\cdot10^{-3}$ mm^2/s respectively.

Table 1. Characteristics of the research population including statistical significance of the differences between the inclusion centers. Number of patients (percentage per center) unless otherwise noted

	Center 1 n (%)	Center 2 n (%)	p-value
Patients (percentage of total)	23 (65.7)	12 (34.3)	
Median age in years (range)	43.0 (39.2-46.8)	43.7 (38.0-49.4)	0.380
Median scan-surgery interval in days (range)	16.8 (9.5-24.0)	19.7 (15.9-23.6)	0.246
FIGO stage			
IB1	20 (87.0)	10 (83.3)	0.890
IB2	2 (8.7)	1 (8.3)	
IIA	1 (4.3)	1 (8.3)	
Histopathological type			
Squamous cell carcinoma	18 (78.3)	6 (50.0)	0.112
Adenocarcinoma	4 (17.4)	6 (50.0)	
Adenosquamous carcinoma	1 (4.3)	0 (0.0)	
Lymph node metastasis			
Present	5 (21.7)	0 (0.0)	0.081
Absent	18 (78.3)	12 (100.0)	

Table 2. Mean ADCs with standard deviations for malignant and benign cervical tissue for each *b*-value combination, with p-values

***b*-value combination (s/mm²)**	**ADC malignant (mm²/s)**	**ADC benign (mm²/s)**	**p-value**
0,500	$1.15 \pm 0.21 \cdot 10^{-3}$	$2.08 \pm 0.31 \cdot 10^{-3}$	<0.001
0,150,500	$1.10 \pm 0.21 \cdot 10^{-3}$	$2.00 \pm 0.29 \cdot 10^{-3}$	<0.001
0,1000	$0.97 \pm 0.18 \cdot 10^{-3}$	$1.62 \pm 0.23 \cdot 10^{-3}$	<0.001
0,150,500,1000	$0.97 \pm 0.23 \cdot 10^{-3}$	$1.54 \pm 0.21 \cdot 10^{-3}$	<0.001
150,500,1000	$0.85 \pm 0.18 \cdot 10^{-3}$	$1.42 \pm 0.22 \cdot 10^{-3}$	<0.001

ADC: Apparent Diffusion Coefficient

Table 3. Optimal ADC cut-off values for each *b*-value combination with corresponding AUC, sensitivity, specificity and Youden Index (sensitivity + specificity – 1)

***b*-value combination (s/mm²)**	**ADC cut-off (mm²/s)**	**AUC (95%CI)**	**Sensitivity**	**Specificity**	**Youden Index**
0,500	$1.650 \cdot 10^{-3}$	0.997 (0.990-1.000)	97.1%	100.0%	0.971
0,150,500	$1.535 \cdot 10^{-3}$	0.998 (0.993-1.000)	97.0%	100.0%	0.970
0,1000	$1.200 \cdot 10^{-3}$	0.982 (0.959-1.000)	93.8%	90.6%	0.844
0,150,500,1000	$1.185 \cdot 10^{-3}$	0.965 (0.924-1.000)	96.9%	90.6%	0.875
150,500,1000	$1.115 \cdot 10^{-3}$	0.978 (0.951-0.998)	90.6%	93.7%	0.843

ADC: Apparent Diffusion Coefficient, AUC: Area Under the Curve, CI: Confidence Interval

Table 4. statistical comparison of AUCs for all *b*-value combinations. Given in p-values

***b*-value combination (s/mm²)**	**0,150,500**	**0,1000**	**0,150,500,1000**	**150,500,1000**
0,500	0.908	0.533	0.442	0.496
0,150,500	X	0.497	0.424	0.466
0,1000	X	X	0.718	0.910
0,150,500,1000	X	X	X	0.791

AUC: Area Under the Curve, X: comparison with identical or reciproke combination

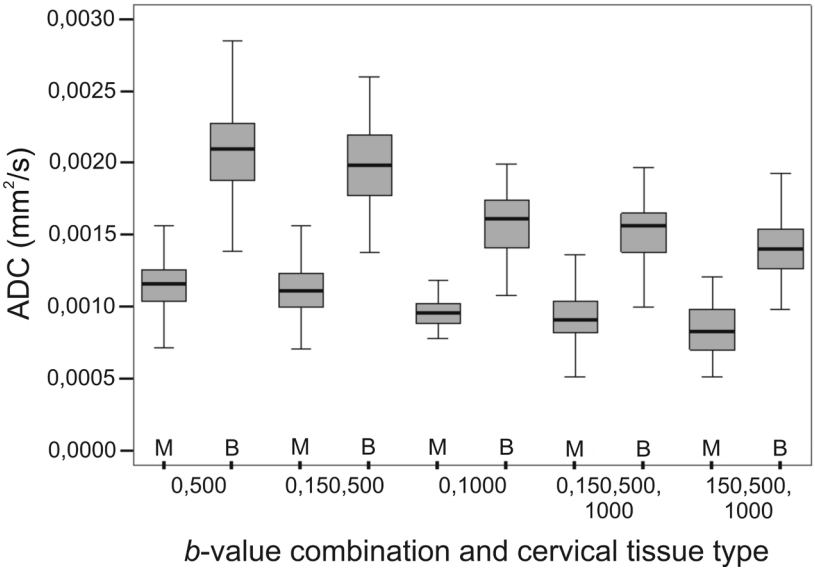

Figure 3. Comparison of apparent diffusion coefficient (ADC) values between malignant (M) and benign (B) cervical tissue, for all *b*-value combinations.

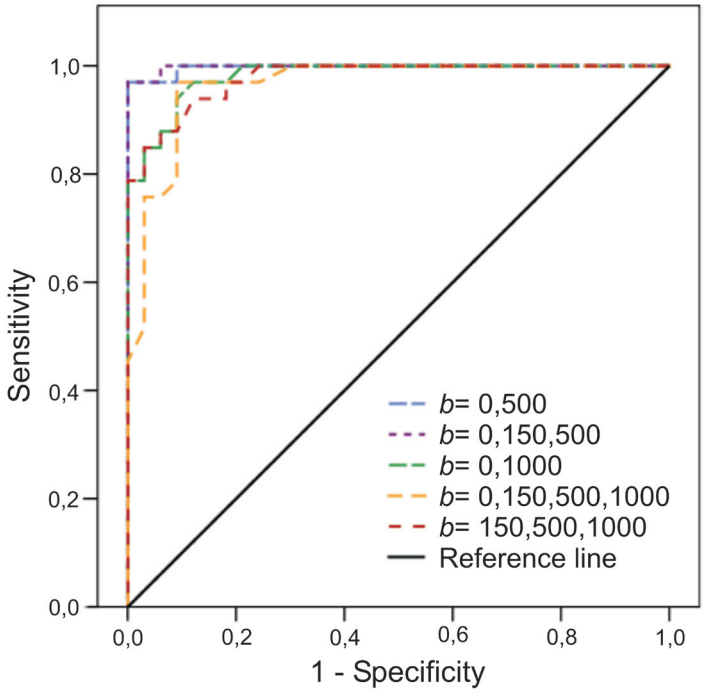

Figure 4. Receiver-Operating-Characteristics (ROC)-curves for the five *b*-value combinations.

DISCUSSION

We have shown that DWI can differentiate between malignant and benign cervical tissue on the basis of ADC, and that the discriminatory power of the ADC is maintained over a range of five frequently used *b*-value combinations.

Two recent studies on cervical cancer used combinations comparable to our lowest two *b*-values (*b*=0,500 and 0,150,500 s/mm²) and found similar results. McVeigh et al [8] scanned 47 patients with cervical cancer and 26 healthy controls at *b*=0,600 s/mm² and reported malignant cervical ADCs of 1.09±0.20·10⁻³ mm²/s compared to benign 2.09±0.46·10⁻³ mm²/s (p<0.001). The second study [9] performed DWI (*b*=0,300,600 s/mm²) to investigate the effect of chemoradiation therapy on the ADC of cervical cancer. In 12 patients a mean malignant ADC of 1.09±0.20·10⁻³ mm²/s and benign of 1.79±0.24·10⁻³ mm²/s (p<0.001) was found before therapy.

Ho et al [15] used *b*=0,1000 s/mm² for ADC calculation at 3.0T and found a mean cervical tumor ADC of 0.89±0.14·10⁻³ mm²/s. Harry et al [16] found a mean cervical tumor ADC of 1.25±0.18·10⁻³ mm²/s using *b*=0,1000 s/mm² for ADC calculation.

One study applied *b*=0,800 s/mm² for cervical cancer patients (n=33) and reported a mean malignant ADC of 1.11±0.18·10⁻³ mm²/s compared to 1.59±0.15·10⁻³ mm²/s (p<0.001) for benign cervix [10]. Their optimal cut-off value, calculated by ROC analysis, was 1.36·10⁻³ mm²/s (AUC 0.971) and had a sensitivity of 100% with specificity of 84.4%. These results are comparable to our findings at *b*=0,1000 s/mm².

In other primary malignancies of the pelvic region, DWI has been successfully adopted. Prostate cancer patients are extensively investigated, with results comparable to ours on cervical cancer. ADC calculation with *b*=0,1000 s/mm² allows for accurate detection of prostate malignancies and shows lower ADCs in malignant tissue relative to benign [17,18,19,20].

In the English literature, no studies on cervical cancer with a combination of four *b*-values identical to ours (*b*=0,150,500,1000 s/mm²) were found. Charles-Edwards et al [21] did use four *b*-values, (*b*=0,300,500,800 s/mm²), and showed a mean malignant cervical ADC of 0.76±0.11·10⁻³ mm²/s (stage IB1, n=19) and a mean benign tissue ADC of 1.33±0.16·10⁻³ mm²/s (p<0.001). At cut-off 1.10·10⁻³ mm²/s a sensitivity of 88.2% and a specificity of 99.9% was found. Another DWI study [22] on uterine pathologies (n=107) with a relatively comparable *b*-value combination of 0,500,1000 s/mm² reported benign cervical ADC of 1.71±0.17·10⁻³ mm²/s and lower ADCs for cervical cancer; 0.91±0.14·10⁻³ mm²/s (p<0.001). No cervical cancer studies excluding *b*=0 s/mm² were identified. By excluding *b*=0 s/mm² (*b*=150,500,1000 s/mm²) we aimed to study the effect

of separating perfusion- or flow-insensitive from flow-sensitive ADC values [11]. This is quantified by lower ADC outcomes [14]. Although we did indeed obtain lower ADCs when excluding *b*=0 s/mm² from the fit, the discriminatory power of ADC was sufficient to allow tissue differentiation when vascular contributions were eliminated. These results are in keeping with existing literature as investigated in brain [23] and parotid gland lesions [24].

Theoretically, lower mean ADC values should be obtained when using a higher maximum *b*-value. Indeed, in our study, combinations with a higher maximum *b*-value produced lower mean ADCs for both benign an malignant tissue. This was paired to a smaller absolute difference in ADCs between malignant and benign tissues. With respect to this effect: when comparing combinations with a lower maximum *b*-value (thus resulting in overall higher mean ADCs) to combinations with a higher maximum *b*-value, the relative decrease in ADC caused by using a higher *b*-value, is stronger in benign tissue than in malignant cervical tissue. Even though all combinations by themselves had ample discriminating power, comparison of relative ADC changes between different *b*-value combinations may make an interesting point for future studies.

Finally, lower maximum *b*-values allow slightly shorter echo–times to be used which is advantageous for sequence planning.

Some limitations of our study merit further explanation. First, a single radiologist reviewed the MRI scans; therefore, the effect of inter-observer variation on the results could not be tested. Additionally, scanning was performed on a 3.0T MR system while most clinical work, including many of the above mentioned DWI studies, used 1.5T scanners. However, in theory ADC values are not influenced by the main magnetic field strength, which is supported by - a limited number of - studies directly comparing ADCs at both field strengths [25,26].

The absence of statistical differences between our optimal ADC-cut-offs from all five *b*-value combinations indicates equal diagnostic performances. However, ultimately, the sensitivity and specificity were calculated on a research population whom all had histologically proven malignancies of the cervix. By identifying benign cervix from the same population, followed by ADC calculation, it functioned as its own control group. By thus enabling paired-samples *t*-testing, statistical significance is more easily reached in this setting. This also means there were no genuinely healthy controls for the sensitivity and specificity calculation of our optimal ADC cut-offs. However, the goal of the current study was not to determine sensitivity and specificity per se, but rather to study the effect of the choice of *b*-value combination on the discriminatory power of the ADC.

In this study we used a mono- instead of a bi-exponential fit for ADC calculation. This was decided from a pragmatic viewpoint. In order to reliable use bi-exponential fitting,

a more substantial range of *b*-values than our current four are required [27,28]. This is disadvantageous for clinical application due to time constraints and would reduce the external validity of our results. Furthermore, the perfusion component from *b*=0 s/mm^2 influences the bi-exponential fit greatly and should therefore be avoided [29], this leaves a maximum of three *b*-values for calculation and reduces possible combinations to be tested.

In conclusion, the ADC reliably differentiated cervical malignancies from benign cervical tissue at all evaluated *b*-value combinations. The potential diagnostic accuracy was independent of the evaluated *b*-value combinations. The results support the inclusion and possible pooling of studies using different *b*-value combinations in future meta-analyses on ADC-based tissue differentiation in cervical cancer.

REFERENCES

1. Namimoto T, Awai K, Nakaura T, Yanaga Y, Hirai T, Yamashita Y. Role of diffusion-weighted imaging in the diagnosis of gynecological diseases. Eur Radiol 2009: 19:745-760.
2. Herneth AM, Guccione S, Bednarski M. Apparent diffusion coefficient: a quantitative parameter for in vivo tumor characterization. Eur J Radiol 2003:45:208-213.
3. Szafer A, Zhong J, Gore JC. Theoretical model for water diffusion in tissues. Magn Reson Med 1995:33:697-712.
4. Anderson AW, Xie J, Pizzonia J, Bronen RA, Spencer DD, Gore JC. Effects of cell volume fraction changes on apparent diffusion in human cells. Magn Reson Imaging 2000:18:689-695.
5. Zelhof B, Pickles M, Liney G et al. Correlation of diffusion-weighted magnetic resonance data with cellularity in prostate cancer. BJU Int 2009:103:883-888.
6. Whittaker CS, Coady A, Culver L, Rustin G, Padwick M, Padhani AR. Diffusion-weighted MR imaging of female pelvic tumors: a pictorial review. Radiographics 2009:29:759-774.
7. Nishie A, Stolpen AH, Obuchi M, Kuehn DM, Dagit A, Andresen K. Evaluation of locally recurrent pelvic malignancy: performance of T2- and diffusion-weighted MRI with image fusion. J Magn Reson Imaging 2008:28:705-713.
8. McVeigh PZ, Syed AM, Milosevic M, Fyles A, Haider MA. Diffusion-weighted MRI in cervical cancer. Eur Radiol 2008:18:1058-1064.
9. Naganawa S, Sato C, Kumada H, Ishigaki T, Miura S, Takizawa O. Apparent diffusion coefficient in cervical cancer of the uterus: comparison with the normal uterine cervix. Eur Radiol 2005:15:71-78.
10. Chen J, Zhang Y, Liang B, Yang Z. The utility of diffusion-weighted MR imaging in cervical cancer. Epub: Eur J Radiol 2009 May 11. DOI 10.1016/j.ejrad.2009.04.025
11. Koh DM, Takahara T, Imai Y, Collins DJ. Practical aspects of assessing tumors using clinical diffusion-weighted imaging in the body. Magn Reson Med Sci 2007:6:211-224.
12. Stejskal EO, Tanner JE. Spin diffusion measurements: spin echoes in the presence of time-dependent field gradient. Journal of Chemical Physics 1965:42:288-292.
13. Koh DM, Padhani AR. Diffusion-weighted MRI: a new functional clinical technique for tumour imaging. Br J Radiol 2006:79:633-635.
14. Koh DM, Collins DJ. Diffusion-weighted MRI in the body: applications and challenges in oncology. AJR Am J Roentgenol 2007:188:1622-1635.
15. Ho KC, Lin G, Wang JJ, Lai CH, Chang CJ, Yen TC. Correlation of apparent diffusion coefficients measured by 3T diffusion-weighted MRI and SUV from FDG PET/CT in

primary cervical cancer. Eur J Nucl Med Mol Imaging 2009:36:200-208.
16. Harry VN, Semple SI, Gilbert FJ, Parkin DE. Diffusion-weighted magnetic resonance imaging in the early detection of response to chemoradiation in cervical cancer. Gynecol Oncol 2008:111:213-220.
17. Kim CK, Park BK, Han JJ, Kang TW, Lee HM. Diffusion-weighted imaging of the prostate at 3 T for differentiation of malignant and benign tissue in transition and peripheral zones: preliminary results. J Comput Assist Tomogr 2007:31:449-454.
18. Issa B. In vivo measurement of the apparent diffusion coefficient in normal and malignant prostatic tissues using echo-planar imaging. J Magn Reson Imaging 2002:16:196-200.
19. Hosseinzadeh K, Schwarz SD. Endorectal diffusion-weighted imaging in prostate cancer to differentiate malignant and benign peripheral zone tissue. J Magn Reson Imaging 2004:20:654-661.
20. Pickles MD, Gibbs P, Sreenivas M, Turnbull LW. Diffusion-weighted imaging of normal and malignant prostate tissue at 3.0T. J Magn Reson Imaging 2006:23:130-134.
21. Charles-Edwards EM, Messiou C, Morgan VA et al. Diffusion-weighted imaging in cervical cancer with an endovaginal technique: potential value for improving tumor detection in stage Ia and Ib1 disease. Radiology 2008: 249:541-550.
22. Kilickesmez O, Bayramoglu S, Inci E, Cimilli T, Kayhan A. Quantitative diffusion-weighted magnetic resonance imaging of normal and diseased uterine zones. Acta Radiol 2009:50:340-347.
23. Le Bihan D, Breton E, Lallemand D, Aubin ML, Vignaud J, Laval-Jeantet M. Separation of diffusion and perfusion in intravoxel incoherent motion MR imaging. Radiology 1988:168:497-505.
24. Thoeny HC, De KF, Boesch C, Hermans R. Diffusion-weighted imaging of the parotid gland: Influence of the choice of b-values on the apparent diffusion coefficient value. J Magn Reson Imaging 2004:20:786-790.
25. Habermann CR, Gossrau P, Kooijman H et al. Monitoring of gustatory stimulation of salivary glands by diffusion-weighted MR imaging: comparison of 1.5T and 3T. AJNR Am J Neuroradiol 2007:28:1547-1551.
26. Matsuoka A, Minato M, Harada M et al. Comparison of 3.0-and 1.5-tesla diffusion-weighted imaging in the visibility of breast cancer. Radiat Med 2008:26:15-20.
27. Shinmoto H, Oshio K, Tanimoto A et al. Biexponential apparent diffusion coefficients in prostate cancer. Magn Reson Imaging. 2009:27:355-359.
28. Mulkern RV, Barnes AS, Haker SJ et al. Biexponential characterization of prostate tissue water diffusion decay curves over an extended b-factor range. Magn Reson Imaging. 2006:24:563-568.

29. Riches SF, Hawtin K, Charles-Edwards EM, de Souza NM. Diffusion-weighted imaging of the prostate and rectal wall: comparison of biexponential and monoexponential modelled diffusion and associated perfusion coefficients. NMR Biomed. 2009:22:318-325.

PART 2:

Sentinel lymph node imaging in cervical cancer

Chapter 6

Preoperative sentinel node mapping with ^{99m}Tc-nanocolloid SPECT-CT significantly reduces the intraoperative sentinel node retrieval time in robot assisted laparoscopic cervical cancer surgery

Jacob P. Hoogendam
Monique G.G. Hobbelink
Wouter B. Veldhuis
René H.M. Verheijen
Paul J. van Diest
Ronald P. Zweemer

Gynecol Oncol. 2013 May; 129(2):389–394.

ABSTRACT

Objective: To compare preoperative sentinel node (SN) mapping with planar lymphoscintigraphy (LSG) to single photon emission computed tomography with computed tomography (SPECT-CT) for differences in intraoperative SN retrieval time in surgically treated cervical cancer patients.

Methods: In cervical cancer patients planned for radical surgery, one day preoperatively, 220-290 MBq technetium-99m-nanocolloid was injected intracervically in four quadrants. Subsequent SN mapping was performed by either LSG (09.2009 – 03.2011) or SPECT-CT (03.2011 – 10.2012). The SN resection, by four armed robot assisted laparoscopy, was based on blue dye and technetium-99m and followed by pelvic lymph node dissection. Timing of perioperative care, including SN procedure times, was prospectively registered.

Results: Out of 62 subjects included, 33 (53.2%) underwent LSG and 29 (46.8%) SPECT-CT. No significant differences in baseline characteristics were observed. Bi- and unilateral SN visualization rates were 75.8% and 15.2% for LSG versus 86.2% and 6.9% for SPECT-CT ($p=0.299$ and $p=0.305$, respectively). Intraoperative bi/unilateral SN detection occurred in 84.8% and 9.1% of LSG subjects versus 89.7% and 3.4% for SPECT-CT ($p=0.573$ and $p=0.616$). Correlation in SN location between mapping and surgery was low for LSG (Spearman $\rho=0.098$; $p=0.449$) but high in SPECT-CT ($\rho=0.798$; $p<0.001$). Bilateral intraoperative SN retrieval times for LSG and SPECT-CT were 75.4±33.5 and 50.1±15.6 minutes, resulting in an average difference of 25.4 minutes ($p=0.003$).

Conclusion: SPECT-CT significantly reduces intraoperative SN retrieval with a clinically relevant time compared to LSG. The trend towards better bilateral visualization rates and significantly higher anatomical concordance may partly explain the observed difference in SN retrieval time.

Keywords: Cervical cancer surgery; sentinel node procedure; preoperative mapping; planar lymphoscintigraphy; SPECT-CT.

INTRODUCTION

In stage IB1 cervical cancer, radical hysterectomy with pelvic lymph node dissection (PLND) is the treatment of choice. Final histopathology will reveal locoregional lymph nodal macrometastasis in 19.5% of cases and an additional 6.2% of micrometastases when ultrastaging is performed [1]. While not an integrative part of the International Federation for Gynecology and Obstetrics (FIGO) staging system, nodal status is an independent prognostic and therapeutic factor [2]. In patients with tumor-positive lymph nodes, additional chemoradiotherapy is warranted, which would have been given as the primary treatment without surgery [3]. Furthermore, the five-year disease specific survival is reduced to 61.8% compared to 94.4% in node negative patients [4].

Sentinel node (SN) procedures in cervical cancer are an increasingly well evaluated patient-tailored practice to assess lymph nodal status at the onset of surgical treatment [1,5,6,7,8]. When performed correctly, false negative rates of 1.3% are achieved [8]. Combined use of technetium-99m-nanocolloid and blue dye enables intraoperative unilateral SN detection in 89–100% of cases, but bilateral detection has been reported in 47–94% of cases [9,10,11]. Efficient intraoperative SN localization of nodes surrounding the retroperitoneal pelvic vasculature remains a practical challenge. Lymph nodes are located in close anatomical relation to the ureters and critical nerves which innervate the legs, bladder, rectum and those essential to sexual functionality. This, and the large surface area of the small pelvis, inhibits efficient surgical retrieval of the SN, often necessitating a complete retroperitoneal exploration. Such a procedure is time-consuming, hazardous and destroys the lymph vessel architecture which would have been spared by a direct SN procedure.

Preoperative SN localization with nuclear medicine imaging techniques is increasingly adopted to alleviate this issue. Currently, this includes planar lymphoscintigraphy (LSG) or single photon emission computed tomography with X-ray computed tomography (SPECT-CT). Studies on preoperative LSG have questioned its predictive value based on the poor correlation to the number and localization of surgically retrieved SN's [12,13,14]. While recent literature has proven superior SN detection rates for SPECT-CT [15,16,17,18], its effect on surgical performance in terms of SN retrieval time has not yet been evaluated.

We primarily investigated the difference in intraoperative SN retrieval times between preoperative SN mapping by LSG and SPECT-CT. Secondarily, quality parameters for both mapping techniques were studied. These include SN visualization and intraoperative detection rates, mapping failure rates, the correlation between mapping and intraoperative procedural failure, and the anatomical concordance in SN locations between mapping and surgery.

METHODS

Patients

We have performed a retrospective analysis of a cervical cancer cohort in which the perioperative time points were prospectively collected. All patients were consecutively treated between September 2009 and October 2012 at our tertiary referral center. Subjects were included when the following criteria were met; 1) histopathologically proven primary cervical cancer, and 2) a planned robot assisted laparoscopic SN procedure with preoperative SN mapping. Subjects who received neo-adjuvant chemotherapy were excluded [19]. Eligible candidates were retrieved from the departmental database for robot assisted surgery in gynecological oncology. All procedures were standard clinical care, for which usual informed consent was obtained.

Planar lymphoscintigraphy

Between September 2009 and March 2011 LSG was the standard preoperative SN mapping technique for cervical cancer patients at our center. Via a speculum aided vaginal examination, 220–290 MBq technetium-99m-nanocolloid (General Electric Healthcare, Eindhoven, The Netherlands) was injected, using a 25 G needle, into the cervical stroma at 4 quadrants directly peripheral of the tumor. Injection was always performed by an experienced gynecological oncologist with assistance of a nuclear medicine consultant. The moment of injection was standardized to 3 o'clock p.m. one day preoperatively, which generated a consistent 17 hour interval to surgery. Approximately 10 minutes post-injection, a dynamic planar LSG sequence (40 images, 30 seconds each) from the anterior and posterior positions was commenced (Forte gamma camera, Philips Healthcare, Best, The Netherlands). At 30 and 90 minutes post-injection, static planar LSG was performed from the anterior, posterior, left and right lateral positions (Figure 1). When SN's could not be visualized bilaterally, a second imaging session with static four-sided LSG could be performed the following day directly preceding surgery.

A nuclear physician reviewed all images preoperatively. A written report was created which minimally included a detailed description of the injection procedure, technetium-99m-nanocolloid dosing, the performed imaging procedure, the number and location of all visualized SN.

SPECT-CT

From March 2011 to October 2012 all cervical cancer patients scheduled for a SN procedure underwent preoperative SN mapping with SPECT-CT. All procedural steps, up to and including the technetium-99m-nanocolloid injection, were identical to the above

described methodology for LSG. No changes in personnel, time of injection or dosing of the radiopharmaceutical were made. SPECT-CT was performed 90 minutes post-injection on a single integrated SPECT-CT system (Symbia T16, Siemens, Erlangen, Germany). The low dosed abdominal CT (0.8–2.0 mSv) was performed with a patient dependent current between 24–60 mAs at 110 kV (Figure 1).
The SPECT-CT dataset was reviewed by the same nuclear physicians and reported in detail, identically to the LSG procedure. Also, when SN visualization was unsuccessful, a second imaging session with four-sided static planar LSG could be performed directly preoperatively.

Intraoperative SN procedure

Stage IA1-2 (multifocal disease and additional risk factors), IB1 and IIA patients were scheduled for a SN procedure, PLND and radical hysterectomy, or if fertility preservation was desired radical vaginal trachelectomy. Criteria for trachelectomy eligibility were: tumor diameter ≤2 cm, clear resection margins at histology and tumor-negative locoregional lymph nodes. In individual cases, considered to have an >10% risk of lymph nodal metastasis, trachelectomy was performed in a separate (second) session after the initial SN procedure and PLND.
Two gynecological oncologists specialized in both conventional and robot assisted laparoscopy (RV/RZ) performed all robot assisted gynecological surgeries. A four armed surgical robotic system, (da Vinci®, Intuitive Surgical, Sunnyvale, USA) was used during the entire study. After general anesthesia, an injection system designed for four quadrant intracervical injection with 2.5% patent blue dye solution (Bleu Patenté V, Guerbet Group, Roissy, France) was positioned. This system enables the surgeon to remotely inject dye (i.e. without vaginal manipulation) immediately before retroperitoneal exploration while the robotic system is docked and regardless of leg positioning, draping or Trendelenburg angles (Figure 2). After peritoneal cavity insufflation to 24 mmHg, a 11 mm supra-umbilical trocar was introduced for the optics. Two 8mm robotic trocars were positioned 8–10 cm laterally to the left and right of the umbilicus. A third 8mm robotic trocar was located above the right iliac crest. Finally, a 12 mm trocar was placed directly lateral of Palmer's point to allow retrieval of specimens by the assistant [20]. In 28 degrees Trendelenburg and reduced intra-abdominal pressure to 14 mmHg, the robotic system was docked and the desired surgical equipment introduced.
Through the prepositioned injection system, 0.5–1.0 ml patent blue was injected intracervically in each quadrant. After inspection and mobilization of the sigmoid colon, the retroperitoneal pelvic space was bilaterally opened. For each hemipelvis, SN exploration started at the lymph nodal station where the preoperative mapping had

predicted a SN. A laparoscopic gamma probe (Europrobe 3 Coelioscopique, Euromedical Instruments, Le Chesnay, France) simultaneously assisted the visual detection of dye stained nodes.

Sentinel nodes were defined as the first lymph node(s) of each hemipelvis to receive afferent lymphatic drainage from the primary cervical tumor, identified by either blue dye or gamma radiation, but preferably both. After SN dissection, residual radioactivity of the surgical site was measured to prevent missing additional SN's and deemed negative if background counts were <10% of the SN count.

After the SN procedure, the PLND was completed by resection of all lymphoid tissue from the obturator fossa and around the common, internal and external iliac vessels. In patients with tumor-negative SN upon cryosectioning, surgery was continued by robot assisted laparoscopic radical hysterectomy or radical vaginal trachelectomy. When planned in a separate second session cryosectioning was omitted. Uterine surgery was abandoned and substituted by chemoradiotherapy when cryosectioning revealed SN metastases.

For monitoring and research purposes, time points of all relevant perioperative steps were prospectively registered. The start of the laparoscopy was defined as the moment of skin incision for pneumoperitoneal insufflation. Time points of left and right SN extraction from the abdominal cavity were scored. The SN retrieval time was defined as the interval between the start of laparoscopy and bilateral SN extraction.

Statistical analysis

Statistical calculations were performed with the 'Statistical Package for the Social Sciences' version 20.0.0 (International Business Machines, New York, USA). Intergroup differences were tested with a X^2-test in categorical data or student's *t*-testing for numeric variables. SN localization for each mapping technique was cross tabulated against surgery, with correlation quantification by Spearman's rank testing. An identical procedure was performed for the correlation between mapping success and intraoperative SN procedural success. SN retrieval times were normality tested. Statistical significance was set at $p<0.05$.

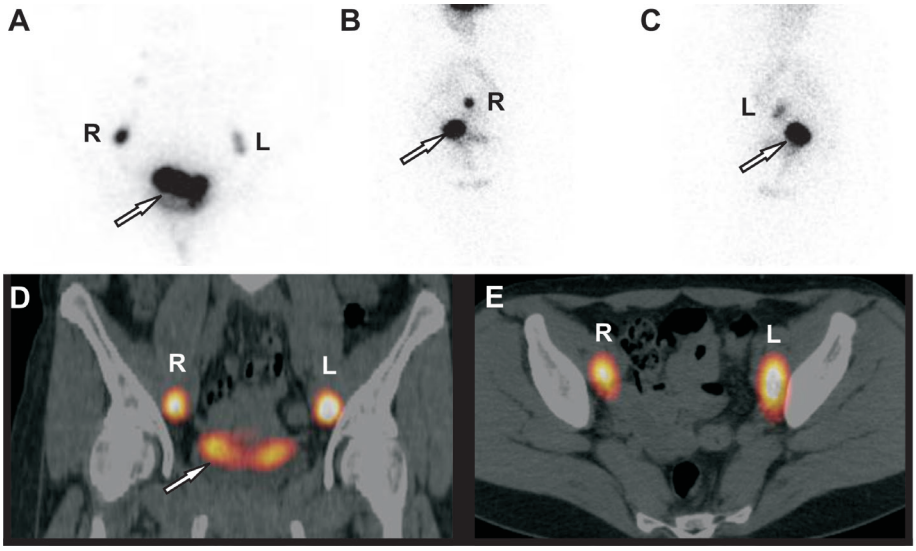

Figure 1. Preoperative sentinel node mapping by LSG and SPECT-CT. A) Static coronal lymphoscintigraphy created 90 minutes post-injection in a 39 year old female with stage IB1 squamous cell carcinoma of the cervix. Corresponding right (B) and left (C) lateral plane. Based on LSG both sentinel nodes (SN) were scored in the general iliac region (R: right, L: left), however, the intra-operative SN procedure (85 minutes) located the right SN at the iliac bifurcation and the left SN in the obturator fossa. Note the residual activity visible from the intracervical injection site (arrow). D) Coronal and axial (E) SPECT-CT at 90 minutes postinjection in a 38 year old women with a stage IB1 squamous cell carcinoma of the cervix. Both SN were localized in the obturator fossa upon SPECT-CT review, which was concordant to the anatomical location during the intra-operative SN procedure (44 minutes).

Figure 2. System for remote dye injection during surgery. After general anesthesia, via a speculum aided vaginal examination, a butterfly type needle is positioned peripherally of the tumor in each cervical quadrant. The connected flexible tubing runs transvaginally to the externally placed system. Color coded valves allow dye injection to be controlled for each quadrant separately, when so desired by the surgeon. A standard 5 or 10ml syringe functions as a reservoir for the patent blue dye and its compression results in intracervical dye injection. Note the unrelated urinary catheter (asterisk).

RESULTS

Population

The study population comprised 62 subjects, of whom 33 (53.2%) underwent planar LSG and 29 (46.8%) SPECT-CT. The median age at diagnosis was 38 years (range 24 – 81 years). Median parity was 1 (range 0 – 5) with 37.1% nulliparous women. Thirteen (21.0%) had a prior conisation and 27 (43.5%) a large loop excision of the transformation zone. Clinical staging resulted in 2 IA1 (3.2%), 1 IA2 (1.6%), 57 IB1 (91.9%), and 2 IIA cases (3.2%). Histopathology showed squamous cell carcinoma, adenocarcinoma and adenosquamous cell carcinoma in 44 (71.0%), 17 (27.4%) and 1 (1.6%) subject(s). Grade I, II, III or undefined tumor differentiation was present in 11 (17.7%), 35 (56.5%), 11 (17.7%) and 5 (8.1%) subjects, respectively. No significant differences in baseline characteristics were observed between the LSG and SPECT-CT population (range p=0.131 – 0.639) (Table 1).

SN mapping

Standard session LSG visualized 71 SN's (left/right 39/32) in 33 subjects with bilateral, unilateral or no SN visualization in 25 (75.8%), 3 (9.1%) and 5 (15.2%) cases, respectively. Eight subjects (24.2%) had a second - preoperative - session which identified 2 additional SN's, totaling 73 SN's (left/right 40/33). Final bi- and unilateral SN visualization was achieved in 25 (75.8%) and 5 (15.2%) cases, with no SN visualization in 3 (9.1%) subjects.
SPECT-CT depicted 58 SN's (left/right 27/31) in 29 subjects with bilateral, unilateral or no SN visualization in 23 (79.3%), 4 (13.8%) and 2 (6.9%) cases, respectively. Four (13.8%) underwent a second imaging session which resulted in 60 SN's (left/right 28/32). The final bi- and unilateral SN visualization was 25 (86.2%) and 2 (6.9%) cases, with no SN visualization in 2 (6.9%) subjects. No significant differences in bi- or unilateral SN visualization rates (range p=0.299 – 0.739) or the need for a second imaging session (p=0.473) were observed between both modalities (Table 2).

Intraoperative SN procedure

In the planar LSG group, 82 SN's were identified intraoperatively of which 62 (75.6%) were preoperatively mapped. Intraoperative SN detection occurred bilaterally in 28 (84.8%), unilaterally in 3 (9.1%) and yielded no SN in 2 (6.1%) subjects. For the SPECT-CT group, 64 SN's were surgically found, of which 53 nodes (82.8%) had been mapped preoperatively. Bi- and unilateral intraoperative SN detection were established in 26 (89.7%) and 1 (3.4%) case(s), with no SN detected in 2 (6.9%) subjects. No significant difference in bilateral (p=0.573) or unilateral (p=0.616) SN detection was observed.
Anatomical SN location as predicted by LSG did not correlate to the intraoperative location

(Spearman ρ=0.098; p=0.449). In contrast, SN localized by SPECT-CT did significantly correlate to surgery (ρ=0.798; p<0.001) (Table 3). Correlation of imaging to blue dye stained SN locations only was not significant for both LSG (ρ=0.214; p=0.096) and SPECT-CT (ρ=0.234; p=0.092). Failure of initial LSG session correlated significantly with failure of the intraoperative procedure (ρ=0.520; p=0.002). In SPECT-CT this correlation was not significant (ρ=0.314; p=0.097).

Time registration was complete in 48 cases, 27 (81.8%) with LSG and 21 (72.4%) with SPECT-CT. The average bilateral SN retrieval time of 75.4±33.5 minutes in planar LSG and 50.1±15.6 minutes in SPECT-CT differed significantly (p=0.003) by 25.4 minutes (95%CI: 9.3 - 41.5). Learning curve effects did not influence SN retrieval times, as tested by comparing the first half of the LSG group against the second half, which did not yield a significant time difference (p=0.252).

Six cases (18.2%) in the LSG group had lymph nodal metastases. Three were correctly identified by a bilaterally successful mapping and intraoperative SN procedure. Two had a tumor-positive non-SN at a hemipelvis where no SN could intraoperatively be detected at that side. One subject had bilaterally tumor-negative SN yet 1 metastatic parametrial non-SN was discovered. In the SPECT-CT group, 4 subjects (13.8%) had lymph nodal metastases which were all exclusively present in their SN. All had bilateral SN visualization on mapping and bilateral intraoperative SN detection.

Table 1. Displays the baseline characteristics for both subgroups with statistical significance testing of the distributions between the respective groups

	Planar LSG (n= 33)	**SPECT-CT** (n= 29)	**p-value**
Median age in years (range)	38 (24-62)	38 (26-81)	0.406
Median parity (range)	1 (0-4)	2 (0-5)	0.236
Prior cervical procedure			
Conisation	5 (15.2%)	8 (27.6%)	0.461
LLETZ	16 (48.5%)	11 (37.9%)	
Biopsy only	12 (36.4%)	10 (34.5%)	
FIGO Stage			
IA1	0 (0.0%)	2 (6.9%)	0.131
IA2	1 (3.0%)	0 (0.0%)	
IB1	32 (97.0%)	25 (86.2%)	
IIA	0 (0.0%)	2 (6.9%)	
Histological type			
Squamous cell carcinoma	23 (69.7%)	21 (72.4%)	0.639
Adenocarcinoma	9 (27.3%)	8 (27.6%)	
Adenosquamous cell carcinoma	1 (3.0%)	0 (0.0%)	
Differentiation			
Grade I	5 (15.2%)	6 (20.7%)	0.436
Grade II	22 (66.7%)	13 (44.8%)	
Grade III	5 (15.2%)	6 (20.7%)	
Undefined	1 (3.0%)	4 (13.8%)	

LSG; lymphoscintigraphy, SPECT-CT; single photon emission computed tomography - computed tomography, LLETZ; large loop excision of the transformation zone, FIGO; International Federation for Gynecology and Obstetrics

Table 2. Sentinel node visualization and detection rates for both subgroups with statistical significance testing between the two respective modalities

		Planar LSG (n= 33)	**SPECT-CT** (n= 29)	**p-value**
		N (%)	**N (%)**	
After 1st Session	Bilateral SN visualization	25 (75.8%)	23 (79.3%)	0.739
	Unilateral SN visualization	3 (9.1%)	4 (13.8%)	0.696
Subjects with a second imaging session[1]		8 (24.2%)	4 (13.8%)	0.299
Including 2nd Session	Bilateral SN visualization[1]	25 (75.8%)	25 (86.2%)	0.299
	Unilateral SN visualization[1]	5 (15.2%)	2 (6.9%)	0.305
Surgery	Bilateral SN detection	28 (84.8%)	26 (89.7%)	0.573
	Unilateral SN detection	3 (9.1%)	1 (3.4%)	0.616

[1] When indicated, by only unilateral or no sentinel nodes detectable during the initial imaging, a second imaging session with static planar LSG was performed directly preoperative.
SN; sentinel node(s), LSG; lymphoscintigraphy, SPECT-CT; single photon emission computed tomography - computed tomography

Table 3. Shows the anatomical sentinel node locations found during mapping (rows) cross tabulated against the locations found at surgery (columns)

		SN location during intraoperative procedure							
	SN location during SN mapping	Parametrium	Obturator	Internal Iliac	External Iliac	Common Iliac	Iliac bifurcation	Other[1]	Total
Planar LSG	Parametrium	2	0	0	0	0	0	1	3
	Obturator	0	8	0	1	0	0	0	9
	Internal Iliac	0	0	0	0	0	0	0	0
	External Iliac	0	0	0	6	0	0	2	8
	Common Iliac	0	1	0	0	0	0	0	1
	Iliac bifurcation	0	0	0	0	0	5	0	5
	Iliac region, unspecified	0	7	10	11	0	5	1	34
	Other[1]	0	0	0	0	0	0	2	2
	Total	2	16	10	18	0	10	6	62
SPECT-CT	Parametrium	0	0	0	0	0	0	0	0
	Obturator	0	19	0	0	0	0	0	19
	Internal Iliac	0	1	2	0	0	0	1	4
	External Iliac	0	2	1	18	0	0	0	21
	Common Iliac	0	0	0	0	1	0	0	1
	Iliac bifurcation	0	0	1	0	0	1	0	2
	Iliac region, unspecified	0	0	2	2	0	0	0	4
	Other[1]	0	0	0	0	0	0	2	2
	Total	0	22	6	20	1	1	3	53

[1] This category comprises incidental SN locations and is condensed for clarity reasons. It includes SN found near the round ligament, uterine artery or in the inguinal, paravesical or presacral region.
SN; sentinel node(s), LSG; lymphoscintigraphy, SPECT-CT; single photon emission computed tomography - computed tomography

DISCUSSION

We observed a reduction in SN retrieval times for SPECT-CT versus LSG. The 3D tomographic nature and anatomical reference of SPECT-CT have likely attributed to the stronger correlation in SN localization to surgery. Indeed, for over half of the SN's discovered on LSG the anatomical location could not be specified beyond 'the general iliac region'. Hence, the preoperative knowledge on where to expect the SN was more accurate in the SPECT-CT group. This allowed less retroperitoneal exploration which consequently reduced the SN retrieval time. Furthermore, the observed trend of higher SN visualization rates on SPECT-CT and the association between mapping failure and intraoperative SN procedural failure may further explain why SPECT-CT reduced retrieval times.

The second correlation calculated between mapping and surgery, selective to the SN found based on their blue dye staining, was not significant for both imaging modalities. This reaffirms the benefit of intra-operative technetium-99m activity measurements, which may even be a prerequisite for achieving an optimal effect from preoperative SPECT-CT mapping.

Strengths of this study are the procedural consistency and independent correlation of the two mapping modalities to the surgical findings. To our knowledge, all studies comparing LSG with SPECT-CT have applied both techniques sequentially in the same patient [15,16,17,18], making the assessment of surgical time reductions impossible. Moreover, SN retrieval times have previously not been compared but constitute a clinically relevant endpoint.

Robot assisted laparoscopy is increasingly adopted in cervical cancer surgery and results in significantly less blood loss and shorter hospital admissions [21]. Its use in this study influences how the presented results and conclusions should be interpreted. The observed SN retrieval times, defined as the interval between first skin incision and SN removal, would be considered long in a non-robotic setting. However, besides insufflation and fivefold trocar placement, this period also includes positioning, docking and testing of the robotic system. Conventional laparoscopic SN procedures may result in shorter time intervals. However, the actual difference is unlikely to be affected since the setup procedure was identical in both groups.

Planar LSG was initially introduced to provide preoperative information on the localization of SN by technetium-99m-nanocolloid uptake, which increased the intraoperative detection [22,23]. However, the two dimensionality limits the accuracy of SN localization and some institutions have omitted LSG despite continuing with technetium-99m-nanocolloid for intraoperative SN detection [24].

Pandit et al compared SPECT-CT against LSG, with both modalities applied in the same patient. In ten cervical cancer subjects, they found a higher unilateral detection rate (100% vs. 80%) and stated that SPECT-CT allowed more accurate SN localization [18]. The high unilateral detection rate of SPECT-CT was confirmed at 95% in a larger cohort (n=41) which similarly indicated superior SN topography [17]. Without reporting detection rates or anatomical concordance, Diaz and colleagues demonstrated that SPECT-CT detected more nodes in five of their 22 subjects [16]. Limitations of these studies are the conclusions on superior SN topography with SPECT-CT, while the correlation between mapping and surgery has not been formally quantified or statistically tested on a node by node basis. A recent report (n=10) observed a 100% concordance in SN location between SPECT-CT and surgery [15]. Our study proves that SPECT-CT does perform significantly better in this respect when compared to LSG.

While evidence for SPECT-CT as a beneficial SN mapping technique is mounting, several disadvantages remain. In our practice, both SPECT-CT and LSG were performed one day preoperatively due to the 6.0h half-life of technetium-99m and their respective waiting interval between injection and imaging. This required admitting patients on the preoperative day which consequently increased the overall in-hospital stay with associated costs. Secondly, although the radiation exposure of SPECT-CT is limited with low-dosed CT, it is still substantially higher than in planar LSG. Thirdly, a caveat of SPECT-CT (and LSG) remains the shine through effect from the technetium-99m injection site, which can potentially obscure nearby and specifically parametrial SN's. Furthermore, lymphogenic metastasis in a SN may prevent radiotracer uptake, which could lead to non-visualization on both imaging modalities [25]. In our series, this could not be confirmed.

Immunofluorescence spectroscopy is an interesting and developing technique for intra-operative SN detection. One preliminary study has reported on robot assisted laparoscopic SN detection for cervical (n=4) (and endometrial, n=16) cancer using immunofluorescence [26]. Unfortunately, concerns have been expressed regarding their limited sensitivity, presence of a false negative case and the generally lower bilateral detection rate (60%) when compared to recent studies using the combined blue dye and technetium-99m approach [27]. More general concerns, remarked in breast cancer studies focused on axillar SN detection, are the limited penetrance of near-infrared fluorescence through bone and a hindered detection of non-superficial nodes [28,29,30]. Larger trials are needed to compare immunofluorescence to the validated standard of dye and technetium-99m for minimally invasive SN detection in early stage cervical cancer.

Although promising, in most institutions that perform SN procedures, these have not yet replaced the systematic PLND. No published evidence exists on the long-term safety

of routine PLND omission after a bilaterally successful SN procedure. Large comparative randomized controlled trials, such as the SENTICOL-studies, should confirm this safety [6,7]. Anyway, whether or not completion of lympadenectomy is warranted, in the presence of tumor-positive SN further radical hysterectomy should be omitted to prevent double modality treatment and its associated additive morbidity. Additionally, in selected cases, fertility sparing surgery is also a safe option if lymph nodes are negative [31,32,33]. In this situation accurate preoperative lymph node assessment is of utmost importance.

Some limitations of this study merit further explanation. A potential advantage of preoperative SN localization could be a reduction in surgical complications due to a more direct SN retrieval. Although relevant as an outcome measure, our study is of insufficient sample size for a valid comparison of such relatively rare endpoints.

The surgeon's learning curve could be regarded as a confounder. Surgical experience during the SPECT-CT phase was inherently greater due to the temporal separation between both techniques. While this is true, we do not deem surgical experience to have added substantially to the time difference found. Scientific and surgical proficiency in robot assisted laparoscopy was adequately present for both surgeons [34,35]. Prior to this study, their clinical experience with this surgical modality was 3 (RV) and 2 years (RZ) and preceded by simulation training. We and others have shown a learning curve of at least 20 robotic procedures is required to stabilize surgical times [21,36]. Furthermore, robot assisted SN procedures were already regular care during the 19 months preceding this study. Unfortunately, these SN procedures were performed without any preoperative SN mapping and more importantly, standardized perioperative time registration was not fully introduced at that time period.

In conclusion, SPECT-CT is a valuable preoperative SN mapping technique in cervical cancer. Its superior anatomical concordance enables more direct intraoperative SN retrieval which reduces surgery by 25 minutes. The trend of higher detection rates during both mapping and surgery, as well as lower or at most equal failure rates for SPECT-CT, further favor it over LSG.

Conflict of interest statement

All authors of the presented manuscript declare to have no conflicts of interest.

REFERENCES

1. Cibula D, Abu-Rustum NR, Dusek L, Zikán M, Zaal A, Sevcik L, Kenter GG, Querleu D, Jach R, Bats AS, Dyduch G, Graf P, Klat J, Lacheta J, Meijer CJ, Mery E, Verheijen R, Zweemer RP. Prognostic significance of low volume sentinel lymph node disease in early-stage cervical cancer. Gynecol Oncol. 2012 Mar;124(3):496-501.
2. Sakuragi N. Up-to-date management of lymph node metastasis and the role of tailored lymphadenectomy in cervical cancer. Int J Clin Oncol. 2007 Jun;12(3):165-75.
3. Landoni F, Maneo A, Colombo A, Placa F, Milani R, Perego P, Favini G, Ferri L, Mangioni C. Randomised study of radical surgery versus radiotherapy for stage Ib-IIa cervical cancer. Lancet. 1997 Aug 23;350(9077):535-40.
4. Takeda N, Sakuragi N, Takeda M, Okamoto K, Kuwabara M, Negishi H, Oikawa M, Yamamoto R, Yamada H, Fujimoto S. Multivariate analysis of histopathologic prognostic factors for invasive cervical cancer treated with radical hysterectomy and systematic retroperitoneal lymphadenectomy. Acta Obstet Gynecol Scand. 2002 Dec;81(12):1144-51.
5. El-Ghobashy AE, Saidi SA. Sentinel lymph node sampling in gynaecological cancers: techniques and clinical applications. Eur J Surg Oncol. 2009 Jul;35(7):675-85.
6. Lécuru F, Mathevet P, Querleu D, Leblanc E, Morice P, Daraï E, Marret H, Magaud L, Gillaizeau F, Chatellier G, Dargent D. Bilateral negative sentinel nodes accurately predict absence of lymph node metastasis in early cervical cancer: results of the SENTICOL study. J Clin Oncol. 2011 May 1;29(13):1686-91.
7. Bats AS, Mathevet P, Buenerd A, Orliaguet I, Mery E, Zerdoud S, Le Frère-Belda MA, Froissart M, Querleu D, Martinez A, Leblanc E, Morice P, Daraï E, Marret H, Gillaizeau F, Lécuru F. The Sentinel Node Technique Detects Unexpected Drainage Pathways and Allows Nodal Ultrastaging in Early Cervical Cancer: Insights from the Multicenter Prospective SENTICOL Study. Ann Surg Oncol. 2012 Aug 22 [Epub ahead of print].
8. Cibula D, Abu-Rustum NR, Dusek L, Slama J, Zikán M, Zaal A, Sevcik L, Kenter G, Querleu D, Jach R, Bats AS, Dyduch G, Graf P, Klat J, Meijer CJ, Mery E, Verheijen R, Zweemer RP. Bilateral ultrastaging of sentinel lymph node in cervical cancer: Lowering the false-negative rate and improving the detection of micrometastasis. Gynecol Oncol. 2012 Aug 31. [Epub ahead of print]
9. van de Lande J, Torrenga B, Raijmakers PG, Hoekstra OS, van Baal MW, Brölmann HA, Verheijen RH. Sentinel lymph node detection in early stage uterine cervix carcinoma: a systematic review. Gynecol Oncol. 2007 Sep;106(3):604-13.
10. Altgassen C, Hertel H, Brandstädt A, Köhler C, Dürst M, Schneider A; AGO Study Group. Multicenter validation study of the sentinel lymph node concept in cervical cancer:

AGO Study Group. J Clin Oncol. 2008 Jun 20;26(18):2943-51.
11. Van Oostrum NH, Makar AP, Van Den Broecke R. Sentinel node procedures in gynecologic cancers: an overview. Acta Obstet Gynecol Scand. 2012 Feb;91(2):174-81.
12. Vieira SC, Sousa RB, Tavares MB, Silva JB, Abreu BA, Santos LG, da Silva BB, Zeferino LC. Preoperative pelvic lymphoscintigraphy is of limited usefulness for sentinel lymph node detection in cervical cancer. Eur J Obstet Gynecol Reprod Biol. 2009 Jul;145(1):96-9.
13. Frumovitz M, Coleman RL, Gayed IW, Ramirez PT, Wolf JK, Gershenson DM, Levenback CF. Usefulness of preoperative lymphoscintigraphy in patients who undergo radical hysterectomy and pelvic lymphadenectomy for cervical cancer. Am J Obstet Gynecol. 2006 Apr;194(4):1186-93;
14. Fotiou S, Zarganis P, Vorgias G, Trivizaki E, Velentzas K, Akrivos T, Creatsas G. Clinical value of preoperative lymphoscintigraphy in patients with early cervical cancer considered for intraoperative lymphatic mapping. Anticancer Res. 2010 Jan;30(1):183-8.
15. Buda A, Elisei F, Arosio M, Dolci C, Signorelli M, Perego P, Giuliani D, Recalcati D, Cattoretti G, Milani R, Messa C. Integration of hybrid single-photon emission computed tomography/computed tomography in the preoperative assessment of sentinel node in patients with cervical and endometrial cancer: our experience and literature review. Int J Gynecol Cancer. 2012 Jun;22(5):830-5.
16. Díaz-Feijoo B, Pérez-Benavente MA, Cabrera-Diaz S, Gil-Moreno A, Roca I, Franco-Camps S, Fernández MS, García-Jiménez A, Xercavins J, Martínez-Palones JM. Change in clinical management of sentinel lymph node location in early stage cervical cancer: the role of SPECT/CT. Gynecol Oncol. 2011 Mar;120(3):353-7.
17. Martínez A, Zerdoud S, Mery E, Bouissou E, Ferron G, Querleu D. Hybrid imaging by SPECT/CT for sentinel lymph node detection in patients with cancer of the uterine cervix. Gynecol Oncol. 2010 Dec;119(3):431-5.
18. Pandit-Taskar N, Gemignani ML, Lyall A, Larson SM, Barakat RR, Abu Rustum NR. Single photon emission computed tomography SPECT-CT improves sentinel node detection and localization in cervical and uterine malignancy. Gynecol Oncol. 2010 Apr;117(1):59-64.
19. European Organization for Research and Treatment of Cancer (EORTC). Chemotherapy followed by surgery vs radiotherapy plus chemotherapy in patients with stage IB2 or IIB cervical cancer. Retrieved from http://clinicaltrials.gov on August 30th 2012, under identifier NCT00039338. Alternative study ID: EORTC-55994. Last update March 12, 2012.
20. Boggess JF, Gehrig PA, Cantrell L, Shafer A, Ridgway M, Skinner EN, Fowler WC. A comparative study of 3 surgical methods for hysterectomy with staging for

endometrial cancer: robotic assistance, laparoscopy, laparotomy. Am J Obstet Gynecol. 2008 Oct;199(4):360.e1-9.

21. Schreuder HW, Zweemer RP, van Baal WM, van de Lande J, Dijkstra JC, Verheijen RH. From open radical hysterectomy to robot-assisted laparoscopic radical hysterectomy for early stage cervical cancer: aspects of a single institution learning curve. Gynecol Surg. 2010 Sep;7(3):253-258.
22. Plante M, Renaud MC, Têtu B, Harel F, Roy M. Laparoscopic sentinel node mapping in early-stage cervical cancer. Gynecol Oncol. 2003 Dec;91(3):494-503.
23. Levenback C, Coleman RL, Burke TW, Lin WM, Erdman W, Deavers M, Delpassand ES. Lymphatic mapping and sentinel node identification in patients with cervix cancer undergoing radical hysterectomy and pelvic lymphadenectomy. J Clin Oncol. 2002 Feb 1;20(3):688-93.
24. Malur S, Krause N, Köhler C, Schneider A. Sentinel lymph node detection in patients with cervical cancer. Gynecol Oncol. 2001 Feb;80(2):254-7.
25. Schneider, A. (2007), The sentinel concept in patients with cervical cancer. J. Surg. Oncol., 96: 337–341.
26. Rossi EC, Ivanova A, Boggess JF. Robotically assisted fluorescence-guided lymph node mapping with ICG for gynecologic malignancies: a feasibility study. Gynecol Oncol. 2012 Jan;124(1):78-82.
27. Bats AS, Mathevet P, Lécuru F. Response to Rossi et al. (Gynecol oncol. 2012; 124(1):78-82). Gynecol Oncol. 2012 Jun;125(3):764-769.
28. Murawa D, Hirche C, Dresel S, Hunerbein M. Authors' reply: Sentinel lymph node biopsy in breast cancer guided by indocyanine green fluorescence British Journal of Surgery 2010; 97: 455–460.
29. Kitai T, Inomoto T, Miwa M, Shikayama T. Fluorescence Navigation with Indocyanine Green for Detecting Sentinel Lymph Nodes in Breast Cancer. Breast Cancer (2005) 12(3): 211-215.
30. Schaafsma B, Mieog J, Hutteman M, van der Vorst J, et al. The clinical use of indocyanine green as a near-infrared fluorescent contrast agent for image-guided oncologic surgery. J Surg Oncol. 2011 Sep 1;104(3):323-332.
31. Rob L, Skapa P, Robova H. Fertility-sparing surgery in patients with cervical cancer. Lancet Oncol. 2011 Feb;12(2):192-200.
32. Du XL, Sheng XG, Jiang T, Li QS, Yu H, Pan CX, Lu CH, Wang C, Song QQ. Sentinel lymph node biopsy as guidance for radical trachelectomy in young patients with early stage cervical cancer. BMC Cancer. 2011 May 2;11:157-164
33. Pahisa J, Alonso I, Torné A. Vaginal approaches to fertility-sparing surgery in invasive cervical cancer. Gynecol Oncol. 2008 Sep;110(3 Suppl 2):S29-32.

34. Schreuder HW, Verheijen RH. Robotic surgery. BJOG. 2009 Jan;116(2):198-213.
35. Verheijen R, Zweemer R. Robotic Surgery for Gynaecologic Cancer: An Overview. Curr Oncol Rep 2012. Epub ahead of print on August 30th 2012.
36. Fanning J, Fenton B, Purohit M. Robotic radical hysterectomy. Am J Obstet Gynecol. 2008 Jun;198(6):649.e1-e4.

Chapter 7

^{99m}Tc SPECT-CT versus planar lymphoscintigraphy for preoperative sentinel lymph node detection in cervical cancer: a systematic review and meta-analysis

Jacob P. Hoogendam
Wouter B. Veldhuis
Monique G.G. Hobbelink
René H.M. Verheijen
Maurice A.A.J. van den Bosch
Ronald P. Zweemer

J Nucl Med. 2015 May; 56(5):675-680.

ABSTRACT

We aim to compare single photon emission computed tomography with computed tomography (SPECT-CT) and lymphoscintigraphy (LSG) on the overall and bilateral sentinel lymph node (SLN) detection in cervical cancer patients.

Methods: A systematic search was performed on August 1st 2014 in PubMed, Embase, Scopus and the Cochrane library. The syntax was based on synonyms of the terms 'cervical cancer', 'SPECT-CT' and 'LSG'. Retrieved articles were title/abstract screened and eligible when a SLN procedure was performed using both imaging modalities and if detection results were reported. Two independent reviewers assessed all included studies on methodological quality using QUADAS-2. Studies were pooled on their odds ratios (OR) with a random effects model.

Results: The search yielded 962 unique articles of which 8 were ultimately included. Studies were recent retrospective or prospective cohort studies of limited size (n = 7–51) but sufficient methodological quality. The median overall detection (≥1 SLN in a patient) was 98.6% for SPECT-CT (range: 92.2–100.0%) and 85.3% for LSG (range: 70.0–100.0%). This corresponded to a pooled overall SLN detection OR of 2.5 (95%CI: 1.2–5.3) in favor of SPECT-CT. The reported median bilateral detection (≥1 SLN in each hemipelvis) was 69.0% for SPECT-CT (range: 62.7–79.3%) and 66.7% for LSG (range: 56.9–75.8%) yielding a pooled OR of 1.2 (95%CI: 0.7–2.1). No significant difference in the number of visualized SLN's was observed at a pooled ratio of 1.2 (95%CI: 0.9–1.6).

Conclusion: In cervical cancer patients, preoperative SLN imaging with SPECT-CT results in a superior overall SLN detection when compared to planar LSG.

Keywords: SPECT-CT, lymphoscintigraphy, sentinel lymph node, cervical cancer, meta-analysis.

INTRODUCTION

In recent years, the sentinel lymph node (SLN) procedure has been increasingly adopted in the staging of cervical cancer patients eligible for surgery. It allows for individualized treatment decisions by accurately ascertaining the lymph nodal status before radical surgery is commenced [1]. This comprises the exclusion of fertility sparing surgery or replacing a radical hysterectomy with chemoradiotherapy in patients with tumor-positive lymph nodes.

Besides blue dye, the colloid bound radionuclide Technetium-99m (^{99m}Tc) is commonly added as a second tracer and has shown to improve the intraoperative SLN detection [2]. A second advantage of this tracer is that preoperative lymphatic mapping by either single photon emission computed tomography with regular computed tomography (SPECT-CT) or planar lymphoscintigraphy (LSG) becomes possible, which predicts the surgical detectability and number of SLN's in an individual patient. This aids the surgeon in a more direct SLN resection, with less disruption of the lymphatic architecture when compared to a full retroperitoneal exploration [3,4,5].

Although SPECT-CT is associated with both increased upfront cost and ionizing radiation, its cross-sectional anatomical reference allows for accurate three-dimensional SLN localization which is considered an important advantage over planar LSG [5,6,7,8,9]. Both SPECT-CT and LSG should ideally have a high detection ability for the SLN which largely determines the clinical value of the entire procedure.

We compared, based on a systematic search of the literature, the detection of SLN's on preoperative mapping by SPECT-CT and LSG in cervical cancer patients. Through a meta-analysis of the retrieved studies, we aimed to quantify both the overall and bilateral SLN detection differences between these two imaging modalities.

MATERIALS AND METHODS

Systematic search

We conducted a systematic review and meta-analysis of the medical literature in adherence to the PRISMA guideline [10]. Before the search was initiated, a protocol was devised which specified the research question, search strategy, in- and exclusion criteria, quality assessment, data-collection and statistical analysis.

A title and abstract based literature search was simultaneously performed on August 1st 2014 for four online databases PubMed/MEDLINE, Embase, Scopus and the Cochrane library. To attain a comprehensive search, the syntax was based on multiple synonyms,

abbreviations and common adjectives of the search terms representing our study domain (i.e. population) and determinants (i.e. intervention and comparison). These search terms were cervical cancer, SPECT-CT and LSG. The outcome measure was deliberately omitted from the search given that this could be a secondary finding in some articles and not included in the title or abstract. As an example, figure 1 outlines the exact search syntax used in PubMed/MEDLINE. Syntaxes for the other databases used identical terms. No Medical Subject Headings, filters or publication date limits were used.
All identified references were exported to the online reference management software RefWorks (RefWorks-COS, ProQuest LLC) for removal of duplicate articles.

Eligibility assessment

All unique articles were screened by a single reviewer (JPH) on their title and abstract for their respective eligibility. The inclusion of individual studies required that a SLN procedure was performed in cervical cancer patients with preoperative SLN mapping by both SPECT-CT and LSG within the same study. Also, the study had to report unilateral and/or bilateral detection results of both these imaging modalities. To allow a valid comparison, we aimed to include only studies which directly compared both techniques. Studies were excluded from the review when they did not contain original data or were not written in English, Dutch, German or French. Conference abstracts and case reports or series with ≤3 valid cases were also excluded. When multiple eligible articles reported on the same patients, only the article demonstrating the most comprehensive results with respect to our research question, was selected.
Full-text assessment was performed when the eligibility of an article, based on title and abstract screening, remained uncertain. Articles deemed eligible based on initial screening were also read in full-text, during which their eligibility was rechecked. The references of all included studies were carefully cross-checked with our initial search result for possible additional literature.

Quality assessment and data-collection

A structured quality assessment of all included studies was performed using the 'Quality Assessment of Diagnostic Accuracy Studies' instrument version 2 (QUADAS-2) [11]. The QUADAS-2 is designed for grading individual diagnostic studies on their respective risk of bias and applicability in the context of systematic reviews and meta-analyses. In adherence to the QUADAS-2 recommendations, signaling questions were optimized for our research aim, though without changing its overall content or structure. The critical appraisal was independently performed by two reviewers (JPH and RPZ). Discrepancies between both reviewers were resolved via consensus discussion or, when persisting, by

an independent third referee (WBV).
The data from the original studies were collected by a single reviewer (JPH) using a standardized form which was created in advance. This form contained variables on the research question, study design, study population, imaging modalities, intraoperative SLN procedure and outcome level effects.

Statistical Analysis

All analyses were performed using the statistical software R, version 3.0.3 (R Foundation for Statistical Computing). Herein, the package 'meta', version 3.7-1, was installed and used for all meta-analyses and corresponding plots. This R package is programmed and kindly provided by G. Schwarzer (Freiburg university, Germany).
The main outcome measures were the differences between SPECT-CT and planar LSG for the overall (≥1 SLN in a patient) and bilateral (≥1 SLN in each hemipelvis) SLN detection. For both outcomes, an inverse variance weighted random effects meta-analysis was performed to pool the original studies based on their odds ratios (OR) [12]. Studies with zero values in any of the boxes in the two by two tables underlying OR calculation were continuity corrected (n +0.5). To facilitate easy interpretation of the OR's and their clinical relevance, pooled OR's and median LSG detection ratios were used to transform the pooled OR into a percentage.
As a secondary analysis, the difference in number of SLN's detected between both imaging modalities was analyzed. This constitutes count-type data for which an inverse variance weighted random effects meta-analysis was performed based on incidence (i.e. detection) rate ratios [12]. Forest plots were created to summarize all studies, the pooled estimate and corresponding 95% confidence intervals (95%CI) in a single overview.
The heterogeneity of the results from the original studies is tested by calculating Cochrane's Q-value, which follows a Chi^2 distribution. Its derived percentage I^2 is calculated and used to represent the variability of results relative to chance. The between study variance is presented by the tau^2-statistic (T^2). Statistical significance was defined as $P < 0.05$.

DOMAIN	(Cervical cancer [Title/Abstract] OR Cervical tumor [Title/Abstract] OR Cervical carcinoma [Title/Abstract] OR Cervical malignancy [Title/Abstract] OR Cervical neoplasm [Title/Abstract] OR Cervical [Title/Abstract] OR Cancer of the uterine cervix [Title/Abstract] OR Neoplasm of the uterine cervix [Title/Abstract] OR Neoplasm of the cervix uteri [Title/Abstract] OR Carcinoma of the uterine cervix [Title/Abstract] OR Carcinoma of the cervix uteri [Title/Abstract] OR Cervical tumour [Title/Abstract] OR Tumor of the uterine cervix [Title/Abstract] OR Tumor of the cervix uteri [Title/Abstract] OR Tumour of the uterine cervix [Title/Abstract] OR Tumour of the cervix uteri [Title/Abstract] OR Cancer of the cervix uteri [Title/Abstract] OR Malignancy of the uterine cervix [Title/Abstract] OR Malignancy of the cervix uteri [Title/Abstract])
	AND
DETERMINANTS	(Single photon emission computed tomography [Title/Abstract] OR Single photon emission computed tomographic [Title/Abstract] OR Single photon emission computerized tomography [Title/Abstract] OR Single photon emission computerised tomography [Title/Abstract] OR Single photon computed tomography [Title/Abstract] OR Single photon computed tomographic [Title/Abstract] OR SPECT [Title/Abstract] OR SPECT-CT [Title/Abstract] OR SPECT/CT [Title/Abstract] OR SPECT\CT [Title/Abstract] OR SPET [Title/Abstract] OR SPET-CT [Title/Abstract] OR SPET/CT [Title/Abstract] OR SPET\CT [Title/Abstract] OR Hybrid Title/Abstract] OR Computed tomography [Title/Abstract] OR CT [Title/Abstract] OR CAT [Title/Abstract])
	AND
	(Lymphoscintigraphy [Title/Abstract] OR Lymphoscintigraphies [Title/Abstract] OR Lymphoscintigraphs [Title/Abstract] OR Lymphoscintigram [Title/Abstract] OR Lymphoscintigrams [Title/Abstract] OR Scintigraphy [Title/Abstract] OR Scintigraphies [Title/Abstract] OR Scintigraphs [Title/Abstract] OR Scintigram [Title/Abstract] OR Scintigrams [Title/Abstract] OR LSG [Title/Abstract] OR Planar [Title/Abstract] OR Conventional imaging [Title/Abstract] OR Gamma [Title/Abstract] OR Lymphatic mapping [Title/Abstract] OR Lymphatic imaging [Title/Abstract] OR Nuclear medicine imaging [Title/Abstract])

Figure 1. The PubMed/MEDLINE search syntax.

RESULTS

Literature search and assessment

The four databases yielded 432 (PubMed), 604 (Embase), 735 (Scopus) and 23 articles (Cochrane library) (Figure 2). After the removal of duplicates, 962 unique articles were screened on their eligibility. Full-text assessment was needed in 22 articles, of which 4 did not meet the inclusion criteria because either SPECT-CT or LSG was not used [13,14,15] or the SLN detection results were not reported for both modalities [6]. A further 9 studies were excluded because of their language (n = 1; [16]), being a conference abstract (n = 7; [17,18,19,20,21,22,23]) or were case report/series (n = 1; [24]). One article [25] was discarded due to an overlap in patients with an included study [8]. The references cited in the remaining 8 articles were cross-checked and did not yield any additional eligible studies [3,4,5,8,9,26,27,28].

These 8 articles were QUADAS-2 assessed (Figure 3). The risk of bias was mainly scored as low or remained unclear due to absent reporting on patient inclusion criteria, consecutiveness of inclusions or details of the SPECT-CT and LSG evaluation procedure. All seven paired studies did not specify if and how blinding between both imaging modalities was assured. No real concerns on the applicability of studies for this meta-analysis existed.

SLN Detection

The characteristics of the studies included in the meta-analysis are outlined in Table 1. Three studies [3,4,5] exclusively investigated patients with cervical cancer, others did so in combination with endometrial cancer (n = 3; [9,26,27]), vulvar cancer (n = 1; [28]) or both (n = 1; [8]). In total, SPECT-CT and LSG were performed in 207 and 208 cervical cancer patients respectively. Except for one single FIGO Stage IIIA case from Klapdor et al., all these subjects had early stage disease (FIGO stage I/II) [5]. Lymph node involvement for cervical cancer was reported in all studies, except Kraft et al. [8], and ranged between 0.0–28.6% (overall mean: 19.8%) [3,4,5,9,26,27,28]. The outlier of 0% lymph node metastasis occurred in a single study with 10 patients [26].

All included studies, with the exception of Diaz et al. [3], reported a higher overall SLN detection for SPECT-CT when compared to LSG. The median overall detection was 98.6% for SPECT-CT (range: 92.2–100.0%) and 85.3% for LSG (range: 70.0–100.0%). At the pooled level, a statistically significant OR of 2.5 (95%CI: 1.2–5.3) was detected, favoring SPECT-CT (Figure 4). The consistency of the detection results was confirmed by the negligible heterogeneity across the included studies. Based on the median 85.3% overall SLN detection for LSG and the pooled OR, a calculated 93.6% (95%CI: 87.3–96.9%) overall detection on SPECT-CT should be achieved. This equals a detection increase of 8.3% (95%CI: 2.0–11.6%).

Three of the 8 studies reported data on the bilateral SLN detection ratios, covering a total of 122 (SPECT-CT) and 123 (LSG) patients. The median bilateral detection was 69.0% for SPECT-CT (range: 62.7–79.3%) and 66.7% for LSG (range: 56.9–75.8%) [4,5,9]. A pooled OR of 1.2 (95%CI: 0.7–2.1) was detected for bilateral SLN detection, indicating absence of a significant difference (Figure 5). This equals to a 4.1% bilateral detection difference (95%CI: -8.1–14.0%).

Five studies could be pooled on the number of SLN's detected by both modalities [3,4,9,26,28]. On SPECT-CT 345 SLN's were visualized in 110 patients, relative to 299 SLN's in 111 patients on LSG. The pooled ratio in SLN count was 1.2 (95%CI: 0.9–1.6) which reflects no significant increase in the number of SLN's detected on SPECT-CT (Figure 6).

Table 1. Characteristics of studies included in the meta-analysis

Study	Design	Data-collection	Sample size	FIGO stages	Tracer and dosing
Pandit 2010 [26]	Prospective cohort	Paired	10	Not specified	37-144 MBq Tc-99m-sulfur colloid
Diaz 2011 [3]	Prospective cohort	Paired	22	IB1 – IIA	144 MBq Tc-99m-albumin nanocolloid
Kraft 2012 [8]	Retrospective cohort	Paired	36	IA1 – II	40 MBq Tc-99m-nanocolloid
Buda 2012 [27]	Retrospective cohort	Paired	10	IA2 – IB1	30-44 MBq Tc-99m-albumin nanocolloid
Hoogendam 2013 [4]	Retrospective cohort	Parallel	33 vs 29	IA1 – IIA	220-290 MBq Tc-99m-nanocolloid
Belhocine 2013 [28]	Prospective cohort	Paired	7	IA – IB1	37 MBq Tc-99m-cysteine rhenium colloid
Bournard 2013 [9]	Retrospective cohort	Paired	42	IA1 – IIA	60-120 MBq Tc-99m-sulfur rhenium colloid
Klapdor 2014 [5]	Prospective cohort	Paired	51	IA1 – IIIA	10 MBq Tc-99m-nanocolloid

FIGO: International Federation of Gynecology and Obstetrics, SPECT-CT: single-photon emission computed tomography and regular computed tomography, LSG: lymphoscintigraphy, SLN: sentinel lymph node, MBq: megabecquerel, Tc-99m: ^{99m}Technetium, min: minutes, vs: versus.

Tracer injection technique	SPECT-CT	LSG	Moment of imaging	Intraoperative SLN procedure
Two quadrant	SPECT and low dose CT, <60 min post-injection	Dynamic and anterior + lateral static, directly post-injection	Preoperative day or day of surgery	Laparotomy or laparoscopy (with blue dye)
Four quadrant	SPECT and CT of unknown dosing, 120-240 min post-injection	Dynamic and 4 directional static, 30-240 min post-injection	Preoperative day	Laparotomy or laparoscopy (with blue dye)
Four quadrant	SPECT and low dose CT, directly after LSG	Anterior and posterior static, 25-60 min post-injection	Day of surgery	Not specified (with blue dye)
Four quadrant	SPECT and low dose CT, 180 min post-injection	Dynamic and anterior static, directly and 180 min post-injection	Preoperative day or day of surgery	Laparotomy or laparoscopy (with blue dye)
Four quadrant	SPECT and low dose CT, 90 min post-injection	Dynamic and 4 directional static, 10-90 min post-injection	Preoperative day	Robot assisted laparoscopy (with blue dye)
Two to four quadrant	SPECT and low dose CT, directly after LSG	Dynamic and 4 directional static, timing not specified	Day of surgery	Laparotomy or laparoscopy (with blue dye)
Four quadrant	SPECT and low dose CT, 60-120 min post-injection	Anterior static, 60-120 min post-injection	Preoperative day or day of surgery	Laparoscopy (with blue dye)
Four quadrant	No details specified, 30 min post-injection	No details specified, 30 min post-injection	Day of surgery	Laparotomy or laparoscopy (with blue dye)

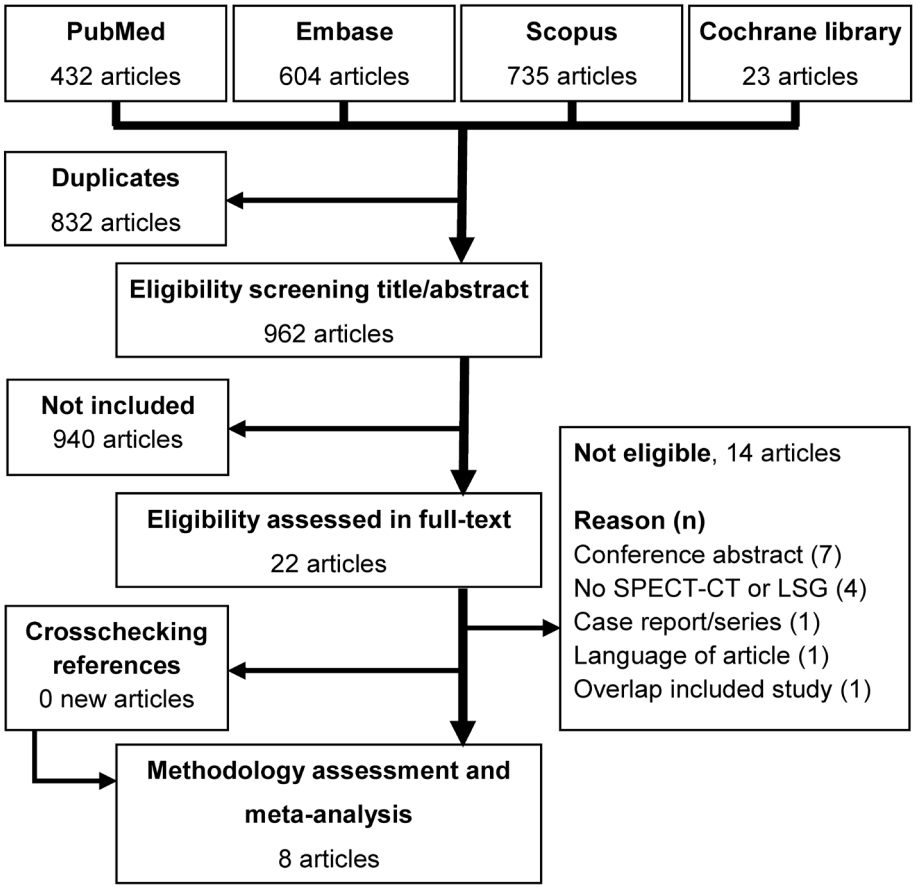

Figure 2. A flow diagram of the performed search and study assessment with the associated number of articles at each stage.

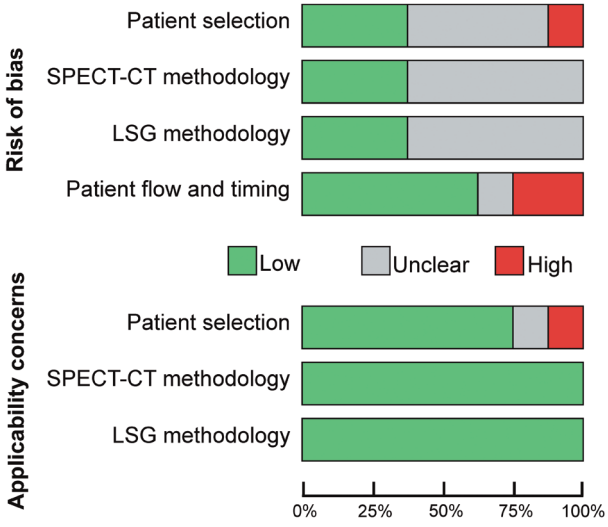

Figure 3. Summary of the methodological quality scored according to the Quality Assessment of Diagnostic Accuracy Studies (QUADAS) version 2.

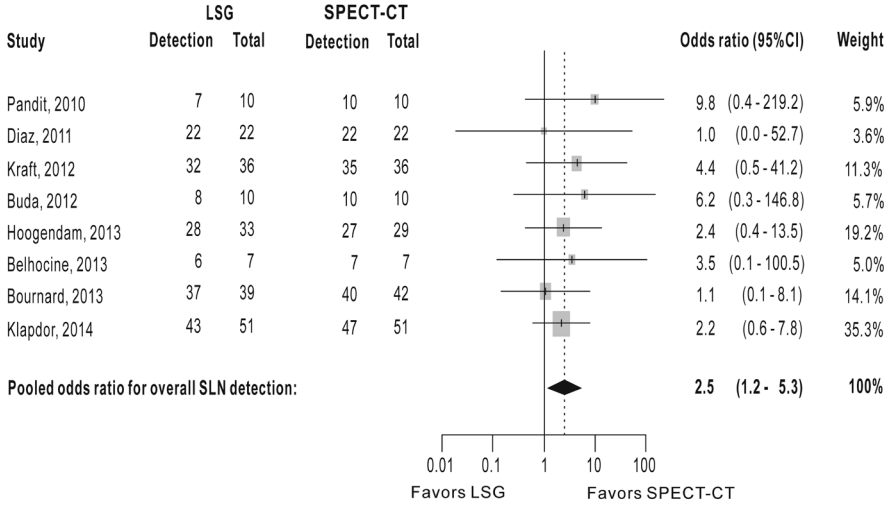

Figure 4. Forest plot of the overall SLN detection (≥1 SLN detected in a patient) on SPECT-CT compared to LSG. Heterogeneity statistics: Cochrane's Q = 2.3 (7 degrees of freedom; P = 0.945), I^2 = 0.0% and T^2 = 0.0. Pandit et al. reports conflicting detection ratios of 70.0% versus 80.0% for their overall SLN detection on lymphoscintigraphy. The most conservative estimate was selected [26].

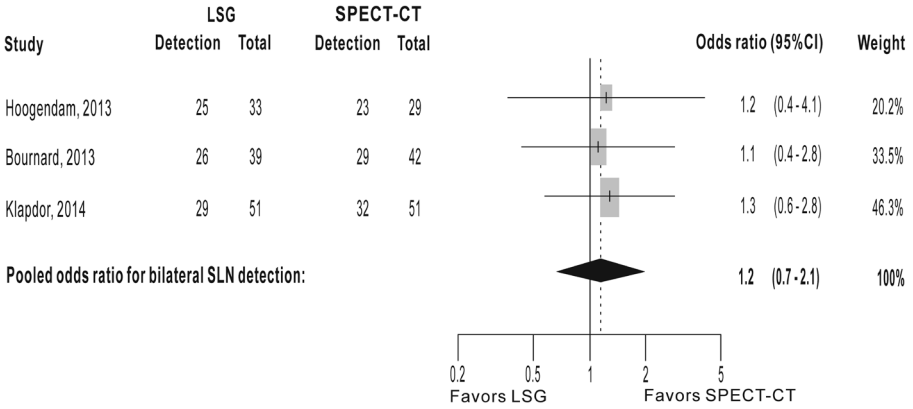

Figure 5. Forest plot of the bilateral SLN detection (≥1 SLN detected in each hemipelvis) on SPECT-CT compared to LSG. Heterogeneity statistics: Cochrane's Q = 0.1 (2 degrees of freedom; *P* = 0.976), I^2 = 0.0% and T^2 = 0.0. Belhocine et al. reports bilateral SLN detection in 71.4% (n = 5/7) without specifying the imaging modality by which this was achieved and was therefore excluded from this sub-analysis [28].

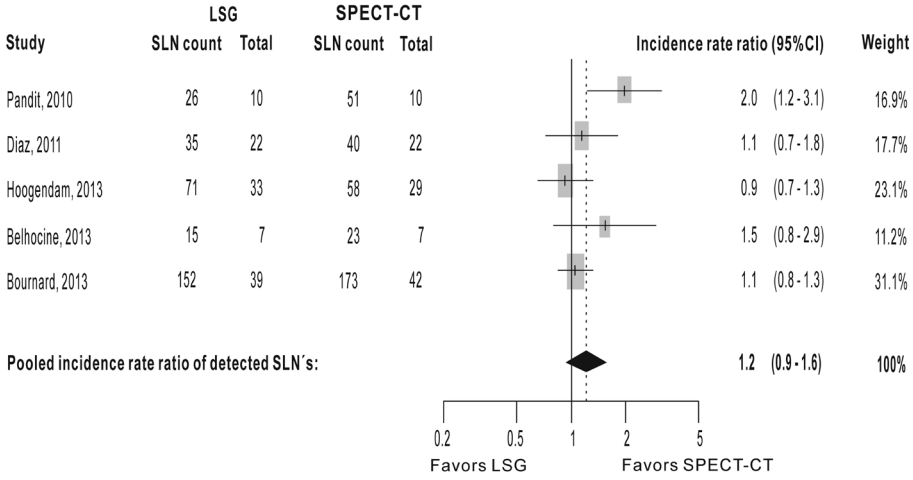

Figure 6. Forest plot of the number of SLN's detected on SPECT-CT compared to planar lymphoscintigraphy. Heterogeneity statistics: Cochrane's Q = 7.7 (4 degrees of freedom; *P* = 0.105), I^2 = 47.8% and T^2 = 0.0.

DISCUSSION

All 8 original studies showed excellent and consistent overall SLN detection ratios for SPECT-CT, ranging between 92.0 and 100.0%. Its pooled SLN detection was superior to LSG with an OR of 2.5 (95%CI: 1.2–5.3) corresponding to a relevant 8.3% (95%CI: 2.0–11.6%) increase. Clinically, this means that of the median 14.7% non-visualization cases on LSG, more than half can be prevented through the use of SPECT-CT (6.4% non-visualization). Its significantly improved overall SLN detection supplements other potential advantages. The cross-sectional nature and anatomical reference of SPECT-CT has been reported, though rarely formally analyzed, to lead to better anatomical SLN localization [4,6,7,8]. This has always been regarded as a weakness of LSG [29]. In addition, a single report has indicated a possible reduction of 25.4 minutes for the intraoperative SLN retrieval length by robot assisted laparoscopy, when preoperative SPECT-CT is used [4].

The cervix is a midline organ with bilateral lymphatic drainage, making it clinically relevant to identify minimally one SLN in each hemipelvis [1,6,30,31,32]. Unfortunately, only 3 studies specifically reported bilateral SLN detection results which led to a meta-analysis of insufficient statistical power to (dis)prove a difference. The wide confidence interval relative to the limited OR of 1.2 (95%CI: 0.7–2.1), indicates that further research is needed before any conclusive statement can be made. In general, researchers should be urged to always report bilateral SLN results in cervical cancer, even though these are often substantially lower and less attractive than the overall detection ability.

Some investigators use ^{99m}Tc-nanocolloid and blue dye via a cervical injection for the sentinel procedure in endometrial cancer patients. While the validity and reliability are not without debate for this indication, the methodology is similar to the cervical cancer approach and identifies the SLN's of the cervix uteri. Four such studies (n = 21–40) from our initial search reported the overall SLN detection results of both SPECT-CT and LSG, which ranged between 84.6–100.0% and 40.0–85.9% respectively [8,9,26,27]. In addition, Garcia et al. demonstrated an overall detection at the first imaging session of 77.8% (n = 14/18) on SPECT-CT compared to 73.7% (n = 14/19) for planar LSG in stage IA-IIIA endometrial cancer patients [33]. While these results, especially for LSG, are lower when compared to the cervical cancer estimates used in our meta-analysis, the superiority of SPECT-CT is maintained.

By definition, the SLN is the first efferent nodal station to receive lymphatic drainage from the tumor and therefore represents the overall lymph nodal status. Consequently, some authors question the necessity of routine pelvic lymphadenectomy when tumor-negative SLN's are identified in cervical cancer [30,32,34,35]. While the as of yet unpublished randomized SENTICOL-2 trial primarily studies the complications after a

SLN procedure, as opposed to full lymphadenectomy, oncological safety is a secondary endpoint of this study [36]. When found to be equal, abstaining from the systematic lymphadenectomy would safeguard lymph node negative patients from an associated 2% intraoperative risk of vascular, nerve, bowel or ureteric injury [37]. Also, long term morbidity caused by lymphedema and (infected) lymphocysts can be minimized and will likely improve quality of life [30,38].

The ability to safely abstain from a systematic lymphadenectomy also depends on the reliability of the SLN procedure. Besides the high SLN detection shown in this meta-analysis, this is mainly determined by the intraoperative risk of a false-negative diagnostic outcome (i.e. misclassifying a patient with lymph node metastases). A large multicenter study (n = 645) by Cibula et al. published a false-negative SLN ratio of 1.3% when bilateral detection with histopathological ultrastaging is performed [1].

Several arguments offer a rationale for the improved SLN detection by SPECT-CT. In addition to its higher spatial resolution, various authors have reported that the anatomical reference and cross-sectional nature of SPECT-CT allows for less frequently overlooked SLN's near the injection depot (e.g. parametrial SLN's) or at unusual anatomical locations (e.g. paravesical, epigastric or pre-sacral SLN's) [5,6,28]. Furthermore, SPECT undergoes superior attenuation correction through the availability of concurrent CT data [39]. This CT based correction reduces the inherent overestimation of (peripheral) background activity (i.e. noise), leading to more valid ^{99m}Tc tracer uptake quantification in the SPECT dataset [40].

Some limitations at the level of the original studies merit further explanation. First, in studies with a paired design, adequate blinding during the review of both imaging modalities is of the utmost importance for an unbiased comparison. However, none of the 7 paired studies had a blinded design. This could possibly favor SPECT-CT because it is commonly performed after LSG. Secondly, all available studies had an observational design (4 prospective, 4 retrospective) with a relatively small sample size. The limited number of original studies did not permit a formal sensitivity analysis wherein only low risk of bias studies are pooled and compared to the effect derived from all studies. Instead, we aimed to clearly asses the methodological quality and pool all studies.

A limitation of this study is our choice of the outcome measure. While the detection on preoperative imaging is relevant and insightful, a more clinically important outcome would be to examine differences in the intraoperative SLN resection. However, this is currently not possible since all but one original study in our meta-analysis followed a paired design and consequently had identical intraoperative SLN resection results for both imaging modalities. The single parallel study included did not report a statistically significant difference between SPECT-CT and LSG for the overall (93.1 vs 93.9%) or bilateral

intraoperative SLN resection (89.7 vs 84.8%) [4].
A limitation of our meta-analysis on the number of SLN detected, which follows a Poisson distribution, is the absence of a uniformly accepted summary statistic for count-type data. We followed a common approach in which pooling was based on the rate ratio (i.e. detection rate LSG divided by detection rate SPECT-CT), instead of treating it as a continuous variable [12]. However, in detection rate calculation the SLN count should be divided by person-time, a nonexistent entity in our imaging setting, which was therefore replaced by the respective number of scans made.

Conclusion

Preoperative SPECT-CT provides a higher overall SLN detection in cervical cancer patients when compared to LSG. Larger studies are still needed before any significant conclusions on bilateral detection, or the number of SLN's visualized, can be reached. Nonetheless, the overall detection ability is high and the difference with LSG substantial. The more than half reduction in non-visualization cases is a relevant clinical improvement achieved through the use of SPECT-CT. This study supplements other advantages of SPECT-CT, including possibly shortened surgical SLN retrieval times and more precise preoperative information on the anatomical location of the SLN's. Combined, few reasons remain for continuing the use of planar LSG for SLN detection in cervical cancer when SPECT-CT is available.

Disclosure

All authors declare to have no conflicts of interest.

Acknowledgments

The authors are grateful to Rob J.P. Scholten as head of the Dutch Cochrane Center for his advice on the manuscript.

REFERENCES

1. Cibula D, Abu-Rustum NR, Dusek L, et al. Bilateral ultrastaging of sentinel lymph node in cervical cancer: Lowering the false-negative rate and improving the detection of micrometastasis. Gynecol Oncol. 2012;127:462-466.
2. Van de Lande J, Torrenga B, Raijmakers PG, et al. Sentinel lymph node detection in early stage uterine cervix carcinoma: a systematic review. Gynecol Oncol. 2007;106:604-613.
3. Díaz-Feijoo B, Pérez-Benavente MA, Cabrera-Diaz S, et al. Change in clinical management of sentinel lymph node location in early stage cervical cancer: the role of SPECT/CT. Gynecol Oncol. 2011;120:353-357.
4. Hoogendam JP, Hobbelink MG, Veldhuis WB, Verheijen RH, van Diest PJ, Zweemer RP. Preoperative sentinel node mapping with (99m)Tc-nanocolloid SPECT-CT significantly reduces the intraoperative sentinel node retrieval time in robot assisted laparoscopic cervical cancer surgery. Gynecol Oncol. 2013;129:389-394.
5. Klapdor R, Mücke J, Schneider M, et al. Value and advantages of preoperative sentinel lymph node imaging with SPECT/CT in cervical cancer. Int J Gynecol Cancer. 2014;24:295-302.
6. Martínez A, Zerdoud S, Mery E, Bouissou E, Ferron G, Querleu D. Hybrid imaging by SPECT/CT for sentinel lymph node detection in patients with cancer of the uterine cervix. Gynecol Oncol. 2010;119:431-435.
7. Holman LL, Levenback CF, Frumovitz M. Sentinel lymph node evaluation in women with cervical cancer. J Minim Invasive Gynecol. 2014;21:540-545.
8. Kraft O, Havel M. Detection of sentinel lymph nodes in gynecologic tumours by planar scintigraphy and SPECT/CT. Mol Imaging Radionucl Ther. 2012;21:47-55.
9. Bournaud C, Le Bail-Carval K, Scheiber C, de Charry C, Mathevet P, Moreau-Triby C. Value of SPECT/CT in lymphatic mapping in cervix and endometrial cancer. Medecine Nucleaire 2013;37:387-396.
10. Moher D, Liberati A, Tetzlaff J, Altman DG. Preferred reporting items for systematic reviews and meta-analyses: the PRISMA statement. Ann Intern Med. 2009;151: 264-269.
11. Whiting PF, Rutjes AW, Westwood ME, et al. QUADAS-2: a revised tool for the quality assessment of diagnostic accuracy studies. Ann Intern Med. 2011;155:529-536.
12. Higgins JPT, Green S (editors). Cochrane Handbook for Systematic Reviews of Interventions Version 5.1.0 [updated March 2011]. The Cochrane Collaboration, 2011. www.cochrane-handbook.org. Accessed 10-03-2015.
13. Kushner DM, Connor JP, Wilson MA, et al. Laparoscopic sentinel lymph node mapping for cervix cancer - A detailed evaluation and time analysis. Gynecol Oncol. 2007;106:507-512.

14. Feigen M, Crocker EF, Read J, Crandon AJ. The value of lymphoscintigraphy, lymphangiography and computer tomography scanning in the preoperative assessment of lymph nodes involved by pelvic malignant conditions. Surg Gynecol Obstet. 1987;165:107-110.
15. Hauspy J, Verkinderen L, De Pooter C, Dirix LY, van Dam PA. Sentinel node metastasis in the groin detected by technetium-labeled nannocolloid in a patient with cervical cancer. Gynecol Oncol. 2002;86:358-360.
16. Zhang WJ, Zheng R, Wu LY, Li XG, Li B, Chen SZ. Clinical application of sentinel lymph node detection to early stage cervical cancer. Ai Zheng. 2006;25:224-228.
17. Asa S, Sager S, Demirayak G, et al. Comparison of SPECT/CT, gamma probe and methylene blue-dye for sentinel lymph node detection in gynecologic tumours [abstract}. Eur J Nucl Med Mol Imaging. 2013;40:S393.
18. Buda A, Arosio M, Elisei F, et al. The role of SPECT/CT for sentinel lymph node detection in uterine cancer: Analysis of 20 cases and literature review [abstract}. Int J Gynecol Cancer. 2011;21:S1108.
19. Chernov VVI, Sinilkin IG, Kolomiets LA, Chernyshova AL, Titskaya AA, Zelchan RV. Sentinel lymph node detection in surgical treatment of cervical cancer [abstract}. Eur J Nucl Med Mol Imaging. 2012;39:S578.
20. Hernandez-Heredia CM, Paredes-Barranco P, Vidal-Sicart S, et al. Contribution of SPECT/CT in the sentinel node detection in early cervical cancer [abstract}. Eur J Nucl Med Mol Imaging. 2013;40:S217.
21. Hertel H, Makowski L, Tjahjadi M, et al. SPECT/CT improved intraoperative detection of sentinel lymph nodes in vaginal and cervical cancer [abstract}. Arch Gynecol Obstet. 2010;282:S246-S247.
22. Miyata H, Tsuji N, Hanada T, et al. Sentinel nodes biopsy can accurately predict lymph nodes metastases in early stage cervical cancer, compared with MRI and PET-CT [abstract}. Int J Gynecol Cancer. 2012;22:E965.
23. Schmidt E, Bozsa S, Gocze P, et al. The significance of additional SPECT/CT imaging in sentinel lymph node scintigraphy of patients with cervical and endometrial cancer [abstract}. Eur J Nucl Med Mol Imaging. 2012;39:S464.
24. Guedec-Ghelfi R, Papathanassiou D, Bruna-Muraille C, et al. Impact of the SPECT/CT in the sentinel lymph node detection. Apropos of 32 cases. Med Nucl. 2011;35:208-218.
25. Kraft O, Havel M. Sentinel lymph nodes and planar scintigraphy and SPECT/CT in various types of tumours. Estimation of some factors influencing detection success. Nucl Med Rev Cent East Eur. 2013;16:17-25.
26. Pandit-Taskar N, Gemignani ML, Lyall A, Larson SM, Barakat RR, Abu-Rustum NR. Single photon emission computed tomography SPECT-CT improves sentinel node detection

and localization in cervical and uterine malignancy. Gynecol Oncol. 2010;117:59-64.
27. Buda A, Elisei F, Arosio M, et al. Integration of hybrid single-photon emission computed tomography/computed tomography in the preoperative assessment of sentinel node in patients with cervical and endometrial cancer: our experience and literature review. Int J Gynecol Cancer. 2012;22:830-835.
28. Belhocine TZ, Prefontaine M, Lanvin D, et al. Added-value of SPECT/CT to lymphatic mapping and sentinel lymphadenectomy in gynaecological cancers. Am J Nucl Med Mol Imaging. 2013;3:182-193.
29. Frumovitz M, Ramirez PT, Levenback CF. Lymphatic mapping and sentinel lymph node detection in women with cervical cancer. Gynecol Oncol. 2008;110(Suppl 2):S17-20.
30. Eiriksson L, Covens A. Sentinel lymph node mapping in cervical cancer: the future? BJOG 2012;119:129-133.
31. El-Ghobashy AE, Saidi SA. Sentinel lymph node sampling in gynaecological cancers: techniques and clinical applications. Eur J Surg Oncol. 2009;35:675-685.
32. Roy M, Bouchard-Fortier G, Popa I, et al. Value of sentinel node mapping in cancer of the cervix. Gynecol Oncol. 2011;122:269-274.
33. Cordero-García JM, López de la Manzanara-Cano CA, García-Vicente AM, et al. Study of the sentinel node in endometrial cancer at early stages: preliminary results. Rev Esp Med Nucl Imagen Mol. 2012;31:243-248.
34. Gortzak-Uzan L, Jimenez W, Nofech-Mozes S, et al. Sentinel lymph node biopsy vs. pelvic lymphadenectomy in early stage cervical cancer: is it time to change the gold standard? Gynecol Oncol. 2010;116:28-32.
35. Hauspy J, Beiner M, Harley I, Ehrlich L, Rasty G, Covens A. Sentinel lymph nodes in early stage cervical cancer. Gynecol Oncol. 2007;105:285-290.
36. Comparison of pelvic lymphadenectomy versus isolated sentinel lymph node biopsy procedure for early stages of cervical cancers: a randomized multicenter study with evaluation of medico-economic impacts. http://clinicaltrials.gov/ct2/show/NCT01639820 Accessed 17-09-2014.
37. Querleu D, Leblanc E, Cartron G, Narducci F, Ferron G, Martel P. Audit of preoperative and early complications of laparoscopic lymph node dissection in 1000 gynecologic cancer patients. Am J Obstet Gynecol. 2006;195:1287-1292.
38. Achouri A, Huchon C, Bats AS, Bensaid C, Nos C, Lécuru F. Complications of lymphadenectomy for gynecologic cancer. Eur J Surg Oncol. 2013;39:81-86.
39. Hasegawa BH, Wong KH, Iwata K, et al. Dual-modality imaging of cancer with SPECT/CT. Technol Cancer Res Treat. 2002;1:449-458.
40. Buck AK, Nekolla S, Ziegler S, et al. SPECT/CT. J Nucl Med. 2008;49:1305-1319.

7

Chapter 8

^{99m}Tc–nanocolloid SPECT–MRI fusion for the selective assessment of non-enlarged sentinel lymph nodes in patients with early stage cervical cancer

Jacob P. Hoogendam
Ronald P. Zweemer
Monique G.G. Hobbelink
Maurice A.A.J. van den Bosch
René H.M. Verheijen
Wouter B. Veldhuis

J Nucl Med. 2016 Apr; 57(4):551-556.

ABSTRACT

We aimed to explore the accuracy of ^{99m}Tc SPECT–MRI fusion for the selective assessment of non-enlarged sentinel lymph nodes (SLNs) for diagnosing metastases in early stage cervical cancer patients.

Methods: We consecutively included stage IA1 – IIB1 cervical cancer patients who presented to our tertiary referral center between March 2011 and February 2015. Patients with enlarged lymph nodes (short axis ≥10mm) on MRI were excluded. Patients underwent a SLN procedure with preoperative ^{99m}Tc-nanocolloid SPECT–CT based SLN mapping. By creating fused datasets of the SPECT and MRI, SLNs could be identified on MRI with accurate correlation to the histological result of each individual SLN. An experienced radiologist, blinded to histology, retrospectively reviewed all fused SPECT–MRI's and scored morphologic SLN parameters on a standardized case report form. Logistic regression and receiver operating curves (ROC) were used to model the parameters against the SLN status.

Results: In 75 cases, 136 SLNs were eligible for analysis of which 13 (9.6%) contained metastases (8 cases). Three parameters, short axis diameter, long axis diameter and absence of sharp demarcation significantly predicted metastatic invasion of non-enlarged SLNs with a quality adjusted odds ratios of 1.42 (95%CI: 1.01 – 1.99), 1.28 (95%CI: 1.03 – 1.57) and 7.55 (95%CI: 1.09 – 52.28) respectively. The area under the curve of the ROC combining these parameters was 0.749 (95%CI: 0.569 – 0.930). Heterogeneous gadolinium enhancement, cortical thickness, round-shape or SLN-size compared to the nearest non-SLN, showed no association with metastases (p 0.055 – 0.795).

Conclusion: In cervical cancer patients without enlarged lymph nodes, selective evaluation of only the SLNs – for size and absence of sharp demarcation – can be used to noninvasively assess the presence of metastases.

Keywords: cervical cancer, sentinel lymph node, metastasis, SPECT-CT, MRI.

INTRODUCTION

Sentinel lymph nodes (SLNs) are defined by the National Cancer Institute as the first nodes to which malignant cells are likely to spread from a primary tumor [1]. There can be one SLN or more than one. Accurate assessment of SLNs in stage I/II cervical cancer patients is important as the presence or absence of metastases is a predictor for survival [2,3]. Also, based on the SLN status, individualized decisions between radical hysterectomy or (chemo)radiation are possible. This allows for a potential morbidity reduction by avoiding double modality treatment [4,5,6].

Before the SLN procedure, assessment of all lymph nodes can be attempted noninvasively by pelvic magnetic resonance imaging (MRI). Current criteria, such as the commonly used 10mm short axis cutoff, are focused on achieving a high specificity, which is reported between 69% and 96% [7,8,9,10,11]. Consequently, this limits sensitivity which ranges from 27% to 71%, indicating that normal sized metastatic lymph nodes (i.e. false negatives) are not uncommon [12,13]. This poses a clinical challenge as early stage patients with <10mm nodes usually do not undergo further non-invasive staging.

We hypothesize that by specifically focusing on SLNs, contrary to reviewing the entire pelvic lymphatic chain, the diagnostic accuracy for detecting metastases on MRI may be improved. This selective identification of SLNs on MRI, can be achieved through fusion with the preoperatively created ^{99m}Tc single photon emission computed tomography (SPECT) –computed tomography (CT) based SLN imaging, which visualizes the number and anatomical location of the bilateral SLNs [14].

In this study, we aim to identify specific SLN parameters on pelvic MRI to explore the accuracy in pre-operatively diagnosing SLN metastases in early stage cervical cancer patients. We focus on patients with <10mm short axis nodes on MRI, as in many centers these are considered non-suspicious and do not undergo further lymph node assessment with positron emission tomography (PET)–CT prior to their intraoperative SLN procedure or lymphadenectomy [15,16].

MATERIALS AND METHODS

Research Population

We reanalyzed preoperative MRI datasets in a retrospective cohort of consecutive stage IA1 – IIB1 cervical cancer patients, treated surgically between March 2011 and February 2015 in our tertiary gynecological oncology referral center. Subjects were eligible for inclusion when cervical cancer was histologically proven and a preoperative pelvic MRI

was performed and contained only lymph nodes with a short axis <10mm. In addition, an intra-operative SLN procedure with preoperative SPECT–CT mapping had to have been completed. Subjects were excluded if no SLN was detected on SPECT–CT or if a concurrent second primary malignancy was diagnosed. The institutional review board approved this retrospective study and the requirement to obtain informed consent was waived. This report follows the STARD guideline for diagnostic accuracy studies [17].

SLN Procedure

Our SLN methodology has recently been published in detail [18]. To summarize, at a standardized 17 hours preoperatively, 202–290 MBq ^{99m}Tc-nanocolloid is submucosally injected into the 4 quadrants of the cervix directly surrounding the tumor. Ninety minutes post-injection a SPECT–CT is performed on a single integrated system (Symbia T16, Siemens, Erlangen, Germany). A board certified nuclear medicine physician reviews the datasets and reports the number of SLNs and locations of the SLNs.

At surgery, the SLN procedure typically precedes a pelvic lymphadenectomy and radical hysterectomy or radical vaginal trachelectomy. Upon incision of the retroperitoneum, 0.5–1.0 ml patent blue dye (Bleu Patenté, Guerbet Group, Roissy, France) is injected intracervically directly surrounding the tumor with the same 4 quadrant technique as used pre-operatively. This allows for both visual and gamma probe aided intraoperative SLN identification.

Histological SLN assessment is performed according to an institutional protocol. After an optional frozen section analysis at the time of operation, definitive histology by paraffin embedding and serial step sectioning at 150 micrometer intervals was performed. Slides (5 micrometer) are stained with heamatoxylin and eosin, followed by routine immunohistochemical staining with cytokeratin AE1/AE3 antibodies. A pathologist who specializes in gynecological oncology reviewed all specimens. Both micrometastases (0.2–2 mm) and macrometastases (>2 mm) indicate a tumor-positive SLN. In contrast, isolated tumor cells (<0.2 mm) are considered as tumor-negative, clinically as well as for the purpose of this study [3].

MRI Based SLN review

As part of routine non-invasive staging, a preoperative pelvic MRI is performed on a 1.5 tesla wide bore MRI system (Achieva / Ingenia, Phillips healthcare, Best, the Netherlands). To reduce bowel movements, 1.0 mg of glucagon is administered intramuscularly. The standardized protocol consists of a T_2-weighted turbo spin echo sequence in both the transversal (repetition time (TR): 6687ms, echo time (TE): 100ms, field of view (FoV): 250mm, matrix; 512x512, flip angle: 90 degrees, slice thickness/gap: 4/0mm) and sagittal

plane (TR: 2800ms, TE: 100ms, FoV: 250mm, matrix; 512x512, flip angle: 90 degrees, slice thickness/gap: 4/0mm), a transversal fat-saturated T_1-weighted THRIVE sequence before and after intravenous gadolinium injection (for both: TR: 5.5ms, TE: 2.7ms, FoV: 395mm, matrix; 512x512, flip angle: 10 degrees, slice thickness/gap: 3/0mm), a transversal proton density sequence (TR: 1705ms, TE: 20ms, FoV: 450mm, matrix; 512x512, flip angle: 90 degrees, slice thickness/gap: 6/0.6mm) which covers the complete abdomen and a transversal diffusion weighted sequence.

To identify the SLNs on MRI an approach with fused datasets, generated in the dedicated fusion software platform syngo.via version 1.1.0.16 (Siemens, Erlangen, Germany), was adopted. First, a fused dataset was created from the CT and T_1 / T_2-weighted MRI datasets using the build in automatic rigid alignment function. The accuracy of this fusion was visually assessed on the criterion of exact 3 dimensional superposition of the ossal anatomy. In rare instances, additional manual alignment was performed. This CT–MRI fusion, and the inherent anatomical link between SPECT and CT, enables a fusion matched for anatomy between the SPECT and T_1 / T_2-weighted MRI datasets (Figure 1). Stills of SLNs on fused SPECT–MRI datasets were created and exported to the picture archiving and communication system (PACS, SECTRA A.B., Linköping, Sweden).

MRI datasets were prospectively reviewed for SLN morphology by a board certified radiologist (WBV) with 5 years of experience in gynecological oncology. Reviews were based on all MRI sequences available and conducted at a clinical PACS workstation. The reviewing radiologist was blinded to the histopathological SLN status and all supporting clinical data, though aware of the study aim. A standardized case report form was used for scoring each SLN and included the following parameters: anatomical location, short and long axis diameter, shape, cortical thickness (when applicable), and presence or absence of sharp demarcation, uniform gadolinium enhancement, fatty center and/or, central necrosis. In addition the short and long axis diameters of the nearest – in any direction – non-sentinel lymph node was recorded. Image quality of the MRI dataset was rated on a 5 point Likert scale.

Statistical Analysis

Statistical calculations were performed with the 'Statistical Package for the Social Sciences' version 21.0.0 (International Business Machines, New York, USA). Baseline characteristics were analyzed in a case wise approach.

For the per node analysis, logistic regression was used to model the parameters scored on MRI against the histopathologically assessed SLN status (i.e. the reference standard). This produces uniformly comparable effect sizes in the form of odds ratios and significance testing with a single test (i.e. the Wald test), regardless of the data type (continuous

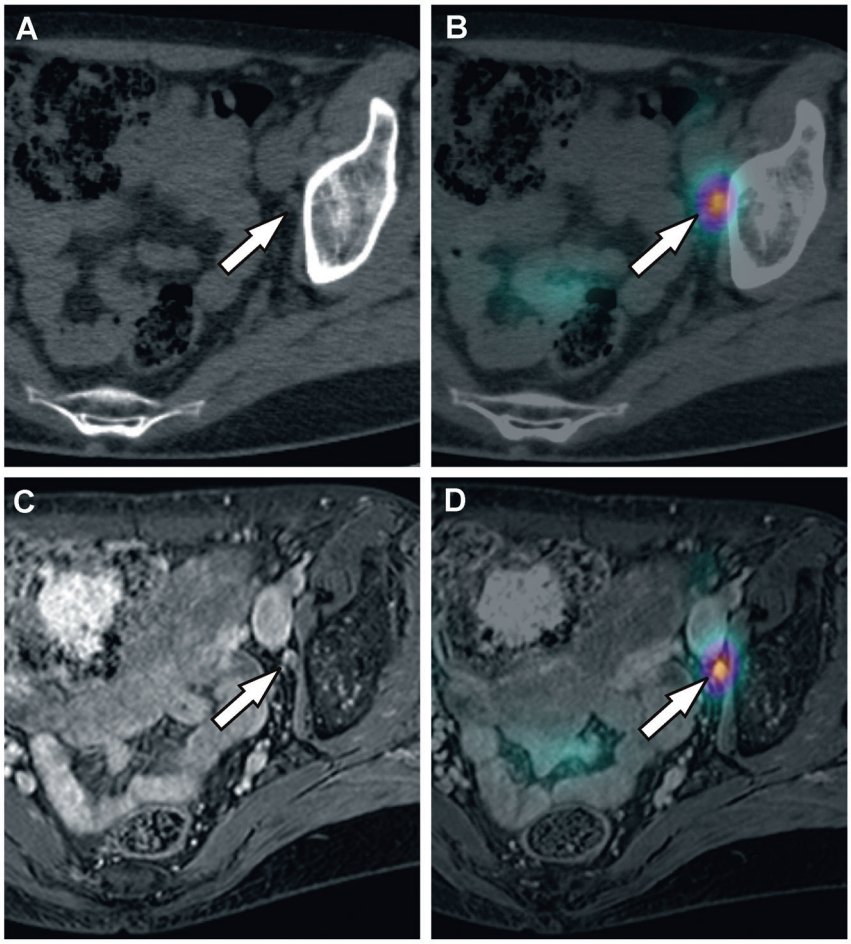

Figure 1. Illustration of the fusion methodology in an exemplary 53 year old patient with a stage IIA squamous cell carcinoma of the cervix. Preoperative SLN imaging with CT (A) as part of the SPECT–CT (B), visualized a SLN (arrow) in the left obturator fossa. The gadolinium enhanced T_1-weighted MRI (C) performed during the routine work-up can, via an anatomy guided fusion between CT and MRI, be used to create a SPECT–MRI fused image (D). At histology, this SLN was found to be tumor negative.

or categorical). The scored MRI quality was added as an additional explanatory variable to the multivariate analysis to adjust the diagnostic odds ratios for the quality of the MRI dataset. The included variables had only 1.9% missing values and no outliers were modified. Significant parameters, defined as $p<0.050$, were combined in a single multivariable model. Predicted individual probabilities were incorporated into a receiver operating curve (ROC) of which the area under the curve (AUC) was calculated, including 95% confidence intervals (95%CI).

RESULTS

Research Population

A total of 75 patients were included, of whom the baseline characteristics are outlined in table 1. In 60 patients (80.0%) bilateral detection (i.e. ≥1 SLN per hemipelvis) was achieved on SPECT–CT. In total, 164 SLNs were visualized on SPECT–CT, of which 141 SLNs (86.0%) could be unequivocally matched to a lymph node visible on MRI. The 23 excluded SLNs were all histologically negative for metastases and came from typical anatomical locations. An additional 5 SLNs (3.5%) could not be intra-operatively identified and were also excluded from the analysis. Of the remaining 136 SLNs, 13 SLNs (9.6%) in 8/75 patients (10.7%) contained micro- or macrometastases. Only one tumor-positive SLN showed extra-nodal growth. Tumor-positive non-sentinel lymph nodes were found in two patients (2.7%), both of whom had macrometastases in their ipsilateral SLN (i.e. no false-negative cases). Isolated tumor cells were identified in 6 SLNs (3.7%) from 6 patients, of whom only one had a contralateral positive SLN. The six cases staged as ≥IB2, who for example underwent the SLN procedure to individualize the radiotherapy field, all had bilaterally detected tumor-negative SLNs.

Of the 136 SLNs analyzed, 74 SLNs were located in the obturator fossa (54.4%), 43 at the external iliac artery (31.6%), 4 dorsal of the internal iliac artery (2.9%) and 15 at various other locations (11.0%).

The mean interval between MRI and the SLN procedure was 22.8 ± 12.8 days and no treatment was administered in between. The image quality of the MRI datasets was graded as poor, limited, intermediate, good or excellent in 0.0% (0/75), 1.3% (1/75), 18.7% (14/75), 50.7% (38/75) and 29.3% (22/75), respectively.

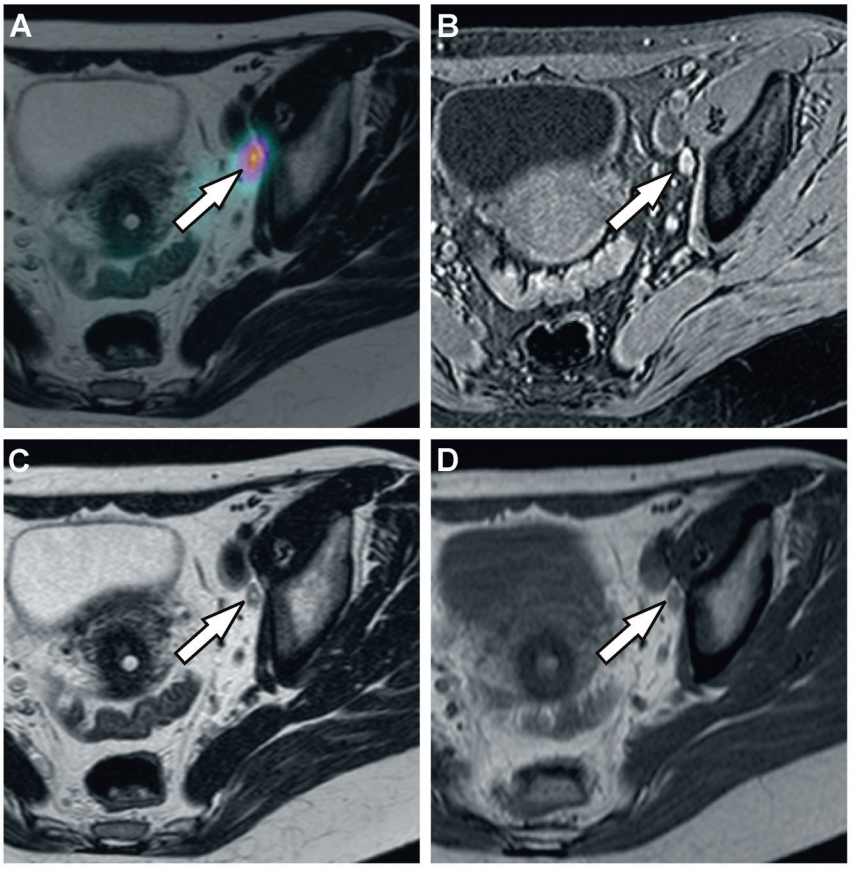

Figure 2. In a 39 year old patient with stage IB1 adenosquamous cervical cancer, a SLN was found on the fused SPECT–T_2-weighted MRI (A) in the left obturator fossa (arrow), in addition to 2 SLNs in the right hemipelvis (not depicted). The left SLN, indeed radioactive and located in the obturator fossa at surgery, showed a 1.0 mm micro-metastasis without extra-nodal growth at histology. The SLN parameters were reviewed blinded on the T_1-weighted (B), T_2-weighted (C) and proton density sequence (D). The SLN measured 6.0 by 12.0mm and was scored as having a lobulated shape with absence of sharp demarcation of its margins and an heterogeneous gadolinium enhancement pattern.

Table 1. Baseline characteristics of the research population

Median age (range)		39.5 (25.3 – 81.2) years
Median BMI (range)		23.5 (18.3 – 41.0) kg/m^2
Median follow-up (range)		17 (0 – 47) months
	N	**%***
Prior cervical procedure		
LLETZ	38	50.7
Conisation	8	10.7
LLETZ and Conisation	2	2.7
None	27	36.0
Stage		
IA1 or IA2	5	6.7
IB1	64	85.3
IB2, IIA1, IIA2 or IIB1	6	8.0
Tumor histology primary tumor		
Squamous cell carcinoma	59	78.7
Adenocarcinoma	12	16.0
Other	4	5.3
Tumor differentiation primary tumor		
Grade 1	10	13.3
Grade 2	35	46.7
Grade 3	22	29.3
Not defined	8	10.7
LVSI in primary tumor		
Present	33	44.0
Absent	42	56.0
SLN procedure approach		
Laparotomy	1	1.3
Conventional laparoscopy	16	21.3
Robot assisted laparoscopy	58	77.3
SLN histology, per patient (n=75)†		
No tumor	62	82.7
Isolated tumor cells	5	6.7
Micrometastasis	2	2.7
Macrometastasis	6	8.0
SLN histology, per sentinel node (n=136)		
No tumor	117	86.0
Isolated tumor cells	6	4.4
Micrometastasis	5	3.7
Macrometastasis	8	5.9

* Percentages are based on 75 cases unless otherwise noted.
† Categorization is based on the severest metastatic SLN load present within each patient.
BMI: body mass index, LLETZ: large loop excision of the transformation zone, LVSI: lymphovascular space invasion, SLN: sentinel lymph node.

Table 2. Results of the reviewed MRI parameters

	Measured result		Diagnostic odds ratio for metastasis detection*		
	123 tumor-negative SLN	13 tumor-positive SLN	Odds ratio	95%CI	p-value
Median SLN size (range)					
Short axis diameter, in mm	4.0 (1.0 – 8.9)	5.6 (2.0 – 6.7)	1.42	1.01 – 1.99	0.042
Long axis diameter, in mm	7.0 (1.0 – 14.3)	8.2 (3.7 – 16.0)	1.28	1.03 – 1.57	0.023
Ratio long relative to short axis†	1.7 (1.0 – 4.6)	1.9 (1.0 – 3.0)	0.75	0.32 – 1.73	0.497
SLN (%) categorized by shape‡					
Bean	47 (38.2%)	3 (23.1%)	0.45	0.12 – 1.75	0.250
Disc	33 (26.8%)	6 (46.2%)	1.98	0.60 – 6.50	0.262
Spherical / ball	38 (30.9%)	3 (23.1%)	0.83	0.21 – 3.30	0.795
Lobulated	5 (4.1%)	1 (7.7%)	2.60	0.27 – 25.46	0.412
SLN (%) with‡					
Absence of sharp demarcation	4 (3.3%)	2 (15.4%)	7.55	1.09 – 52.28	0.040
Heterogeneous gadolinium enhancement	17 (13.8%)	4 (30.8%)	3.06	0.79 – 11.89	0.107
Fat hilum visible	17 (13.8%)	1 (7.7%)	0.60	0.07 – 5.06	0.637
Central necrosis	0 (0.0%)	0 (0.0%)	na	na	na
Cystic component	0 (0.0%)	0 (0.0%)	na	na	na
SLN (%) categorized by cortex‡					
Cortex cannot be discerned	90 (73.2%)	9 (69.2%)	0.59	1.56 – 2.24	0.438
Cortex < 3mm	29 (23.6%)	3 (23.1%)	1.27	0.31 – 5.29	0.738
Cortex ≥ 3mm	4 (3.3%)	1 (7.7%)	3.79	0.33 – 43.09	0.282

Table 2 continued. Results of the reviewed MRI parameters

	Measured result		Diagnostic odds ratio for metastasis detection*		
	123 tumor-negative SLN	13 tumor-positive SLN	Odds ratio	95%CI	p-value
Median nearest non-sentinel LN size (range)					
Short axis diameter, in mm	3.0 (1.0 – 9.0)	3.5 (1.0 – 5.2)	1.35	0.95 – 1.92	0.092
Long axis diameter, in mm	4.9 (1.0 – 15.0)	7.9 (3.5 – 12.0)	1.19	1.00 – 1.42	0.055
Ratio short axis relative to short axis SLN†	1.4 (0.4 – 5.5)	1.3 (0.6 – 6.0)	1.09	0.63 – 1.88	0.755
Ratio long axis relative to long axis SLN†	1.2 (0.1 – 9.7)	1.1 (0.8 – 2.1)	0.58	0.25 – 1.37	0.216

* Values are multivariable adjusted for the quality of the MRI datasets.
† Calculated variable based on scored parameters.
‡ Depending on either a tumor-negative or tumor-positive SLN status, percentages in the measured result columns are fractions of 123 or 13 SLNs, respectively.
MRI: magnetic resonance imaging, SLN: sentinel lymph node, 95%CI: 95% confidence interval, na: not applicable, LN: lymph node.

Diagnostic Accuracy

The scored MRI parameters are descriptively outlined in table 2 and an example case is shown in figure 2. After adjusting for MRI dataset quality, only the short axis SLN diameter (p 0.042), long axis SLN diameter (p 0.023) and the absence of sharp SLN demarcation (p 0.040) were significantly associated with a tumor-positive SLN (Table 2). Interestingly, the SLN was significantly larger – in both short ($p<0.001$) and long axis ($p<0.001$) diameter – than the anatomically nearest non-sentinel lymph node whether the SLN was tumor-positive or not. The SLN shape (p 0.250 – 0.795), cortex thickness (p 0.282 – 0.738), and presence or absence of heterogeneous gadolinium enhancement (p 0.107) or fatty hilum (p 0.637), all showed no significant positive or negative association with nodal metastases. A subgroup analysis on macrometastases, by recoding micrometastatic SLNs as negative, did not identify additional significant parameters.

The ROC's of the short axis SLN diameter, long axis SLN diameter and the absence of sharp SLN demarcation had an AUC of 0.668 (95%CI: 0.528 – 0.808), 0.655 (95%CI: 0.482 – 0.829) and 0.574 (95%CI: 0.381 – 0.768), respectively. See supplemental file 1 for the ROC plots. A short axis SLN diameter cutoff of 5.6mm yielded the highest combined sensitivity (53.8%) and specificity (81.3%). For the long axis SLN diameter this cutoff was 10.5mm for the sensitivity (38.5%) and specificity (94.3%).

The moderate increase to an AUC of 0.749 (95%CI: 0.569 – 0.930) for the multivariable model – based on all three MRI parameters – when compared to the AUC's of the individual parameters, is likely attributable to the significant correlation (Pearson's r: 0.669, $p<0.001$) between the short and long axis of the SLN (i.e. multicollinearity).

DISCUSSION

We have used SPECT–MRI fusion to enable a selective assessment of SLNs in early stage cervical cancer patients. We purposely focused our analysis on non-enlarged, <10mm lymph nodes because in clinical practice these nodes are commonly considered 'non-metastatic'. Women with early stage cervical cancer and non-enlarged nodes generally do not undergo PET-CT, unless there is an alternative indication (e.g. MRI findings) [15]. This is in contrast to the routine use of PET-CT for advanced (stage III-IV) disease. Our approach was based on the premise that a focused review of a few lymph nodes – with the knowledge that these are the SLNs – instead of indiscriminately assessing all non-enlarged lymph nodes, could improve the detection of metastases.

We have shown that selective SLN assessment on MRI is feasible. The analysis further identified three clinically usable MRI parameters – the short and long axis diameters and absence of a sharp demarcation – that all had a significant association with nodal metastases from cervical cancer. As expected in <10mm nodes, the univariable and combined diagnostic accuracy was only moderate at best, but reducing false-negatives in these nodes is an attractive clinical goal. Even after this <10mm short axis selection, SLN size remained significantly correlated with the odds of metastases. This is in line with Choi et al. (n=55) who found a comparable result in a node-by-node analysis for the short axis of metastatic non-sentinel lymph nodes on MRI [19]. Unfortunately, other studies often present only a single size cut-off, instead of maintaining it as a continuous variable (such as in a ROC analysis) which better reflects the inverse dependency between sensitivity and specificity.

The cervical cancer study by Choi et al. also observed significantly less often smooth margins in metastatic lymph nodes, regardless of their size [19]. Likewise, absence of smooth margins has been linked by Brown et al. to nodal metastases in rectal cancer with a sensitivity of 75% and specificity of 98%. However, their inclusion of large metastatic lymph nodes – up to 15mm – could have potentially influenced the margin assessment and inflated the diagnostic accuracy outcome; this in contrast to the selective inclusion of small, < 10mm lymph nodes in the current study [20]. In terms of SLN shape, various authors consider spherical (i.e. round in a single orthogonal plane) lymph nodes intrinsically more suspicious than those with a bean or oval appearance [13,21,22]. In our results, both direct SLN shape judgments and long/short axis ratios did not have a significant association with metastatic invasion.

Although the intraoperative SLN procedure is invasive, laborious and carries a risk of adverse events, it remains diagnostically superior to conventional MRI assessment wherein all pelvic lymph nodes – not specifically SLNs – are reviewed. A meta-analysis

from 2008 (72 studies, n=5042) by Selman et al. reported a pooled sensitivity of 91.4%, 74.7% and 55.5% and a specificity of 100.0%, 97.6% and 93.2% in detecting lymph node metastases from cervical cancer for the SLN procedure, PET–CT and MRI, respectively [23]. Studies on MRI published after this meta-analysis, have shown comparable results for its diagnostic accuracy in cervical cancer [7,24,25,26,27,28]. However, a recent study on the intraoperative SLN procedure by Cibula et al. (8 centers, n=645) reported a further increase to 97% sensitivity when SLNs are bilaterally detected and histopathologically ultrastaged [2].

Certain limitations of our study merit further explanation. Firstly, the number of tumor-positive SLNs (i.e. 'events') was limited to 13 SLNs in 8 cases. Although this represents the normal incidence of metastases in a stage I/II cohort conditioned on <10mm short axis lymph nodes, the statistical power to prove associations is restricted. Secondly, we adopted a single reviewer approach which inherently challenges reproducibility when compared to consensus statements by multiple independent reviewers. However, this issue is at least partly alleviated by adequate blinding, the use of measurable criteria (e.g. SLN diameter) and a review by an experienced radiologist specialized in gynecological and oncological imaging. Thirdly, our approach still requires CT for accurate anatomy based fusion of the SPECT dataset with the work-up MRI. However, this can be overcome when hybrid SPECT–MRI scanners become commercially available in the future. Finally, our research is exploratory and requires external validation in larger series.

Conclusion

In conclusion, we have shown that a SPECT–MRI review specifically focused on detecting cervical cancer metastases in <10mm short axis SLNs is feasible, and – as hypothesized – may reduce the number of false negatives in these patients. While it cannot match the intraoperative SLN procedure in terms of accuracy, a clinical benefit is that it may allow for selecting early stage patients for PET–CT. Also, our MRI based SLN assessment noninvasively provides the radiologist with information on the nodal site where metastatic disease may first appear, deemphasizing non-sentinel lymph nodes in the review process. Three easy to use SLN parameters were identified, namely the short and long axis diameter and absence of sharp demarcation, which could be of potential value for future research or patients wherein SLNs cannot be intra-operatively retrieved. These exploratory results justify larger and prospective series focused on the value of selective SLN assessment on MRI.

Supplemental file 1. Receiver-operating-curves for detection of metastases in sentinel lymph nodes.

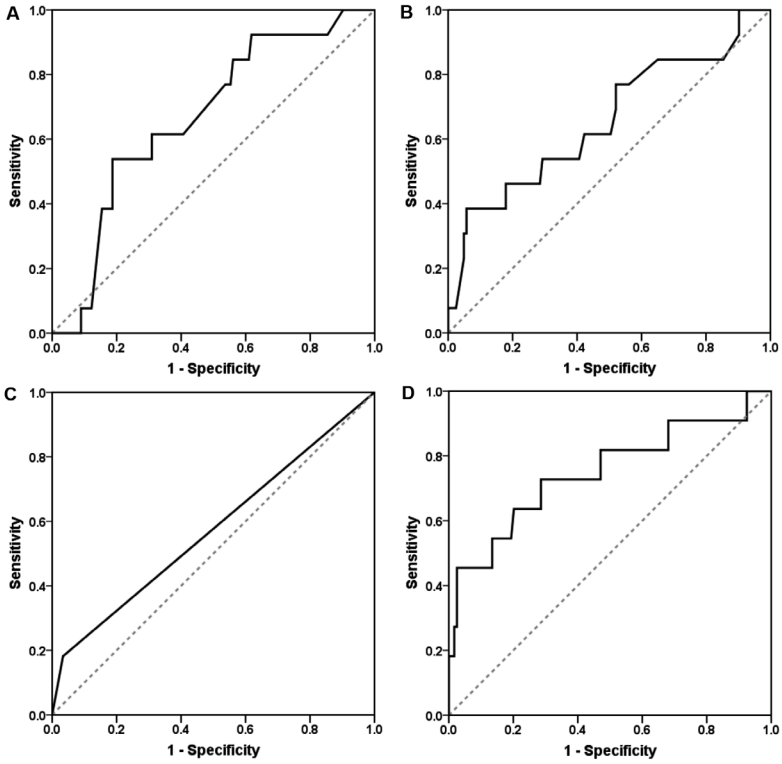

Univariable receiver-operating-curve for detecting metastases based on MRI measurement of the SLN short axis (A) which produces an area under the curve (AUC) of 0.668 (95%CI: 0.528 – 0.808). The SLN long axis (B) has an AUC of 0.655 (95%CI: 0.482 – 0.829) and absence of sharp demarcation of the SLN (C) an AUC of 0.574 (95%CI: 0.381 – 0.768). The MRI quality adjusted multivariable model which combines these three significant SLN parameters (D) has an AUC of 0.749 (95%CI: 0.569 – 0.930).

Funding

None

Conflict of interest

The authors declare that they have no conflicts of interest relevant to the presented work.

Acknowledgments

None

REFERENCES

1. National Cancer Institute, department of Health and Human Services, United States government. Sentinel lymph node biopsy. National Cancer Institute website. http://www.cancer.gov/about-cancer/diagnosis-staging/staging/sentinel-node-biopsy-fact-sheet#q2. Updated: August 11, 2011. Retrieved: September 22, 2015.
2. Cibula D, Abu-Rustum NR, Dusek L, et al. Bilateral ultrastaging of sentinel lymph node in cervical cancer: lowering the false-negative rate and improving the detection of micrometastasis. Gynecol Oncol. 2012;127:462-466.
3. Cibula D, Abu-Rustum NR, Dusek L, et al. Prognostic significance of low volume sentinel lymph node disease in early-stage cervical cancer. Gynecol Oncol. 2012;124:496-501.
4. Baalbergen A, Veenstra Y, Stalpers L. Primary surgery versus primary radiotherapy with or without chemotherapy for early adenocarcinoma of the uterine cervix. Cochrane Database Syst Rev. 2013;31:CD006248.
5. Landoni F, Maneo A, Colombo A, et al. Randomised study of radical surgery versus radiotherapy for stage Ib-IIa cervical cancer. Lancet. 1997;350:535-540.
6. Eiriksson L, Covens A. Sentinel lymph node mapping in cervical cancer: the future? BJOG 2012;119:129–133.
7. Chung HH, Kang KW, Cho JY, et al. Role of magnetic resonance imaging and positron emission tomography/computed tomography in preoperative lymph node detection of uterine cervical cancer. Am J Obstet Gynecol. 2010;203:156.e1-156.e5.
8. Hori M, Kim T, Murakami T, et al. Uterine cervical carcinoma: preoperative staging with 3.0-T MR imaging--comparison with 1.5-T MR imaging. Radiology. 2009;251:96-104.
9. Testa AC, Ludovisi M, Manfredi R, et al. Transvaginal ultrasonography and magnetic resonance imaging for assessment of presence, size and extent of invasive cervical cancer. Ultrasound Obstet Gynecol. 2009;34:335-344.
10. Sheu M, Chang C, Wang J, Yen M. MR staging of clinical stage I and IIa cervical carcinoma: a reappraisal of efficacy and pitfalls. Eur J Radiol. 2001;38:225-231.
11. Choi HJ, Roh JW, Seo SS, et al. Comparison of the accuracy of magnetic resonance imaging and positron emission tomography/computed tomography in the presurgical detection of lymph node metastases in patients with uterine cervical carcinoma: a prospective study. Cancer. 2006;106:914-922.
12. Sala E, Rockall AG, Freeman SJ, Mitchell DG, Reinhold C. The added role of MR imaging in treatment stratification of patients with gynecologic malignancies: what the radiologist needs to know. Radiology. 2013;266:717-740.
13. Lai G, Rockall AG. Lymph node imaging in gynecologic malignancy. Semin Ultrasound CT MR. 2010;31:363-376.

14. Hoogendam JP, Veldhuis WB, Hobbelink MG, Verheijen RH, van den Bosch MA, Zweemer RP. Technetium-99m SPECT-CT versus planar lymphoscintigraphy for preoperative sentinel lymph node detection in cervical cancer: a systematic review and meta-analysis. J Nucl Med. 2015;56:675-680.
15. Chou HH, Chang TC, Yen TC, et al. Low value of [18F]-fluoro-2-deoxy-D-glucose positron emission tomography in primary staging of early-stage cervical cancer before radical hysterectomy. J Clin Oncol. 2006;24:123-128.
16. Driscoll DO, Halpenny D, Johnston C, Sheehy N, Keogan M. 18F-FDG-PET/CT is of limited value in primary staging of early stage cervical cancer. Abdom Imaging. 2015;40:127-133.
17. Bossuyt PM, Reitsma JB, Bruns DE, et al. Standards for reporting of diagnostic accuracy. towards complete and accurate reporting of studies of diagnostic accuracy: the STARD initiative. BMJ. 2003;326:41-44.
18. Hoogendam JP, Hobbelink MG, Veldhuis WB, Verheijen RH, van Diest PJ, Zweemer RP. Preoperative sentinel node mapping with (99m)Tc-nanocolloid SPECT-CT significantly reduces the intraoperative sentinel node retrieval time in robot assisted laparoscopic cervical cancer surgery. Gynecol Oncol. 2013;129:389-394.
19. Choi HJ, Kim SH, Seo SS, et al. MRI for pretreatment lymph node staging in uterine cervical cancer. AJR Am J Roentgenol. 2006;187:W538-W543.
20. Brown G, Richards CJ, Bourne MW, et al. Morphologic predictors of lymph node status in rectal cancer with use of high-spatial-resolution MR imaging with histopathologic comparison. Radiology. 2003;227:371-377.
21. Kim SH, Kim SC, Choi BI, Han MC. Uterine cervical carcinoma: evaluation of pelvic lymph node metastasis with MR imaging. Radiology. 1994;190:807-811.
22. Torabi M, Aquino SL, Harisinghani MG. Current concepts in lymph node imaging. J Nucl Med. 2004;45:1509-1518.
23. Selman TJ, Mann C, Zamora J, Appleyard TL, Khan K. Diagnostic accuracy of tests for lymph node status in primary cervical cancer: a systematic review and meta-analysis. CMAJ. 2008;178:855-862.
24. Zhang W, Zhang J, Yang J, et al. The role of magnetic resonance imaging in pretreatment evaluation of early-stage cervical cancer. Int J Gynecol Cancer. 2014;24:1292-1298.
25. Lv K, Guo HM, Lu YJ, Wu ZX, Zhang K, Han JK. Role of 18F-FDG PET/CT in detecting pelvic lymph-node metastases in patients with early-stage uterine cervical cancer: comparison with MRI findings. Nucl Med Commun. 2014;35:1204-1211.
26. Klerkx WM, Veldhuis WB, Spijkerboer AM, et al. The value of 3.0 tesla diffusion-weighted MRI for pelvic nodal staging in patients with early stage cervical cancer. Eur J Cancer. 2012;48:3414-3421.

27. Hong KS, Ju W, Choi HJ, Kim JK, Kim MH, Cho KS. Differential diagnostic performance of magnetic resonance imaging in the detection of lymph node metastases according to the tumor size in early-stage cervical cancer patients. Int J Gynecol Cancer. 2010;20:841-846.
28. Mitchell DG, Snyder B, Coakley F, et al. Early invasive cervical cancer: MRI and CT predictors of lymphatic metastases in the ACRIN 6651/GOG 183 intergroup study. Gynecol Oncol. 2009;112:95-103.

8

Chapter 9

General discussion

IMAGING IN EARLY STAGE CERVICAL CANCER

We focused our research on both the evaluation of existing and development of new imaging strategies applicable to women diagnosed with stage I – II cervical cancer. In the first half of this thesis we investigated the clinical value of routine chest radiography and possible improvements to pelvic MRI. Both are currently incorporated into the primary (staging) evaluation of cervical cancer. The second part of this thesis was directed at sentinel lymph node imaging and includes a comparison between lymphoscintigraphy and SPECT-CT.

Routine chest radiography

The cohort presented in chapter 2 confirmed the anticipated absent value for chest radiography as a screening tool for thoracic metastatic disease detection, as part of the routine work-up of patients suspected of early stage cervical cancer [1]. In none of these women did the radiograph identify pulmonary metastases or adjust the FIGO stage.

We found that even in the era in which a pretreatment radiograph was routinely recommend by the guidelines – perhaps intuitively – they were ordered at a disproportionally lower rate in early stage patients. In our study, only 36.8% of stage IA cases and 83.5% for IB1 underwent radiography during their work-up. This may indicate that during the study period (2006-2013) physicians already questioned its efficacy in early stage disease. Comparable findings have been reported in studies on 'patterns of care' which demonstrate a slow but steady decline in radiograph use worldwide. Russell et al [2]. illustrated that from 1984 to 1990 its pretreatment use in the United States dropped from 63.2% to 58.5% (stage IA) and 81.2% to 78.8% (stage IB and IIA), respectively. A multicenter study (trial GOG183) by the American Gynecologic Oncology Group recorded a further drop to 62.9% (stages ≥IB1) by 2000-2002 [3]. A nationwide Japanese survey (all FIGO stages) also demonstrated a significant ($p<0.001$) decline, though from a relatively high 97% (1999-2001) to 88% (2003-2005) [4,5]. These interstudy differences emphasize the marked geographical differences in the use of a work-up chest radiography.

Our study was deliberately not focused on diagnostic test accuracy, but on the clinical efficacy of the current unselective use of chest radiography. Quantitative diagnostic test accuracy parameters would have appeared deceptively good due to the very low incidence of thoracic metastases. In our cohort, true negative cases will fill >97% of the underlying two-by-two-table, yielding a high area under the curve (i.e. 0.989; 95%CI: 0.975 - 1.000) at a receiver operating characteristics (ROC) analysis. However, such an approach obscures the absence of true positives cases in the early stage subgroup, a clinically relevant finding. In addition, advantages of our approach include the presentation of

undesired clinical consequences from false positive findings and the absent detection of any relevant thoracic comorbidities unrelated to cervical cancer.
In the literature, only a limited number of comparable radiography studies exist, though with uniformly similar results. In an analysis by Griffin et al [6]. (1970-1975, n=227) two patients, considered to have pre-radiograph stage IIB and IIIB, were identified and upstaged to IVB based on chest radiography abnormalities. This study contained 178 suspected of stage I-II prior to radiography, yielding a 0.6% upstaging ratio for this early stage subgroup. Gordon et al [7]. (1975-1981, n=211) reported nearly identical results. They found one positive radiograph in 156 pre-radiograph stage I-II patients (0.6%) after excluding one patient with a synchronous second primary tumor (stage III oral cancer). Thirdly, a study from the United States by Massad et al [8]. (1994-1999, n=133) which excluded stage IA or IB1, identified one positive chest radiograph in 66 cases with IB2, IIA or IIB. She was subsequently upstaged from IIB to IVB. Unfortunately, results from various other radiography studies cannot be interpreted in terms of their staging implications, mainly due to absent pre-radiograph stage descriptions or the combining of follow-up and staging radiographs [9,10,11,12].
Nearly all (inter)national guidelines do not support their recommendations on radiography use with specific references, except for citing the expert FIGO opinion on clinical staging [13,14,15,16,17,18]. At present, formal guideline changes have not been made in the Netherlands and chest radiography remains unselectively recommended for all cervical cancer patients [17]. Thus, the recently implemented practice at our center in which it is no longer routinely used in early stage patients should be regarded as a motivated deviation from the current guideline. Based on the current evidence – and anticipating that further large trials will not be carried out – we advocate to omit routine chest radiography for staging purposes in cervical cancer patients suspected of an early stage.

Pelvic 7.0T MRI of cervical cancer

Prior to the publication of our feasibility study, no literature existed on in-vivo cervical cancer imaging at ultra-high field strengths. In 2013 a research group from Germany published results on pelvic imaging in healthy volunteers using a 7.0T whole-body MR system (Magnetom, Siemens) with an external 8 channel coil [19]. Ten women (25-33 years) of unknown body mass index underwent T_1 and T_2-weighted imaging following individualised B_1 shimming in a manner comparable to our study [20]. In contrast to our study, 0.1 mmol/kg Gadobutrol and 20 mg N-butylcopalamin were intravenously administered. The authors concluded that T_1-weighted gradient echo sequences, with and without gadolinium contrast enhancement, were feasible and yielded satisfactory

image quality as judged independently by two radiologists. The T_2-weighted turbo spin echo sequences provided only moderate image results and were mostly considered of insufficient quality for diagnostic purposes. Challenges discussed by the investigators include Specific Absorption Rate (SAR) constraints and artefacts caused by the B_1 inhomogeneity associated with MRI at an ultra-high field strength.

In chapters 3 and 4 we present the feasibility and added value of using an receive only endorectal antenna for ultra-high field MR imaging of cervical cancer. The beneficial effect, in terms of signal to noise ratio (SNR) gain, of the monopole receive antenna was substantial in both the healthy female volunteer (3.2 fold increase) and the scanned patients (1.8-2.2 fold increase). The SNR increase is relatively local and thus the achieved benefit depends on adequate antenna positioning to minimize the distance between its receive optimum and the anatomical region of interest (i.e. cervix). Endorectal positioning is relatively straightforward and not regarded as uncomfortable by the study participants, nor did they report adverse events or request to end their participation prematurely. Nor was there any indication during the execution of the presented study that patient accrual was hindered by its use. In conclusion, the use of an endorectal monopole should not be discarded by researchers (or review boards) out of a misplaced fear for the loss of patient comfort during imaging.

While we have demonstrated the feasibility of T_2-weighted imaging at 7.0T for stage IB1-IIB cervical cancer, further improvements in image quality remain desirable, particularly in improving the field of view to allow better visualization of the draining lymph nodes and in the reduction of artefacts [21]. This imaging method can also be of interest to researchers on other pathology of the inner pelvis such as endometriosis and malignancies of the endometrium, prostate and rectum.

A future research perspective should be to objectify the clinical benefit of ultra-high field MRI in cervical cancer. For the moment, its diagnostic test accuracy and the associated observer variability – relative to 1.5/3.0T MRI or the clinical rectovaginal examination – remain unknown. Especially the accuracy in detecting parametrial invasion would be relevant, whereas this is largely a resolution dependent assessment for which increases in field strength have been suggested to improve accuracy [22]. The sample size of the presented pilot study is insufficient for such an analysis and patients considered IIB did not undergo radical surgery and thus no histopathological proof (i.e. reference standard) of invasion exists.

MR spectroscopy non-invasively studies the biochemical composition by measuring the signal from metabolites that resonate at detectable frequencies [23]. The experience with MR spectroscopy on cervical cancer is limited to either field strengths ≤3.0T or, when performed at higher field strengths, on an ex-vivo basis (i.e. resected tissue) which

may negatively influence the representativeness of the identified metabolites [24,25,26]. Besides a possible choline increase, these preliminary studies have repeatedly indicated elevated lipid levels in cervical cancer. Such increases in lipid levels are consistent with the results of a range of other solid malignancies [27,28,29]. Furthermore, reports have significantly correlated these spectra to 0.3–2.0 micrometer cytoplasmic lipid droplets identified at histopathology of the scanned cervical cancer biopsies [30,31]. In a study conducted by Zietkowski et al [32], both the extent of apoptosis and sensitivity to paclitaxel were associated with a fourfold increase in the unsaturated triglyceride droplets, indicating that these triglyceride spectroscopy profiles may be of interest as a marker for chemotherapy resistance.

The use of ultra high field strengths, aided by local antennas which further increase the SNR, is very advantageous to MR spectroscopy because a higher spectral resolution (i.e. better signal separation of individual metabolites) can be achieved. Obtaining spectra in-vivo from early stage cervical cancer at ultra high field strengths, including the study of spectral differences between invaded and non-invaded parametria, is an active aim for our research group in the near future [33].

Pelvic MRI: diffusion weighted imaging

The sensitivity of diffusion weighted imaging (DWI) to differences in diffusivity is governed by the choice of *b*-values. In chapter 5 we demonstrated that although, as expected, the *b*-value combination affects the calculated apparent diffusion coefficient (ADC), its diagnostic ability to discriminate malignant from benign cervical tissue remains uniformly good across different combinations [34]. The importance of the ADC lies with its quantification of water diffusion from the DWI signal of a scanned voxel.

A methodological limitation of our study was that benign regions of interest (ROI) were not derived from a separate control group, proven to be without cervical disease. Such an approach could have provided more valid ADC values than our method wherein 'benign' ADC results were calculated from cervical areas without visible tumor. However, our study was not focused on diagnosing cervical cancer by ADC calculation, instead the diagnostic accuracy parameters were a method to compare *b*-value combinations. This approach follows daily clinical practice since DWI is not a tool for diagnosing cervical cancer, instead it is used to aid tumor delineation for size and regional invasion assessments [35]. Such delineation is in essence an (image based) comparison between benign versus malignant tissue performed within a single patient.

As outlined in the discussion of chapter 5 of this thesis, a range of DWI studies (with different *b*-value combinations) have shown hindered water diffusion (i.e. reduced ADC's) of cervical malignancies. These encouraging results from studies on primary

tumor evaluation sparked research on the benefits of DWI with respect to lymph node visualization and metastasis detection. From our institution, Klerkx et al [36]. demonstrated a considerable increase in lymph node detection through the use of DWI when compared to conventional T_1 and T_2 MRI. The extra nodes detected were predominately small sized, inherently carrying a low probability of containing metastatic disease.

In 2015, a meta-analysis by Shen et al [37]. (15 studies, n=1021) was published in which the diagnostic accuracy of DWI for detection of nodal metastases was investigated for cervical cancer. Eleven studies were deemed to be of high quality based on a QUADAS assessment and had a pooled sensitivity and specificity of 86% (95%CI: 82–89%) and 84% (95%CI: 83–86%). Surprisingly, only Korean and Chinese studies were included, limiting global generalizability, nevertheless substantial interstudy heterogeneity remained at pooling (I^2 = 91%). In the included studies, accuracy outcomes were typically calculated for ADC cut-off values which were retrospectively established and optimized to have the highest discriminatory power. Without external validation, such an approach could drastically overestimate the diagnostic performance of DWI [38]. Equally, the review authors did not address nodal size as an important covariate which will in a regular clinical setting influence a reviewer in his judgment on nodal status. The results of this meta-analysis do not include and even conflict with the prospective multicenter study (n=62) conducted at our center, in which a blinded multirater approach to assess nodes was adopted [39]. This trial found that both the short (AUC: 0.81, 95%CI: 0.70–0.91) and long axis nodal diameter (AUC: 0.69, 95%CI: 0.54–0.84) were diagnostically superior to the poor accuracy of ADC (AUC: 0.62, 95%CI: 0.48–0.76) for diagnosing nodal metastases in IA2–IIB cervical cancer.

Published research is increasingly directed towards using the ADC as a functional biomarker for tumor aggressiveness, monitoring the response to (chemo)radiotherapy and predicting both survival and detecting recurrence [40,41,42,43]. While most of these studies should be considered preliminary, a convincing body of evidence exists for the relation between ADC's measured directly after treatment and the long term treatment response. A review by Schreuder et al (9 studies, n=231) identified a larger relative ADC increase, when comparing pre-(chemo)radiotherapy (i.e. baseline) values to those at the end of treatment on an intrapatient basis, for those who had a complete response [44]. Besides relative increases, absolute post-treatment ADC values were also markedly higher in complete ($1.50{\cdot}10^{-3}$ mm^2/s) and partial responders ($1.42{\cdot}10^{-3}$ mm^2/s) when compared to non-responders ($1.18{\cdot}10^{-3}$ mm^2/s). Some authors have hypothesized that in this situation the ADC functions as a marker for the extent of edema and necrosis induced by the administered treatment [35,45].

Sentinel lymph node imaging: Lymphoscintigraphy versus SPECT-CT

A range of cervical cancer studies on planar lymphoscintigraphy have stated that its added value to the intraoperative gamma-probe and blue dye aided sentinel lymph node (SLN) detection is limited [46,47,48,49,50]. This would be due to the lack of anatomical reference and non-cross-sectional nature of planar imaging, hampering correlation between images and the intra-operative view of the pelvis. However, the concept of preoperative imaging aimed at facilitating the intraoperative retroperitoneal SLN detection (i.e. minimizing the damage to lymphatic structures while removing the SLN) continued to exist and SPECT-CT became increasingly adopted as an alternative to lymphoscintigraphy. In chapter 6 of this thesis, shorter SLN retrieval time, an increased intra-operative detection and a higher SLN visualization on SPECT-CT were found. The latter two of these outcomes were not statistically significant, likely due to the limited sample size of the studied cohort.

After pooling our results with seven comparable observational studies, SPECT-CT had a superior overall SLN visualization ratio with 8.3% (95%CI: 2.0–11.6%) more cases in which minimally one SLN was depicted when compared to lymphoscintigraphy. In this meta-analysis, presented in chapter 7, we had preferred an approach focused on comparing the intraoperative SLN resection result between both imaging modalities. It is possible that lymphoscintigraphy and SPECT-CT cause differences in the intraoperative uni- and bilateral SLN resection ratio and the total number of SLN's found during surgery. This may be a clinically more relevant outcome measure compared to the current analysis limited to imaging (i.e. visualization) results. However, seven of the eight studies followed a design in which SPECT-CT and lymphoscintigraphy were consecutively performed within the same patient (i.e. paired design), consequently yielding identical intraoperative SLN resection results. Besides considering the benefits of an unpaired (or even randomized) design, future studies should preferably present bilateral visualization and intra-operative detection ratios.

From a clinical perspective, the identified benefits of SPECT-CT should outweigh its associated disadvantages. An increased ionizing radiation exposure due to the CT addition could be considered an important disadvantage of SPECT-CT. Currently, both low (i.e. with a reduction in image quality) and regular dosed (abdomino)pelvic CT, with or without intravenous contrast enhancement, are used for SLN imaging. New CT algorithms using iterative image reconstruction instead of filtered back projection are able to increase the signal to noise ratio, thus conversely allowing substantial reductions in ionizing radiation dose [51]. A review by Willemink et al. on 49 studies reported a relative dose reduction between 23% and 76% when using iterative reconstruction at an equal image quality to filtered back projection [52,53]. Furthermore, given that in SLN

imaging CT serves as an anatomical reference only, without a direct diagnostic aim, ultra-low dose CT (<1 mSv) could possible yield sufficient image quality for this purpose [54].
A second concern voiced for SPECT-CT is that it is considered to be more expensive when directly compared to lymphoscintigraphy. For both modalities the exact costs can differ substantially between clinics due to a variety of logistical and medical factors. At our center, the internal fee in 2016 to compensate the modality itself (i.e. a subpart of the entire SLN imaging procedure cost) is 106 euro for lymphoscintigraphy and 112 euro for SPECT-CT. Moreover, additional costs are likely identical due the overlap in methodology with respect to the injection technique, radiotracer dosing, review time and overhead costs.
This thesis demonstrated that SPECT-CT yields a reduction of 25 minutes for the intra-operative robotic SLN retrieval [55]. This raises the question whether its added costs are offset by the reduction in theatre time. Unfortunately, no formal economic evaluation exists wherein both modalities for preoperative SLN imaging are compared in women with early stage cervical cancer. However, a 2013 study published in the JAMA calculated the actual cost of a hysterectomy based on 264758 procedures in 441 hospitals in the United States [56]. For benign uterine pathology, a hysterectomy by a robot-assisted laparoscopic approach would cost a median 8868 dollar, with an interquartile range between 6787 and 11830 dollar. This entails all fixed and variable costs of the surgery itself, a non-radical hysterectomy without a SLN procedure or pelvic lymph node dissection. Theatre lengths are not provided by the investigators, however, when a median length is assumed between 120 and 180 minutes per hysterectomy, a robotic theatre would cost between 74 and 49 dollar per minute. For a 25 minute reduction in theatre time, this corresponds to a total of 1850 to 1225 dollar (i.e. 1665 to 1103 euro, exchange rate: 1 euro / 1.10 dollar). This could even be a relative underestimation whereas more qualified personnel and the additional instruments required for radical surgery may further increase the per minute cost.
All maters considered, when pre-operative SLN imaging is desired in early stage cervical cancer, a clear preference for SPECT-CT over lymphoscintigraphy exists. As a next research step in this field, we wanted to investigate whether our standard SPECT-CT approach could facilitate a MRI review focused solely on the SLN for the imaging based detection of nodal metastases.

MRI based SLN assessment

In chapter 8 we described a new imaging technique focused on the detection of metastases in non-enlarged (i.e. short axis <10mm) lymph nodes [57]. More precisely, via SPECT-MRI fusions we aimed at focusing MRI assessment on only a very select number

of lymph nodes, namely those where metastases are first expected (i.e. sentinel lymph nodes). The studied cohort consisted solely of women with early stage cervical cancer whom had a routine work-up MRI in which all pelvic nodes were indiscriminately reviewed and considered unsuspicious.

An advantage of the presented approach is that only already available datasets are used without a need for extra imaging. Also, creating a SPECT-MRI fusion is one, relatively straightforward, post-processing step extra for the technologist after creating the SPECT-CT. It can be created on the day before surgery and reviewed side-by-side with the SPECT-CT, in which the good soft tissue contrast of MRI can be exploited. When considered suspicious for lymph nodal metastases on MRI, theoretically, it is than still possible to select those patients for same day (i.e. still prior to surgery) PET-CT. Based on the PET-CT findings a decision can be reached whether to abstain from radical surgery and select chemoradiation as the primary treatment modality.

The scored MRI parameters for nodal assessment (e.g. absence of sharp SLN demarcation) and their associated test accuracy outcomes are informative, especially for comparisons with alternative strategies for detection of nodal metastases. We incorporated it into our methodology to assist in the feasibility demonstration and highlight the possibilities of the SPECT-MRI approach. Though, a study limitation is our single reviewer approach for scoring these parameters. This makes the reproducibility of the accuracy outcomes unknown. Though, observer variability will be partly alleviated by the adequate blinding, substantial clinical experience of the reviewer and addition of less subjective MRI parameters (e.g. size measurements). A second limitation of our study is its sample size (n=75), and particularly the relatively small number of tumor positive lymph nodes (13 SLN, 8 patients), which restricts the statistical precision. This is noticeable in the broad confidence intervals of the test accuracy outcomes. These limitations indicate that while our preliminary results are interesting, they require external validation in larger series.

Imaging in early stage cervical cancer

In conclusion, imaging plays a central role in the care for women with early stage cervical cancer. This thesis was focused on a range of imaging studies which assess both disease extent and aid in the selection of treatment, typically performed after diagnosis and before treatment. We questioned the clinical value of existing practices such as the routine use of chest radiography, and presented the first developmental steps in new strategies. The latter were focused on ultra high field MRI and preoperative SLN imaging. In addition to these work-up strategies, though beyond the scope of this thesis, imaging is also increasingly integrated into treatment itself (e.g. radiotherapy), tumor response evaluation and the assessment of disease recurrence. The rapid technological advances, in part illustrated by this thesis, will likely increase rather than decrease this role in the near future. This affirms the important role of the radiologist in the multidisciplinary approach to cervical cancer.

REFERENCES

1. Hoogendam JP, Zweemer RP, Verkooijen HM, de Jong PA, van den Bosch MA, Verheijen RH, Veldhuis WB. No Value for Routine Chest Radiography in the Work-Up of Early Stage Cervical Cancer Patients. PLoS One. 2015 Jul 2;10(7):e0131899
2. Russell AH, Shingleton HM, Jones WB, Fremgen A, Winchester DP, Clive R, Chmiel JS. Diagnostic assessments in patients with invasive cancer of the cervix: a national patterns of care study of the American College of Surgeons. Gynecol Oncol. 1996 Nov;63(2):159-65.
3. Amendola MA, Hricak H, Mitchell DG, Snyder B, Chi DS, Long HJ 3rd, Fiorica JV, Gatsonis C. Utilization of diagnostic studies in the pretreatment evaluation of invasive cervical cancer in the United States: results of intergroup protocol ACRIN 6651/GOG 183. J Clin Oncol. 2005 Oct 20;23(30):7454-9.
4. Tomita N, Toita T, Kodaira T, Shinoda A, Uno T, Numasaki H, Teshima T, Mitsumori M. Changing trend in the patterns of pretreatment diagnostic assessment for patients with cervical cancer in Japan. Gynecol Oncol. 2011 Dec;123(3):577-80.
5. Toita T, Kodaira T, Uno T, Shinoda A, Akino Y, Mitsumori M, Teshima T. Patterns of pretreatment diagnostic assessment and staging for patients with cervical cancer (1999-2001): patterns of care study in Japan. Jpn J Clin Oncol. 2008 Jan;38(1):26-30.
6. Griffin TW, Parker RG, Taylor WJ. An evaluation of procedures used in staging carcinoma of the cervix. Am J Roentgenol. 1976 Nov;127(5):825-7.
7. Gordon RE, Mettler FA Jr, Wicks JD, Bartow SA. Chest X-rays and full lung tomograms in gynecologic malignancy. Cancer. 1983 Aug 1;52(3):559-62.
8. Massad LS, Calvello C, Gilkey SH, Abu-Rustum NR. Assessing disease extent in women with bulky or clinically evident metastatic cervical cancer: yield of pretreatment studies. Gynecol Oncol. 2000 Mar;76(3):383-7.
9. Barter JF, Soong SJ, Hatch KD, Orr JW, Shingleton HM. Diagnosis and treatment of pulmonary metastases from cervical carcinoma. Gynecol Oncol. 1990 Sep;38(3):347-51.
10. Imachi M, Tsukamoto N, Matsuyama T, Nakano H.Pulmonary metastasis from carcinoma of the uterine cervix. Gynecol Oncol. 1989 May;33(2):189-92.
11. Gunasekera PC, Fernando RJ, Abeykoon SC. Pulmonary metastases from cervical cancer in Sri Lanka. J Obstet Gynaecol. 1999 Jan;19(1):65-8.
12. Tellis CJ, Beechler CR. Pulmonary metastasis of carcinoma of the cervix: a retrospective study. Cancer. 1982 Apr 15;49(8):1705-9.
13. Colombo N, Carinelli S, Colombo A, Marini C, Rollo D, Sessa C; ESMO Guidelines Working Group. Cervical cancer: ESMO Clinical Practice Guidelines for diagnosis, treatment and follow-up. Ann Oncol. 2012 Oct;23 (Suppl 7:vii 27-32).

14. National Comprehensive Cancer Network (NCCN). NCCN Clinical Practice Guidelines in Oncology: Cervical Cancer. Version 3.2013. Available from "http://www.nccn.org", retrieved on Jan 20th, 2014.
15. World Health Organization, department of reproductive health and research and department of chronic diseases and health promotion. Comprehensive Cervical Cancer Control: A guide to essential practice (2006). Available from: http://www.who.int/reproductivehealth/publications/cancers/en/, retrieved on Jan 20th, 2014.
16. Kesic V, Cibula D, Kimmig R, Lopes A, Marth C, Reed N, et al (ESGO Educational Committee). Algorithms for management of Cervical cancer. Available from: http://www.esgo.org/Education/Pages/Algorithms.aspx, retrieved on Jan 20th, 2014.
17. Comprehensive Cancer Centre the Netherlands (IKNL). National cervical cancer guideline. Version 3.0 (approved on march 22th, 2012). Available from: http://oncoline.nl/cervixcarcinoom, retrieved on Jan 23th, 2014.
18. Oaknin A, Díaz de Corcuera I, Rodríguez-Freixinós V, Rivera F, del Campo JM; SEOM (Spanish Society of Clinical Oncology). SEOM guidelines for cervical cancer. Clin Transl Oncol. 2012 Jul;14(7):516-9.
19. Umutlu L, Kraff O, Fischer A, Kinner S, Maderwald S, Nassenstein K, Nensa F, Grüneisen J, Orzada S, Bitz AK, Forsting M, Ladd ME, Lauenstein TC. Seven-Tesla MRI of the female pelvis. Eur Radiol. 2013 Sep;23(9):2364-73.
20. Metzger GJ, Auerbach EJ, Akgun C, Simonson J, Bi X, Uğurbil K, van de Moortele PF. Dynamically applied B1+ shimming solutions for non-contrast enhanced renal angiography at 7.0 Tesla. Magn Reson Med. 2013 Jan;69(1):114-26.
21. Hoogendam JP, van Kalleveen IML, Arteaga de Castro CS, Raaijmakers AJE, Verheijen RHM, van den Bosch MAAJ, Klomp DWJ, Zweemer RP, Veldhuis WB. High resolution T2-weighted cervical cancer imaging: a feasibility study on ultra-high field 7.0T MRI with an endorectal monopole antenna. Eur Radiol 2016, in press.
22. Thomeer MG, Gerestein C, Spronk S, van Doorn HC, van der Ham E, Hunink MG. Clinical examination versus magnetic resonance imaging in the pretreatment staging of cervical carcinoma: systematic review and meta-analysis. Eur Radiol. 2013 Jul;23(7):2005-18.
23. Sala E, Rockall AG, Freeman SJ, Mitchell DG, Reinhold C. The added role of MR imaging in treatment stratification of patients with gynecologic malignancies: what the radiologist needs to know. Radiology. 2013 Mar;266(3):717-40.
24. Lin G, Lai CH, Tsai SY, Lin YC, Huang YT, Wu RC, Yang LY, Lu HY, Chao A, Wang CC, Ng KK, Ng SH, Chou HH, Yen TC, Hung JH. 1H MR spectroscopy in cervical carcinoma using external phase array body coil at 3.0 Tesla: Prediction of poor prognostic human papillomavirus genotypes. J Magn Reson Imaging. 2016 Jul 19. [Epub ahead of print]

25. Delikatny EJ, Russell P, Hunter JC, et al.. Proton MR and human cervical neoplasia: ex vivo spectroscopy allows distinction of invasive carcinoma of the cervix from carcinoma in situ and other preinvasive lesions. Radiology 1993;188(3):791–796
26. De Silva SS, Payne GS, Morgan VA, Ind TE, Shepherd JH, Barton DP, deSouza NM. Epithelial and stromal metabolite changes in the transition from cervical intraepithelial neoplasia to cervical cancer: an in vivo 1H magnetic resonance spectroscopic imaging study with ex vivo correlation. Eur Radiol. 2009 Aug;19(8):2041-8.
27. Calabrese C, Pisi A, Di Febo G, Liguori G, Filippini G, Cervellera M, Righi V, Lucchi P, Mucci A, Schenetti L, Tonini V, Tosi MR, Tugnoli V. Biochemical alterations from normal mucosa to gastric cancer by ex vivo magnetic resonance spectroscopy. Cancer Epidemiol. Biomarkers Prev. 2008; 17: 1386–1395.
28. Righi V, Mucci A, Schenetti L, Tosi MR, Grigioni WF, Corti B, Bertaccini A, Franceschelli A, Sanguedolce F, Schiavina R, Martorana G, Tugnoli V. Ex vivo HR-MAS magnetic resonance spectroscopy of normal and malignant human renal tissues. Anticancer Res. 2007; 27: 3195–3204.
29. Astrakas LG, Zurakowski D, Tzika AA, Zarifi MK, Anthony DC, De Girolami U, Tarbell NJ, Black PM. Noninvasive magnetic resonance spectroscopic imaging biomarkers to predict the clinical grade of pediatric brain tumors. Clin Cancer Res. 2004 Dec 15;10(24):8220-8.
30. Zietkowski D, deSouza NM, Davidson RL, Payne GS. Characterisation of mobile lipid resonances in tissue biopsies from patients with cervical cancer and correlation with cytoplasmic lipid droplets. NMR Biomed. 2013 Sep;26(9):1096-102.
31. Zietkowski D, Davidson RL, Eykyn TR, De Silva SS, Desouza NM, Payne GS. Detection of cancer in cervical tissue biopsies using mobile lipid resonances measured with diffusion-weighted (1)H magnetic resonance spectroscopy. NMR Biomed. 2010; 23: 382–390.
32. Zietkowski D, Payne GS, Nagy E, Mobberley MA, Ryder TA, deSouza NM. Comparison of NMR lipid profiles in mitotic arrest and apoptosis as indicators of paclitaxel resistance in cervical cell lines. Magn Reson Med. 2012 Aug;68(2):369-77.
33. Arteaga de Castro CS, Hoogendam JP, Raaijmakers AJ, van Kalleveen IML, Veldhuis WB, Zweemer RP, Luijten PR, Klomp DWJ. Shortened Fatty Acid Chains in Cervical Cancer using 1H MRSI at 7T. Abstract 3895, ISMRM 24th Annual Meeting & Exhibition, 7-13 May 2016, Singapore.
34. Hoogendam JP, Klerkx WM, de Kort GA, Bipat S, Zweemer RP, Sie-Go DM, Verheijen RH, Mali WP, Veldhuis WB. The influence of the b-value combination on apparent diffusion coefficient based differentiation between malignant and benign tissue in cervical cancer. J Magn Reson Imaging. 2010 Aug;32(2):376-82.
35. Thoeny HC, Forstner R, De Keyzer F. Genitourinary applications of diffusion-weighted

MR imaging in the pelvis. Radiology. 2012 May;263(2):326-42.
36. Klerkx WM, Mali WP, de Kort GA, Heintz AP, Takahara T, Sie-Go DM, Peeters PH. Diffusion weighted imaging added to eonventional MRI increases pelvic lymph node detection. Doctorate thesis; MR Imaging of lymph nodes. 2009. ISBN 9789039351918.
37. Shen G, Zhou H, Jia Z, Deng H. Diagnostic performance of diffusion-weighted MRI for detection of pelvic metastatic lymph nodes in patients with cervical cancer: a systematic review and meta-analysis. Br J Radiol. 2015 Aug;88(1052):20150063.
38. Whiting P, Rutjes AW, Reitsma JB, Glas AS, Bossuyt PM, Kleijnen J. Sources of variation and bias in studies of diagnostic accuracy: a systematic review. Ann Intern Med. 2004 Feb 3;140(3):189-202.
39. Klerkx WM, Veldhuis WB, Spijkerboer AM, van den Bosch MA, Mali WP, Heintz AP, Bipat S, Sie-Go DM, van der Velden J, Schreuder HW, Stoker J, Peeters PH. The value of 3.0Tesla diffusion-weighted MRI for pelvic nodal staging in patients with early stage cervical cancer. Eur J Cancer. 2012 Dec;48(18):3414-21.
40. Hameeduddin A, Sahdev A. Diffusion-weighted imaging and dynamic contrast-enhanced MRI in assessing response and recurrent disease in gynaecological malignancies. Cancer Imaging. 2015 Mar 15;15:3.
41. Bollineni VR, Kramer G, Liu Y, Melidis C, deSouza NM. A literature review of the association between diffusion-weighted MRI derived apparent diffusion coefficient and tumour aggressiveness in pelvic cancer. Cancer Treat Rev. 2015 Jun;41(6):496-502.
42. Rizzo S, Buscarino V, Origgi D, Summers P, Raimondi S, Lazzari R, Landoni F, Bellomi M. Evaluation of diffusion-weighted imaging (DWI) and MR spectroscopy (MRS) as early response biomarkers in cervical cancer patients. Radiol Med. 2016 Jul 2. [Epub ahead of print]
43. Marconi DG, Fregnani JH, Rossini RR, Netto AK, Lucchesi FR, Tsunoda AT, Kamrava M. Pre-treatment MRI minimum apparent diffusion coefficient value is a potential prognostic imaging biomarker in cervical cancer patients treated with definitive chemoradiation. BMC Cancer. 2016 Jul 28;16:556.
44. Schreuder SM, Lensing R, Stoker J, Bipat S. Monitoring treatment response in patients undergoing chemoradiotherapy for locally advanced uterine cervical cancer by additional diffusion-weighted imaging: A systematic review. J Magn Reson Imaging. 2015 Sep;42(3):572-94.
45. Harry VN, Semple SI, Gilbert FJ, Parkin DE. Diffusion-weighted magnetic resonance imaging in the early detection of response to chemoradiation in cervical cancer. Gynecol Oncol. 2008 Nov;111(2):213-20.
46. Frumovitz M, Coleman RL, Gayed IW, Ramirez PT, Wolf JK, Gershenson DM, Levenback CF. Usefulness of preoperative lymphoscintigraphy in patients who undergo radical

hysterectomy and pelvic lymphadenectomy for cervical cancer. Am J Obstet Gynecol. 2006 Apr;194(4):1186-93; discussion 1193-5.
47. Vieira SC, Sousa RB, Tavares MB, Silva JB, Abreu BA, Santos LG, da Silva BB, Zeferino LC. Preoperative pelvic lymphoscintigraphy is of limited usefulness for sentinel lymph node detection in cervical cancer. Eur J Obstet Gynecol Reprod Biol. 2009 Jul;145(1):96-9.
48. Holman LL, Levenback CF, Frumovitz M. Sentinel lymph node evaluation in women with cervical cancer. J Minim Invasive Gynecol. 2014 Jul-Aug;21(4):540-5.
49. Bats AS, Lavoué V, Rouzier R, Coutant C, Kerrou K, Daraï E. Limits of day-before lymphoscintigraphy to localize sentinel nodes in women with cervical cancer. Ann Surg Oncol. 2008 Aug;15(8):2173-9.
50. Fotiou S, Zarganis P, Vorgias G, Trivizaki E, Velentzas K, Akrivos T, Creatsas G. Clinical value of preoperative lymphoscintigraphy in patients with early cervical cancer considered for intraoperative lymphatic mapping. Anticancer Res. 2010 Jan;30(1):183-8.
51. Patino M, Fuentes JM, Singh S, Hahn PF, Sahani DV. Iterative Reconstruction Techniques in Abdominopelvic CT: Technical Concepts and Clinical Implementation. AJR Am J Roentgenol. 2015 Jul;205(1):W19-31.
52. Willemink MJ, de Jong PA, Leiner T, de Heer LM, Nievelstein RA, Budde RP, Schilham AM. Iterative reconstruction techniques for computed tomography Part 1: technical principles. Eur Radiol. 2013 Jun;23(6):1623-31.
53. Willemink MJ, Leiner T, de Jong PA, de Heer LM, Nievelstein RA, Schilham AM, Budde RP. Iterative reconstruction techniques for computed tomography part 2: initial results in dose reduction and image quality. Eur Radiol. 2013 Jun;23(6):1632-42.
54. Khawaja RD, Singh S, Blake M, Harisinghani M, Choy G, Karaosmanoglu A, Padole A, Do S, Brown K, Thompson R, Morton T, Raihani N, Koehler T, Kalra MK. Ultra-low dose abdominal MDCT: using a knowledge-based Iterative Model Reconstruction technique for substantial dose reduction in a prospective clinical study. Eur J Radiol. 2015 Jan;84(1):2-10.
55. Hoogendam JP, Hobbelink MG, Veldhuis WB, Verheijen RH, van Diest PJ, Zweemer RP. Preoperative sentinel node mapping with (99m)Tc-nanocolloid SPECT-CT significantly reduces the intraoperative sentinel node retrieval time in robot assisted laparoscopic cervical cancer surgery. Gynecol Oncol. 2013 May;129(2):389-94.
56. Wright JD, Ananth CV, Lewin SN, Burke WM, Lu YS, Neugut AI, Herzog TJ, Hershman DL. Robotically assisted vs laparoscopic hysterectomy among women with benign gynecologic disease. JAMA. 2013 Feb 20;309(7):689-98.
57. Hoogendam JP, Zweemer RP, Hobbelink MG, van den Bosch MA, Verheijen RH, Veldhuis WB. 99mTc-Nanocolloid SPECT/MRI Fusion for the Selective Assessment of Nonenlarged Sentinel Lymph Nodes in Patients with Early-Stage Cervical Cancer. J Nucl Med. 2016 Apr;57(4):551-6

Chapter 10

English summary

IMAGING FOR THE PRIMARY EVALUATION OF CERVICAL CANCER

As outlined in **chapter 1**, plain film urography, skeletal and chest radiography were traditionally the only image based diagnostics allowed within the FIGO framework of clinical cervical cancer staging. Following changes in clinical practice, the 2009 updated edition of the FIGO stage classification system started to allow cross-sectional imaging to assist with staging, prognosis estimates and better treatment selection. Currently, (in the Netherlands) for women suspected of having early stage (I/II) disease, the radiological part of the standardized work-up typically includes traditional chest radiography and a pelvic MRI, and exceptionally CT is allowed.

A range of international cervical cancer guidelines, including the Dutch guideline, recommend routine chest radiography as the first work-up test for objectifying thoracic metastatic disease. **Chapter 2** investigated the clinical value of this practice in which radiography is unselectively used at staging of women with cervical cancer. None of the studied 244 women with pre-radiograph early stage disease had evidence of pulmonary or skeletal metastases at initial radiography, nor at 6 months follow up. Hence, no stage adjustment was induced by the screening radiograph. Four early stage patients were considered suspicious of metastatic disease on radiography, however the subsequent chest CT or PET-CT were all negative (i.e. false positive radiograph findings). Two of 44 women with advanced pre-radiograph stage disease were upstaged to IVB – from IIIB and IVA, respectively – due to pulmonary metastases identified on radiography. While a range of pathology unrelated to cervical cancer (e.g. pulmonary emphysema) was identified in 61 of a total 288 women, in none immediate intervention was required. In conclusion, no real benefit of routine chest radiography during the workup of women suspected of stage I/II cervical cancer was identified in this study. The current practice is inefficient and associated with – however little – unnecessary ionizing radiation exposure and raises cost-utility concerns. Thus, abandoning unselective radiography use in stage I/II patients should be strongly considered, and is now standard practice in our hospital.

In **chapters 3 and 4** we explored the feasibility of ultra-high field 7.0T MRI to qualitatively improve T_2-weighted imaging of primary early stage cervical cancer. Following a pilot study on healthy volunteers, a prospective feasibility study (DETECT study) of 20 women with stage IB1 – IIB2 cervical cancer was conducted. All had routine 1.5T MRI in their work-up, and subsequently underwent 7.0T MRI which included transversal, sagittal and oblique T_2-weighted turbo spin echo sequences. Seven external transmit and receive dipole antennas were positioned around the pelvis, and combined with an endorectal

monopole antenna. Its signal receive optimum was placed 6 – 10cm beyond the anal verge. The addition of this endorectal antenna increased the signal-to-noise ratio (SNR) at the cervix and tumor by a mean factor of 1.8, and even up to 2.2 when cases with suboptimal positioning were excluded. The SNR increase within a 30mm radius from the antenna was a mean factor of 2.9, and 3.7 for cases with optimal antenna position. Patient-reported discomfort – on a 10 point scale – associated with the endorectal antenna was minimal for its placement with a median score of 1 (range: 0 – 5) and 0 (range: 0 – 2) for its removal. None of the participants requested preterm MRI session discontinuation or reported adverse events related to the antenna. The T_2-weighted acquisitions from 7.0T MRI are visually presented in these chapters, and compared to those from 1.5T MRI to illustrate its feasibility. Likewise, image artefacts encountered on the T_2-weighted acquisitions at 7.0T are illustrated and discussed. In conclusion, we demonstrated the feasibility of high resolution T_2-weighted cervical cancer imaging with 7.0T MRI. The use of an endorectal antenna is well tolerated by patients and allows for substantial SNR increases.

In **chapter 5** we studied the effect of the choice of *b*-values in diffusion weighted magnetic resonance imaging (DWI) on apparent diffusion coefficient (ADC)-based differentiation between malignant and healthy cervical tissue. The ADC is a parameter quantifying the ease of water diffusion in a scanned voxel and is calculated from the signal intensities in DWI datasets, acquired with a minimum of two different *b*-values (i.e. the *b*-value combination). Hindered water diffusion due to cellular changes in cervical cancer makes DWI a promising part of the imaging work-up, though unfortunately the choice of *b*-values varied substantially between investigators, challenging study comparisons. Within the prospective DINGO trial, 35 patients with stage IB1 – IIA cervical cancer underwent a pelvic 3.0T MRI (b= 0, 150, 500, 1000 s/mm^2) with ADC maps created with five different combinations (0,500 – 0,150,500 – 0,1000 – 0,150,500,1000 – 150,500,1000 s/mm^2). For all these combinations, the calculated ADC's were significantly lower in cervical malignancies compared to healthy cervical tissue. This yielded equally high area's under the curve (AUC, all ≥0.965) at ROC analysis, indicating that the discriminatory power is high and uniformly maintained over a range of frequently used *b*-value combinations. Hence, the diagnostic accuracy of DWI in early stage cervical cancer appears independent of the evaluated *b*-value combinations – as long as the highest *b*-value is at least 500 s/mm^2. This supports the pooling of DWI accuracy results from cervical cancer studies that use different *b*-value combinations.

SENTINEL LYMPH NODE IMAGING IN CERVICAL CANCER

Chapter 1 introduced the sentinel lymph node (SLN) concept and both its ability and limitations to ascertain the lymph nodal status, an independent prognostic and therapeutic factor in early stage cervical cancer. When, in addition to blue dye, ^{99m}Tc-nanocolloid is used as a radionuclide for SLN detection, preoperative imaging becomes possible with either single photon emission computed tomography (SPECT) - computed tomography (CT) or dynamic/planar lymphoscintigraphy (LSG). Both modalities aim to provide the surgeon with preoperative information on the anatomical location, radioactive detectability and SLN count per hemipelvis to assist in efficient intraoperative SLN localization.

In **chapters 6 and 7** we directly compared SPECT-CT and LSG based SLN imaging in early stage cervical cancer patients. In **chapter 6** both modalities were retrospectively compared with respect to their effect on their intraoperative SLN retrieval time in a robot assisted laparoscopy setting. Perioperative time points had been prospectively registered in a standardized fashion during the surgeries of two sequentially treated cohorts (33 versus 29 cases) with comparable baseline characteristics. Also, the injection methodology, ^{99m}Tc-nanocolloid dosing, reviewing physicians and perioperative care were identical between both groups. Results on the bilateral intraoperative SN retrieval time (i.e. skin incision for pneumoperitoneal insufflation to bilateral SLN externalization) showed a significant 25.4 minutes reduction for the SPECT-CT group (50.1 ± 15.6 minutes) compared to LSG (75.4 ± 33.5 minutes). Additional analyses confirmed the anticipated poor correlation in anatomical SLN location between LSG imaging and surgery and a strong correlation with SPECT-CT. In more than half of the SLN's visualized on LSG the anatomical location could not be specified beyond 'the general iliac region'. Furthermore, also favoring SPECT-CT over LSG, a trend without statistical significance was observed of higher bilateral SLN visualization (86.2% versus 75.8%) and intraoperative detection ratios (89.7% versus 84.8%), respectively. Our limited sample size could be a reason why significance was not reached (i.e. lack of discriminatory power), thus in **chapter 7** we pooled our results with detection data from comparable cervical cancer studies. A systematic search identified 7 other applicable studies which were, after an internal QUADAS-2 based quality assessment, pooled on their odds ratios (OR) with a random effects model. The median overall detection (≥1 SLN in a patient) was 98.6% on SPECT-CT and 85.3% on LSG which corresponded to a significantly higher pooled detection OR of 2.5 (95%CI: 1.2 – 5.3) for SPECT-CT. Only 3 studies reported the bilateral detection (≥1 SLN in each hemipelvis) which, at a pooled OR of 1.2 (95%CI: 0.7–2.1), yielded no significant

difference. Likewise, no difference in the absolute number of visualized SLN's was present between both modalities. In conclusion, SPECT-CT offers several advantages over LSG such as better anatomical SLN localization and a higher overall detection ratio, possibly contributing to the shortened intraoperative SLN retrieval time found in chapter 6. Combined, these arguments support the preference of SPECT-CT over LSG for preoperative SLN imaging in early stage cervical cancer. In our hospital SPECT-CT is now the standard of pre-operative care for cervical cancer patients.

In **Chapter 8** we hypothesized that a focused SLN assessment on MRI, contrary to indiscriminately reviewing the entire pelvic lymphatic chain, may reduce the number of missed nodal metastases. This is particularly relevant for early stage cervical cancer patients with exclusively <10mm short axis nodes, since they are typically considered non-suspicious (i.e. false negative when metastases are found at histology) and do not undergo PET–CT prior to surgery. Here, we investigated an approach with SPECT–MRI fusions to enable selective SLN assessment and studied MRI based parameters for their association with SLN metastases. An existing cohort of 75 stage IA1 – IIB1 cervical cancer patients was re-analyzed. All patients had a work-up 1.5T MRI and a SLN procedure with preoperative ^{99m}Tc-nanocolloid SPECT–CT based SLN imaging. A fused dataset was created from the CT and MRI datasets using automatic rigid alignment and visual verification of exact 3 dimensional superposition of the pelvic ossal anatomy. This CT–MRI fusion, combined with the inherent link between SPECT and CT, enabled an anatomy matched SPECT–MRI fusion. These fused datasets guided a standardized SLN assessment on MRI, performed by a radiologist blinded to histology. Of the 136 SLN's assessed, 13 (9.6%) contained metastases (8 cases). The short axis diameter (OR: 1.42, 95%CI: 1.01 – 1.99), long axis diameter (OR: 1.28, 95%CI: 1.03 – 1.57) and absence of sharp demarcation (OR: 7.55, 95%CI: 1.09 – 52.28) were significantly associated with nodal metastases. Their combined area under the curve in ROC analysis was 0.749 (95%CI: 0.569 – 0.930) after adjusting for the scored MRI dataset quality. In conclusion, we demonstrated the feasibility of a SPECT–MRI review specifically focused on detecting cervical cancer metastases in <10mm short axis SLNs, an approach not published before. This may aid the selection of early stage patients for PET–CT. The attained accuracy with MRI is substantially lower than the intraoperative SLN procedure, though also cheaper, less laborious and carries a lower adverse event risk.

Chapter 10

Nederlandse samenvatting

BEELDVORMING VOOR DE PRIMAIRE EVALUATIE VAN BAARMOEDERHALSKANKER

In **hoofdstuk 1** wordt uiteengezet dat het intraveneus pyelo-ureterogram, röntgenfoto's van het skelet en de x-thorax lange tijd de enige beeldvormende diagnostiek waren binnen de FIGO richtlijn voor klinische stadiering van baarmoederhalskanker. Volgend op veranderingen in de klinische praktijk werd vanaf de herziende 2009 editie van deze richtlijn ook cross-sectionele beeldvorming toegestaan ter ondersteuning van de stadiering, het inschatten van de prognose alsmede het faciliteren van een betere selectie binnen de behandelmogelijkheden. Bij vrouwen met baarmoederhalskanker (in Nederland) waar een vroeg stadium (I/II) wordt verwacht omvat het radiologische deel van het onderzoek momenteel een x-thorax en een MRI kleine bekken, of bij uitzondering een CT abdomen.

Diverse internationale richtlijnen voor baarmoederhalskanker, inclusief de Nederlandse richtlijn, adviseren routinematig een x-thorax te verrichten als eerste onderzoek voor het vinden van thoracale metastasen. In **hoofdstuk 2** werd de klinische waarde onderzocht van deze methode, waarbij de x-thorax zonder enige selectie wordt ingezet voor de stadiering van vrouwen met baarmoederhalskanker. Geen van de 244 vrouwen verdacht voor een vroeg stadium, vooraf aan deze x-thorax, bleken long- of skeletmetastasen te hebben. Ook presenteerden zij zich daar niet mee in de eerste 6 maanden. Ergo, er deed zich geen stadiumwijziging voor op basis van de gemaakte x-thorax. In tegendeel: vier patiënten hadden bevindingen welke zouden kunnen passen bij metastasen, maar die bij de daaropvolgende CT-thorax of PET-CT allen negatief bleken (oftewel: fout positieve x-thorax bevindingen). Twee van in totaal 44 vrouwen met gevorderd stadium baarmoederhalskanker werden omhoog gestadieerd naar IVB – van IIIB en IVA – doordat er pulmonale metastasen werden gezien op de x-thorax. In 61 van de 288 vrouwen werden toevalsbevindingen, allen zonder relatie met baarmoederhalskanker (bijvoorbeeld longemfyseem), gerapporteerd en in geen van hen was direct medisch handelen geïndiceerd. Concluderend werd in onze evaluatie geen reëel voordeel gezien van het routinematig maken van een x-thorax in vrouwen verdacht voor stadium I/II baarmoederhalskanker. De huidige methode is inefficiënt, geassocieerd met – weliswaar beperkte – expositie aan ioniserende straling en roept vragen op over de kosteneffectiviteit. Het verlaten van het zonder selectie inzetten van x-thorax in vrouwen verdacht voor stadium I/II dient te worden overwogen en is in ons ziekenhuis reeds beleid.

In **hoofdstuk 3 en 4** hebben we de haalbaarheid onderzocht van ultra-hoog veld 7.0T MRI voor de kwalitatieve verbetering van T_2-gewogen beeldvorming van vroeg stadium baarmoederhalskanker. Na een pilotproject met gezonde vrijwilligsters, werd een prospectieve haalbaarheidsstudie (DETECT studie) opgezet met 20 vrouwen gediagnosticeerd met stadium IB1 – IIB2 baarmoederhalskanker. Allen ondergingen hun klinische 1.5T MRI gevolgd door de 7.0T MRI met transversale, sagittale en oblique T_2-gewogen turbo spin echo sequenties. Hierbij werden zeven externe zend en ontvang dipool antennes rond het bekken gepositioneerd en gecombineerd met één endorectale monopool antenne. Het signaalontvangst optimum werd ingebracht tot 6 – 10 cm voorbij de anus. De toevoeging van deze endorectale antenne verhoogde de signaal-ruisverhouding ter plaatse van de cervix en de tumor met een factor van gemiddeld 1.8, en wel tot 2.2 indien casus met een suboptimale antenne positionering werden geëxcludeerd. De signaal-ruisverhouding binnen een straal van 30 mm rondom de antenne nam gemiddeld toe met een factor 2.9, en zelfs 3.7 voor de casus met optimale positionering. Het door patiënten gerapporteerde verlies aan comfort – op een 10 puntenschaal – geassocieerd met de plaatsing en verwijdering van de endorectale antenne was minimaal met een mediane score van 1 (bereik: 0 – 5) en 0 (bereik: 0 – 2) respectievelijk. Geen van de deelneemsters verzocht om vroegtijdig staken van de MRI sessie of had complicaties gerelateerd aan de endorectale antenne. De T_2-gewogen acquisities met 7.0T MRI zijn visueel gerapporteerd – en vergeleken met de 1.5T MRI – in de beschreven hoofdstukken om zo de haalbaarheid te tonen. Ook de beeldartefacten op de T_2-gewogen acquisities op 7.0T zijn geïllustreerd. Concluderend hebben we de haalbaarheid gedemonstreerd van hoge resolutie T_2-gewogen baarmoederhalskanker beeldvorming met 7.0T MRI. Het gebruik van een endorectale antenne is minimaal belastend voor patiënten en bewerkstelligt een substantiële toename in de signaal-ruisverhouding.

In **hoofdstuk 5** hebben we het effect van de *b*-waarden combinatie tijdens diffusie gewogen magnetische resonantie beeldvorming (DWI) op de apparent diffusion coefficient (ADC) gebaseerde differentiatie tussen maligne en gezond cervicaal weefsel bestudeerd. De ADC is een kwantificatie van waterdiffusie in een afgebeeld voxel en wordt berekend met de signaalintensiteiten van DWI datasets verkregen met minimaal twee verschillende *b*-waardes (de *b*-waarden combinatie). De gehinderde cellulaire waterdiffusie in baarmoederhalskanker maakt DWI een veelbelovend beeldvormend MRI onderdeel, echter *b*-waardes verschillen substantieel tussen studies wat het vergelijken van resultaten bemoeilijkt. Binnen de prospectieve DINGO studie ondergingen 35 patiënten met stadium IB1 – IIA baarmoederhalskanker een 3.0T MRI (*b*= 0, 150, 500, 1000

s/mm²) van het kleine bekken. Hierbij werden ADC maps gecreëerd met vijf verschillende combinaties (0,500 – 0,150,500 – 0,1000 – 0,150,500,1000 – 150,500,1000 s/mm²). Voor alle combinaties waren de berekende ADC's significant lager voor baarmoederhalskanker in vergelijking met het gezonde cervixweefsel. Dit produceerde vergelijkbaar hoge resultaten in de ROC analyse (allen AUC ≥0.965), duidend op een goed discriminerend vermogen welke uniform aanwezig is over de frequent gebruikte *b*-waarden combinaties. De diagnostische accuratesse van DWI in vroeg stadium baarmoederhalskanker lijkt dus onafhankelijk van de geëvalueerde combinaties, wanneer de hoogste *b*-waarde minimaal 500 s/mm² is. Dit ondersteunt het vergelijken van DWI resultaten voor baarmoederhalskanker uit studies die verschillende *b*-waardes gebruiken.

SCHILDWACHTLYMFKLIER BEELDVORMING BIJ BAARMOEDERHALSKANKER

Hoofdstuk 1 introduceerde de schildwachtklier (SWK) procedure met een uiteenzetting van de daaraan verbonden mogelijkheden en beperkingen in het achterhalen van de lymfklierstatus, een onafhankelijk prognostische en therapeutische factor in vroeg stadium baarmoederhalskanker. Indien, naast een blauwe kleurstof, ^{99m}Tc-nanocolloid wordt gebruikt als radionuclide voor SWK detectie, wordt preoperatieve beeldvorming mogelijk middels single photon emission computed tomography (SPECT) - computed tomography (CT) of lymfoscintigrafie (LSG). Beide modaliteiten beogen de operateur preoperatief te voorzien van informatie betreffende de anatomische locatie, radioactieve detecteerbaarheid en het aantal SWK's per hemipelvis. Dit ondersteunt een efficiënte intra-operatieve SWK lokalisatie.

In **hoofstukken 6 en 7** hebben we bij vrouwen met vroeg stadium baarmoederhalskanker een directe vergelijking gemaakt tussen SPECT-CT en LSG gebaseerde SWK beeldvorming. In **hoofdstuk 6** hebben we beide modaliteiten retrospectief vergeleken op de intra-operatieve SWK verwijdertijd bij gebruik van robot geassisteerde laparoscopie. De hiertoe gebruikte perioperatieve tijdspunten werden prospectief en op gestandaardiseerde wijze geregistreerd tijdens de operaties van twee sequentiële cohorten (33 versus 29 casus) met vergelijkbare patiëntkenmerken. Ook de injectiemethode, ^{99m}Tc-nanocolloid dosering, de beoordelend nucleair geneeskundigen en overige perioperatieve zorg waren identiek in beide groepen. De resultaten wat betreft de bilaterale SWK verwijdertijd (definitie: tijdsinterval van huidincisie tot het extracorporeel halen van de SWK's) toonden een significante reductie van 25.4 minuten voor de SPECT-CT groep (50.1 ± 15.6

minuten) ten opzichte van de LSG groep (75.4 ± 33.5 minuten). Aanvullende analyses bevestigden de geanticipeerde slechte correlatie tussen LSG en de intra-operatieve anatomische SWK locatie, dit in tegenstelling tot SPECT-CT. In meer dan de helft van de SWK's op LSG kon de anatomische locatie niet nader geduid worden dan de 'iliacale regio'. Verder, ten voordele van SPECT-CT boven LSG, werd een niet significante trend gezien voor hogere bilaterale SWK visualisatie (86.2% versus 75.8%) en intra-operatieve SWK detectie (89.7% versus 84.8%). Onze onderzoekspopulatie had een beperkte omvang wat mogelijk kan verklaren waarom er geen statische significantie werd bereikt. Daarom hebben we in **hoofdstuk 7** onze detectie resultaten samengevoegd met vergelijkbare baarmoederhalskankerstudies. Het systematisch doorzoeken van de literatuur leverde 7 studies op die, na een kwaliteitsbeoordeling met QUADAS-2, werden samengevoegd op basis van odds ratios (OR) met een zogenaamd random effects model. De mediane totale detectie (≥1 SWK in een patiënt) was 98.6% voor SPECT-CT en 85.3% voor LSG wat samenhangt met een significant hogere detectie OR van 2.5 (95%CI: 1.2 – 5.3) voor SPECT-CT. Slechts 3 studies rapporteerden de bilaterale detectie (≥1 SWK in ieder hemipelvis) welke na samenvoeging een OR van 1.2 (95%CI: 0.7–2.1) zonder statistische significantie gaf. Ook werd er tussen beide modaliteiten geen verschil gevonden in het absolute aantal SWK's dat werd gevisualiseerd. In conclusie, SPECT-CT beidt een aantal voordelen ten opzichte van LSG, waaronder betere anatomische SWK lokalisatie en een hogere totale detectie ratio welke mogelijk bijdragen aan de kortere bilaterale SWK verwijdertijd gevonden in hoofdstuk 6. Op basis van deze argumenten geniet SPECT-CT de voorkeur boven LSG voor preoperatieve SWK beeldvorming bij vroeg stadium baarmoederhalskanker. In ons ziekenhuis is SPECT-CT de standaard geworden in de preoperatieve zorg voor patiënten met baarmoederhalskanker.

In **hoofdstuk 8** hadden we de hypothese dat een gerichte SWK beoordeling op MRI, ten opzichte van het aselect beoordelen van alle afgebeelde pelviene lymfklieren, mogelijk het aantal gemiste lymfkliermetastasen kan reduceren. Dit is met name relevant voor vrouwen met vroeg stadium baarmoederhalskanker die enkel lymfklieren met een korte as <10mm hebben. Zij worden doorgaans als onverdacht beschouwd (fout-negatief indien metastasen histologisch worden bewezen) en ondergaan geen PET-CT voor hun operatie. Dit onderzoek richt zich op SPECT–MRI fusies waarop we selectief de SWK's hebben beoordeeld en MRI parameters hebben onderzocht die geassocieerd zijn met SWK metastasen. Een bestaand cohort van 75 vrouwen met stadium IA1 – IIB1 baarmoederhalskanker werd geanalyseerd. Al deze patiënten hadden een routine 1.5T MRI en SWK procedure met preoperatieve ^{99m}Tc-nanocolloid SPECT–CT beeldvorming ondergaan. Een gefuseerde dataset werd gecreëerd van de CT en MRI middels

automatische uitlijning met visuele verificatie of er exact 3 dimensionale superpositie van de benige bekkenstructuren was. Deze CT–MRI fusie, gecombineerd met de inherente SPECT en CT verbinding, maakt een anatomisch correcte SPECT-MRI fusie mogelijk. Deze SPECT-MRI datasets begeleide een gestandaardiseerde SWK beoordeling op MRI, uitgevoerd door een radioloog geblindeerd voor de histologische bevindingen. Er werden 136 SWK's beoordeeld, waarvan 13 (9.6%) een metastase hadden (8 casus). De korte as diameter (OR: 1.42, 95%CI: 1.01 – 1.99), lange as diameter (OR: 1.28, 95%CI: 1.03 – 1.57) en afwezigheid van een scherpe begrenzing (OR: 7.55, 95%CI: 1.09 – 52.28) waren significant geassocieerd met kliermetastasen. De gecombineerde AUC was 0.749 (95%CI: 0.569 – 0.930) na correctie voor de MRI kwaliteit. In conclusie, de haalbaarheid van SPECT–MRI voor de beoordeling van SWK's, specifiek gericht op de detectie van metastasen in <10mm korte as klieren, is hier getoond. Mogelijk kan dit de selectie van vroeg stadium baarmoederhalskankerpatiënten voor PET-CT bevorderen. Echter, de verkregen diagnostische accuratesse blijft substantieel lager dan de intra-operatieve SWK procedure, doch het is wel minder kostbaar en bewerkelijk en heeft een lager complicatierisico.

10

Chapter 11

Bibliography

Articles in peer reviewed journals

Hoogendam JP, Vlek CA, Witteveen PO, Verheijen RHM, Zweemer RP. Surgical lymph node assessment during the staging of primary mucinous ovarian carcinoma: a systematic review and meta-analysis. BJOG 2016, in press.

Hoogendam JP, van Kalleveen IML, Arteaga de Castro CS, Raaijmakers AJE, Verheijen RHM, van den Bosch MAAJ, Klomp DWJ, Zweemer RP, Veldhuis WB. High resolution T2-weighted cervical cancer imaging: a feasibility study on ultra-high field 7.0T MRI with an endorectal monopole antenna. Eur Radiol 2016, in press.

Hoogendam JP, Zweemer RP, Hobbelink MGG, van den Bosch MAAJ, Verheijen RHM, Veldhuis WB. ^{99m}Tc SPECT – MRI fusion for the selective assessment of non-enlarged sentinel lymph nodes for diagnosing cervical cancer metastases. J Nucl Med. 2016 Apr; 57(4):551-556.

Van der Aa JE, **Hoogendam JP**, Butter ESF, Ausems MGEM, Verheijen RHM, Zweemer RP. Effect of personal medical history and family history of cancer in uptake of risk-reducing salpingo-oophorectomy. Fam Cancer. 2015 Dec; 14(4):539-544.

Hoogendam JP, Zweemer RP, Verkooijen HM, de Jong PA, van den Bosch MAAJ, Verheijen RHM, Veldhuis WB. No value for routine chest radiography in the work-up of early stage cervical cancer patients. PLoS ONE. 2015. 10(7): e0131899.

Hoogendam JP, Veldhuis WB, Hobbelink MGG, Verheijen RHM, van den Bosch MAAJ, Zweemer RP. Technetium-99m SPECT-CT versus planar lymphoscintigraphy for preoperative sentinel lymph node detection in cervical cancer: a systematic review and meta-analysis. J Nucl Med 2015 May; 56(5):675-680.

Hoogendam JP, Zweemer RP, Schaap TS, Schreuder HWR, Veldhuis WB. CT, MRI and laparoscopy findings of a retroperitoneally herniated ovary causing acute abdominal pain. Hernia 2014 Dec; 18(6):915-917.

Hoogendam JP, Verheijen RH, Wegner I, Zweemer RP. Oncological outcome and long term complications in robot assisted radical surgery for early stage cervical cancer: an observational cohort study. BJOG. 2014 Nov; 121(12): 1538-1545.

Hoogendam JP, Zaal A, Rutten EG, Heijnen CJ, Kenter GG, Veldhuis WB, Verheijen RHM, Zweemer RP. Detection of cervical cancer recurrence during follow-up: a multivariable comparison of 9 frequently investigated serum biomarkers. Gynecol Oncol. 2013 Dec; 131(3): 655-660.

Hoogendam JP, Hobbelink MGG, Veldhuis WB, Verheijen RH, van Diest PJ, Zweemer RP. Preoperative sentinel node mapping with ^{99m}Tc-nanocolloid SPECT-CT significantly reduces the intraoperative sentinel node retrieval time in robot assisted laparoscopic cervical cancer surgery. Gynecol Oncol 2013 May; 129(2): 389–394.

Hoogendam JP, Klerkx WM, de Kort GA, Bipat S, Zweemer RP, Sie-Go DM, Verheijen RH, Mali WP, Veldhuis WB. The influence of the *b*-value combination on apparent diffusion coefficient based differentiation between malignant and benign tissue in cervical cancer. J Magn Reson Imaging. 2010 Aug; 32(2): 376-382.

Articles in non-peer reviewed media

Hoogendam JP, Zweemer RP. De schilwachtklierprocedure bij het stadium I/II cervixcarcinoom. Kanker Breed (NVvO journal) 2014 Nov; 6(2): 3-6.

Hoogendam JP (on behalf of Zweemer RP, Hobbelink MGG, van den Bosch MAAJ, Verheijen RHM, Veldhuis WB). SPECT-MRI Fusion Minimizes Surgery for Diagnosis of Early-stage Cervical Cancer Patients. Interview / press release by the Society of Nuclear Medicine and Molecular Imaging, April 2016.

Evidence based GCP guidelines

Vergote I, Vlayen J, Heus P, **Hoogendam JP**, Damen JAAG, van de Wetering FT, van der Baan FH, Bourgain C, De Grève J, Debruyne D, Fastrez M, Goffin F, Huizing M, Kerger J, Kridelka F, Stroobants S, Tjalma W, Van Dam P, Van de Caveye V, Villeirs G, Vuylsteke P, Fairon N, Zweemer RP, Hooft L, Scholten RJPM, Verleye L. Ovarian cancer: diagnosis, treatment and follow-up. Good Clinical Practice (GCP) Brussels: Belgian Health Care Knowledge Centre (KCE). 2016. KCE Reports 268. D/2016/10.273/49.

Awards

Best presentation, WGE symposium, Noordwijk, 2014.

Alavi-Mandell Award, Society of Nuclear Medicine and Molecular Imaging, 2016.

Chapter 11

Dankwoord

Allereerst wil ik alle patiënten en gezonde vrijwilligsters hartelijk danken voor hun belangeloze bijdrage aan het onderzoek in dit proefschrift. Voorts wil ik expliciet bedanken:

Prof. dr. R.H.M. Verheijen, beste René, ik heb je leren kennen als een scherpe, fijnzinnige en bovenal eloquente promotor. Je wilde met dit promotietraject de vorming van een academicus bereiken. Zo gaf je me, naast mijn wetenschappelijke werk, de ruimte voor zowel het volgen als het verzorgen van onderwijs. Voor je visie 'kwaliteit boven kwantiteit' en de volwaardige promotietijd die je me gegund hebt, ben ik je uiterst dankbaar. Het was een eer om een van jouw laatste promovendi te mogen zijn. Merci en geniet van la douce France!

Prof. dr. M.A.A.J. van den Bosch, beste Maurice, onze contactmomenten waren altijd waardevol: ik kreeg er zowel nieuwe energie als inspiratie van! Ondanks je overvolle agenda blijf je toegankelijk en heb je oog voor de mens achter de promovendus, zo ook voor de fase na zijn promotie. En dat zelfs bij deze niet-radioloog in spé! Ik heb veel respect voor je indrukwekkende wetenschappelijke en organisatorische prestaties en ik ben blij dat je deel van dit promotieteam wilde zijn.

Dr. R.P. Zweemer, beste Ronald, Ronnie, ome Roon, Ronaldo, pink panther (indien in roze OK jas over de stafgang sluipend) of gewoon: de grote baas. Zo groen als gras kwam ik 8 jaar geleden als student onderzoek bij je doen. Sindsdien, tijdens onze ontelbare vandaag-is-het-krokettendag lunches, leerde ik je kennen als een open, eerlijk en positief ingestelde wetenschapper met een goed gevoel voor humor. Zo kreeg ik de afgelopen jaren 1 doorlopende opdracht van je: "Zorg dat je nooit terecht komt in mijn what-the-f*ck-is-going-on-met-dit-project-map...". Ik leerde over het nut van paashazen en het schrijven zonder de fameuze 'Jaap speak' (een nobel streven, maar of het haalbaar is gebleken...). Zullen we de aankomende jaren nog veel wetenschap samen verrichten? Ik kijk er naar uit.

Dr. W.B. Veldhuis, beste Wouter, door je doelgerichte, heldere en 'we can do it' attitude ben je enorm waardevol geweest voor het slagen van dit promotietraject. Je hebt een scherp oog voor goede wetenschap (en mooie techniek!), zoekt enthousiast uitdagingen op en weet wat doorpakken is. Dat bewonder ik enorm in je. Je bent een uitstekende leermeester en je toekomstige promovendi weten nog niet half hoeveel geluk ze gaan hebben met jouw begeleiding.

Prof. dr. P.J. van Diest, Prof. dr. P.A. de Jong, Prof. dr. G.G. Kenter, Prof. dr. P.R. Luijten en Prof. dr. W.P.T.M. Mali ben ik dankbaar voor het zitting nemen in de beoordelingscommissie.

Dr. I.M.L. Kalleveen, dr. C.S. Arteaga de Castro, dr. D.W.J. Klomp en dr. A.J.E. Raaijmakers, beste Irene, Catalina, Dennis, Alexander (en vele anderen), in mijn ogen zijn jullie allemaal MRI kunstenaars en technische helden! Voor deze simpele ziel was jullie werk voor/achter/in/naast/bij de 7T MRI soms onnavolgbaar, maar altijd indrukwekkend. Samen vormen jullie een hechte en succesvolle onderzoeksgroep waarmee het fijn samenwerken was.

Prof. dr. R.J.P.M. Scholten, beste Rob, onze samenwerking met het KCE voor de Belgische richtlijn (en het Cochrane manuscript) ovariumcarcinoom heb ik als uiterst leerzaam en leuk ervaren. Het was een ware masterclass literatuur zoeken en beoordelen. Ook de samenwerking met Leen, Fleur, Lotty, Pauline en René beschouw ik als een verrijking van dit project.

Dr. H.M. Verkooijen, beste Lenny, als mentor tijdens mijn master epidemiologie heb ik een aantal waardevolle lessen over diagnostisch onderzoek van je gekregen. Ik bewonder je directe doch integere benadering en je unieke gave om met een paar scherpe vragen alle hiaten in een projectvoorstel of manuscript bloot te leggen. Daar werd het zeker beter van!

Drs. S. van Amelsvoort-van de Vorst, beste Saskia, vanuit het trialbureau hielp je me met de gehele procedurele ondersteuning van de DETECT studie (waaraan ik anders hopeloos ten onder zou zijn gegaan). Je kennis en kunde over GCP, METC procedures, WMO verplichtingen, interne SOP's, datamonitoring, investigator site files en alle aanverwante narigheid is indrukwekkend. Duizend maal dank!

Drs. M.G.G. Hobbelink, beste Monique, je enthousiaste bijdrage vanuit de nucleaire geneeskunde was stimulerend en creëerde absoluut meerwaarde voor onze sentinel node manuscripten. Je hebt een warm en stralend karakter!

Dr. A. Zaal, beste Afra, onze onderzoeksonderwerpen verschilden, maar toch is het een eer om in je voetsporen te mogen treden bij de gynaecologische oncologie. Met je positieve instelling ben je altijd een voorbeeld voor me geweest. Het serumproject en de ESGO in Liverpool waren voor mij een hoogtepunt in onze samenwerking.

Dr. W.M. Klerkx, beste Wenche, in 2008 begon de wetenschap voor me en ik ben je dankbaar dat we samen, op basis van jouw DINGO trial, het eerste hoofdstukje hebben kunnen schrijven.

Alle coauteurs die ik nog niet bij naam heb genoemd, wil ik van harte bedanken voor al hun tijd, energie, zinnige revisies, oprechte interesse en kritische vragen.

Dr. H.W.R. Schreuder, beste Henk, als onderwijs-tutor heb je me richting en structuur geboden bij het vergroten van mijn didactische vaardigheden. Uiteindelijk is die doctorstitel afgeleid van het Latijnse werkwoord *docere* (lesgeven) en ben je na het promoveren meer dan ooit een docent. Jij begrijpt dit als geen ander. Ik ben je zeer dankbaar voor de inzichten en adviezen die je me hebt gegeven tijdens het BKO traject.

Mw. E.S.F. Butter, beste Els, door onze gezamenlijke inspanningen hebben we – o.a. met de FSFI vragenlijst en het erfelijke tumoren project – de gynaecologische oncologische zorg in het UMC Utrecht een beetje kunnen verrijken. Ik denk met veel plezier en tevredenheid terug aan onze gezamenlijke projecten.

Drs. C.J. de Witte en Drs. J.F. Roze, beste Chris en Joline, wat ontzettend tof dat jullie het stokje overnemen bij de gynaecologische oncologie, uiteraard op een veel ingewikkelder onderwerp. Ik wens jullie een mooie tijd toe!

Drs. J.E. van der Aa en mw. C.A. Vlek, beste Jessica en Caroline, ik ben jullie dankbaar dat jullie het als student met mij hebben uitgehouden tijdens jullie wetenschappelijke stages. De mooie artikelen die uit deze stages zijn voort gekomen zijn een prestatie van wereldformaat.

Alle UMC Utrecht staf, A(N)IOS en anderszins geïnteresseerden wil ik hartelijk bedanken voor hun zinvolle bijdrage, de getoonde interesse en verrichte DETECT inclusies. Ik ben Tessa en Ellis dankbaar voor hun organisatorische hulp, in het bijzonder voor al mijn onmogelijke vergaderverzoeken die toch gerealiseerd konden worden.

Alle gynaecologen, arts-assistenten, verloskundigen en verpleging vanuit het Elisabeth-TweeSteden ziekenhuis wil ik bedanken voor de goede sfeer en het fijne begin van de opleiding.

Alle arts-onderzoekers van de divisie Vrouw en Baby wil ik bedanken voor de koffie-

met-taart-momenten, maandaglunches, klaagmuurtirades, uitgedeelde moederpunten en leuke borrelactiviteiten. De (ex-)PhD ladies met wie ik ergens gedurende de 4 jaar lotgenotencontact heb gehad in het Côte d'AZU ben ik bijzonder dankbaar: Charine, Annegreet, Annelien, Eline, Felicia, Janine, Jolijn, Juliënne, Kim, Kristine, Madeleine, Marlieke, Marlies, Marlise, Martine, Nadine, Ouijdane, Simone en Yvonne. Zoveel beeldschone dames, zoveel nieuwe inzichten in de wonderlijk fluïde, licht theatrale en soms onnavolgbare psyché van de moderne, hoogopgeleide vrouw. Geloof me, het was bij tijd en wijle een echte openbaring!
(P.S. Beste hoogleraren, wanneer komen er weer een paar promovendi die in het bezit zijn van een robuust Y-chromosoom, zodat deze ovariocratie wordt doorbroken?)

Drs. T.C. van Tilborg en Drs. C.J. de Witte, beste Charine en Chris, ik wil jullie expliciet bedanken voor alle activiteiten als paranimf. Mijn keuze voor jullie was logisch, lang voor deze promotie deelden we al harde grappen en diep inhoudelijke wetenschappelijke discussies. Geen verrassing dus dat jullie ook deze rol als paranimf fantastisch hebben ingevuld. Mijn dank is groot!

Beste Hans, en met liefdevolle nagedachtenis aan Astrid, ik wil jullie bedanken voor alle interesse door de jaren heen. Het was een donderslag op een regenachtige dinsdag toen dit onderwerp ineens persoonlijk werd en heel dichtbij kwam. Gedurende het gehele traject daarna ben ik diep onder de indruk geraakt van jullie veerkracht en aanhoudende optimisme, dit ondanks de vele tegenslagen. Het was en is nog steeds buitengewoon aangenaam om naar Haarlem te komen voor goede wijn, een mooie dis en alle andere fijne dingen des leven die jullie ons keer op keer hebben gegund. Ik ben gelukkiger met jullie in mijn leven en wil jullie daarvoor hartelijk bedanken.

Lieve pap en mam, jullie zijn een steunpilaar in deze drukke periode geweest, maar zeker ook in de periode ervoor en ongetwijfeld nog lang hierna. Jullie onvoorwaardelijke liefde heeft bijgedragen aan waar ik nu sta in het leven. Dit boekje is daar slechts één (kleine) uiting van. Ik wil jullie vanuit het diepste van mijn hart bedanken voor het vertrouwen, de warmte en alle goede zorgen. Ook Suzan en Sjoerd ben ik in deze dankbaar voor de aanhoudende oprechte belangstelling (en dat jullie deze carnetariër hebben overtuigd dat vegetarisch dineren ook erg lekker kan zijn!).

Frea, amore, je bent alles voor me en ik wil de rest van mijn leven met je delen. Met geen duizend zinnen kan ik hier mijn liefde voor je duidelijker beschrijven dan met de allesomvattende waarheid: Ik hou van je!

Chapter 11

Curriculum Vitae

On June 8th 1986, after an uncomplicated multiparous delivery, Jacob Pieter (Jaap) Hoogendam was born in Leidschendam. After graduating from the Huygens Lyceum in 2004, he moved to Utrecht where he attended the medical curriculum. During his fourth year, he completed an internship in paediatrics at the Teygerberg hospital in Cape Town, South Africa. That same year, a cervical cancer project with diffusion weighted MRI became his first research encounter. After receiving his MD degree in 2010, he worked for 14 months as a gynaecology and obstetrics resident (ANIOS) in the St. Antonius Hospital in Nieuwegein (supervision: J.H. Schagen van Leeuwen).

In 2012 Jaap started his PhD program which culminated in this thesis as its final product. The performed research was presented at conferences in Honolulu (ISMRM), Liverpool (ESGO), Brussels (ESGE), Istanbul (SERGS) and Nice (ESGO). To further sharpen his theoretical and practical competences in the field of medical research, a MSc. degree in epidemiology was obtained at the University of Utrecht in 2015 (supervision: H.M. Verkooijen). This entailed a double specialisation program of 'clinical epidemiology' and 'medical statistics'. During these PhD years, he enjoyed supervising medical students during their research projects and assisted with the core oncology course in the medical curriculum. In 2015 a university teaching qualification (BKO) was granted (supervision: H.W.R. Schreuder). Furthermore, in close collaboration with the Dutch Cochrane Center and the KCE in Brussels, Jaap participated in preparation of the Belgian ovarian cancer guideline which was published in April 2016.

In January 2016 he started his specialty training as a resident in gynaecology and proactive obstetrics at the Elisabeth – TweeSteden hospital in Tilburg (supervision: I.A.J. van Rooij and J.M.J. Smeenk).